Title
Signaling properties of the sigma E activation pathway

Author
Grigorova, Irina L

Publication Date
2005

Peer reviewed|Thesis/dissertation

Signaling properties of the σ^E activation pathway

by

Irina L. Grigorova

DISSERTATION

Submitted in partial satisfaction of the requirements for the degree of

DOCTOR OF PHIOLOSOPHY

in

Biophysics

in the

GRADUATE DIVISION

of the

UNIVERSITY OF CALIFORNIA, SAN FRANCISCO

This thesis is dedicated to my grandfathers,

Victor and Naum

Acknowledgements

I take this opportunity to thank everyone who supported me throughout my graduate school making these years interesting and fulfilling. I want to acknowledge all those who contributed towards my research and encouraged me by setting examples in both scientific and humane fields.

First, I want to express my gratitude to my Ph. D. advisor and mentor, Carol Gross. Carol taught me using a perfect combination of freedom and guidance. She allowed me to try and explore various possible projects and helped me to develop a personalized view on research. She always encouraged my attempts to combine experiments with modeling and supported new ideas. Carol was very involved in my research and she made sure that science was good, that the questions were addressed correctly and in completion. She also showed me how to finalize a project and bring it to the publication level. Throughout my graduation Carol provided me with her ultimate support, trust and help, both in research and life in general. I am very grateful to her for being a great advisor and a friend.

I would like to specifically thank two former lab members, Sarah Ades and Benjamin Alba. Working with Sarah helped me to develop a critical attitude towards experimentation. Ben generously introduced me to bacterial genetics and gave me many good advices. I am thankful to Hong Ji Zhong for voluntarily providing me with technical assistance which saved me many hours of mundane work. I also want to thank former and current lab members including, Brian Yong, Virgil Rhodius, Christopher Herman, Tanja Gruber, Eric Guisbert and Rachna Chaba, for their technical advices and for providing fruitful discussions and constructive criticism. My

life in graduate school was enlightened by the presence of Chi Zen Lu, an outstandingly warm person who took care of each one of us in the lab. I greatly appreciate and respect her wisdom, kindliness and love for life. I also want to mention Julie Ransom, the "mama" of biophysical students, who was very supportive and really fun to be around.

I can not express my grief about the untimely passing of Naum Phleger, a gifted graduate student in Biophysics from Davis. We collaborated with Naum on modeling RNA polymerase binding to DNA and I always enjoyed talking to him, his brilliant ideas, friendliness and enthusiasm about science.

I also take this opportunity to express my love and gratitude towards my family. Not only have my family members encouraged and supported me throughout the years of my education, they have also been my role models in science. I have always been amazed by my mom's ability to combine research and managerial skills, at the same time being a thoughtful and caring advisor. My father has always been the ideal Scientist for me. He is one of the few persons in science, I have come across, capable of combining his deep knowledge and understanding of the various areas of physics with original unconventional ideas and above all, the courage to stand for them. This attitude in the family comes from my grandfathers, to whom science meant their entire life. Their personal example and philosophy have been a great source of inspiration to me.

In the end, I want to thank my husband Ilya for his encouragement and reassurances, despite his personal sacrifices. His constant support made it possible for me to sail through the graduate school years and make the most out of them.

Statement Regarding Previously Published Material with Multiple Authors

Chapter Two contains the data that I contributed to (Ades, S.E., Grigorova, I.L. and Gross, C.A. (2003) Regulation of the alternative sigma factor σ^E during initiation, adaptation, and shutoff of the extracytoplasmic heat shock response in *Escherichia coli*. J. Bacteriol. 185: 2512-2519), and is reprinted here with permission from American Society for Microbiology (page vii), who retains all copyright privileges. I conceived of and carried out experiments included in Table 2-1, Figure 2-3, Figure 2-4, Figure 2-5 A,B.

Chapter Three contains work previously published in (Grigorova, I.L., Chaba, R., Zhong, H.J., Alba, B.M., Rhodius, V., Herman, C., and Gross, C.A. (2004) Fine-tuning of the *Escherichia coli* σ^E envelope stress response relies on multiple mechanisms to inhibit signal-independent proteolysis of the transmembrane anti-sigma factor, RseA. Genes. Dev. 18: 2686-2697), which is reprinted here with permission from Cold Spring Harbor Laboratory Press (page viii) who retains all copyright privileges. I conceived of and carried out all experiments in this publication. H. J. Zhong provided laboratory assistance. R. Chaba collected additional relevant data that did not appear in the paper. I wrote the entire text, which was edited by Carol A. Gross.

UCSF
University of California
San Francisco

November 18, 2005

Carol A. Gross, PhD
Department of Stomatology
Department of Microbiology
and Immunology

600-16th Street
Genentech Hall, S372E
San Francisco CA 94143-2200

Telephone: 415/476-4161
Facsimile: 415/514-4080
E-mail: agross@cgl.ucsf.edu

Journals Dept.,
American Society for Microbiology
1752 N street,
N.W., Washington, DC
20036-2904, USA
fax: (202) 942-9355

To whom it may concern:

I am writing to request permission to include the following publication in its entirety in my doctoral thesis dissertation:

Sarah E. Ades, Irina L. Grigorova, and Carol A. Gross. 2003. Regulation of the alternative sigma factor σ^E during initiation, adaptation and shutoff of the extracytoplasmic heat shock response in *Escherichia coli*. *Journal of Bacteriology*. 185, 8: 2512-2519.

The dissertation will be archived by University Microfilms International, which requests written permission to supply single copies of the thesis upon demand. Please respond by fax to fax: 415-514-4080 or by e-mail to igricor@itsa.ucsf.edu.

Thank you for assistance in this matter.

Sincerely,

Irina Grigorova

PERMISSION GRANTED
CONTINGENT ON AUTHOR PERMISSION (which you must obtain)
AND APPROPRIATE CREDIT
American Society for Microbiology
Journals Department
Date 11-22-05

UCSF
University of California
San Francisco

November 18, 2005

Carol A. Gross, PhD
Department of Stomatology
Department of Microbiology
and Immunology

600-16th Street
Genentech Hall, S372E
San Francisco CA 94143-2200

Telephone: 415/476-4161
Facsimile: 415/514-4080
E-mail: cgross@cgl.ucsf.edu

Journals Dept.,
American Society for Microbiology
1752 N street,
N.W., Washington, DC
20036-2904, USA
fax: (202) 942-9355

To whom it may concern:

I am writing to request permission to include the following publication in its entirety in my doctoral thesis dissertation:

Sarah E. Ades, Irina L. Grigorova, and Carol A. Gross. 2003. Regulation of the alternative sigma factor σ^E during initiation, adaptation and shutoff of the extracytoplasmic heat shock response in *Escherichia coli*. *Journal of Bacteriology*. 185, 8: 2512-2519.

The dissertation will be archived by University Microfilms International, which requests written permission to supply single copies of the thesis upon demand. Please respond by fax to fax: 415-514-4080 or by e-mail to igricor@itsa.ucsf.edu.

Thank you for assistance in this matter.

Sincerely,

Irina Grigorova

PERMISSION GRANTED
CONTINGENT ON AUTHOR PERMISSION (which you must obtain)
AND APPROPRIATE CREDIT
American Society for Microbiology
Journals Department
Date 11-22-05

UCSF
University of California
San Francisco

November 18, 2005

Carol A. Gross, PhD
Department of Stomatology
Department of Microbiology and Immunology

600-16th Street
Genentech Hall, S372E
San Francisco CA 94143-2200

Telephone: 415/476-4161
Facsimile: 415/514-4080
E-mail: cgross@cgl.ucsf.edu

Genes and Development
Cold Spring Harbor Laboratory
Attn: Bibi Garite, Editorial Secretary
500 Sunnyside Boulevard
Woodbury, NY 11797-2924
Phone: 516-422-4015; FAX: 516-422-4093

To whom it may concern:

I am writing to request permission to include the following publication in its entirety in my doctoral thesis dissertation:

Irina L. Grigorova, Rachna Chaba, Hong Ji Zhong, Benjamin M. Alba, Virgil Rhodius, Christophe Herman, and Carol A. Gross. 2004. Fine-tuning of the *Escherichia coli* σ^E envelope stress response relies on multiple mechanisms to inhibit signal-independent proteolysis of the transmembrane anti-sigma factor, RseA. *Genes & Development*. 18: 2686-2697

The dissertation will be archived by University Microfilms International, which requests written permission to supply single copies of the thesis upon demand. Please respond by fax to fax: 415-514-4080 or by e-mail to igrigor@itsa.ucsf.edu.

Thank you for assistance in this matter.

Sincerely,

Irina Grigorova

Permission granted by the copyright owner, contingent upon the consent of the original author, provided complete credit is given to the original source and copyright date.

By [signature] 10/22/05

COLD SPRING HARBOR LABORATORY PRESS

TOTAL P.02

Signaling properties of the σ^E activation pathway

by

Irina L. Grigorova

Carol A. Gross, Ph.D.
Thesis Advisor

Abstract

σ^E activity is required to diminish general stress in the envelope of *Escherichia coli* and to ensure proper insertion of outer membrane porins (OMP) into the outer membrane. Accumulation of unassembled OMP monomers in the periplasm generates a signal that is communicated through the inner membrane to the cytoplasm, where it activates the transcription factor, σ^E. The signal is conveyed by proteolytic cascade that carries out regulated proteolysis of RseA, a membrane-spanning anti-sigma factor whose cytoplasmic domain inhibits σ^E - dependent transcription. Upon binding to OMP C-termini, the membrane localized DegS protease is activated to cleave RseA in its periplasmic domain. The membrane embedded protease, RseP, then cleaves RseA close to the inner membrane, and σ^E is released in complex with cytoplasmic RseA fragment that is subsequently degraded. The transcriptional

activity of σ^E varies over 40-fold in a graded manner depending on the expression level of OMP. In this thesis I have addressed the organization of the pathway. First, I have shown that σ^E activity correlates with the rate of RseA proteolysis because RseA degradation determines the rate of σ^E release into the cytoplasm. This mechanism enables cells to respond to the changes in RseA degradation rate rapidly, prior to changes in the relative levels of RseA and σ^E. I also present evidence that RseB (a periplasmic protein) and DegS function to make the system sensitive to a wide range of OMP concentrations and unresponsive to variations in the levels of DegS and RseP proteases. These features rely on the inability of RseP to cleave intact RseA. I demonstrate that RseB, which binds to the periplasmic face of RseA, and DegS each independently inhibit RseP cleavage of intact RseA.

In a separate project, I measured the levels of RNA polymerase, σ^{70}, σ^E and σ^{32} in *E. coli*. I use these values in an equilibrium model that considers RNA polymerase binding to DNA to explore theoretically two aspects of general regulation of transcription: recruitment of RNA polymerase to promoters by activators and competition between σ's.

Table of Contents

List of Tables

List of Figures

Chapter One

Principal organization of σ^E pathway in *Escherichia coli*.

Comparison to RIP pathways in other bacteria.

Prologue

To receive information from the extracellular environment or to transmit it between sub-compartments, cells must communicate signals across lipid membranes. Most transmembrane signaling pathways employ membrane-spanning proteins, which undergo signal-induced changes in their conformation, oligomerization state, or stability. Stability of membrane proteins is often regulated by intra-membrane proteolysis (RIP) [1, 2], which is carried out by membrane metalloproteases [3, 4]. These proteases are believed to cleave their transmembrane substrates in the plane of the membrane or near its surface [5]; the released cleavage products often act downstream as transcription factors or signaling molecules.

The founding RIP proteases, SpoIVFB and S2P, were discovered in organisms as diverse as bacteria and humans [2, 5-8]. In eukaryotic cells RIP proteases are involved in regulation of various cellular processes, such as ATF6-dependent induction of the unfolded protein response in the endoplasmic reticulum [9, 10], SREBP dependent regulation of cholesterol biosynthesis [8, 11], activation of Notch and NF-κB transcription factors [12, 13]. RIP proteases are very widespread in bacteria, as they are found in almost all known bacterial subgroups. Although most of them have not yet been extensively studied, it is clear that RIP proteases are used in many different signaling pathways. These signaling pathways have evolved in concert with the diverse cellular functions that they regulate.

In this review, we examine the well-studied bacterial RIP signaling pathways and discuss how the properties of these pathways, such as the timing and type of response (e.g. graded or all-or-none) relate to the functions regulated. We first discuss the

organizational principles of one of the best-studied bacterial RIP signaling pathways, the *Escherichia coli* σ^E-dependent envelope stress response. We then compare this response to the *Pseudomonas aeruginosa* σ^E response, which uses similar components. We end by reviewing other bacterial RIP signaling pathways, whose other components are unrelated to those in the *E. coli* σ^E pathway.

The *E. coli* σ^E-dependent envelope stress response

Introduction

As a gram-negative bacterium, *E. coli* has two compartments: the cytoplasmic compartment and the cell envelope, which consists of the periplasm bounded by the inner and outer membranes [14-17]. The outer membrane provides an extra barrier between the harsh extracellular milieu and the cytoplasm, and contains two unique molecules: lipopolysaccharide (LPS), and porins [14]. LPS constitutes about 80% of the surface area of the outer membrane and is responsible for the relative impermeability of gram negative bacteria [18]. Porins are trimeric β-barrel proteins that form aqueous channels in the outer membrane and constitute most of the remaining 20% of the surface area of the bacterium. Porins permit nutrient uptake and solute exchange with the environment [14]. Porins are translocated across the inner membrane as monomers; their insertion into the outer membrane and assembly into trimers requires a complex maturation pathway, including several protein folding agents, several LPS intermediates and a machinery that inserts β-barrel proteins into

the membrane [19-21]. The integrity of the outer membrane requires the proper insertion of porins and the proper ratio of porins to LPS [14].

Outer membrane integrity is crucial for cellular viability [14-17], therefore it is not surprising that the cell carefully monitors the status of porin maturation in the envelope. Accumulation of unassembled porin monomers generates a signal that is communicated through the inner membrane to the cytoplasm, where it activates the transcription factor, σ^E [22, 23]. σ^E binds to core RNA polymerase and directs it to transcribe target genes that ensure the synthesis, assembly and homeostasis of outer membrane porins and LPS [24]. Interestingly, the transcriptional activity of σ^E varies over 40-fold in a graded manner depending on the expression level of OMPs [22, 25]. Here, we describe the components of this transmembrane signal transduction pathway and simultaneously discuss properties that make it graded and sensitive to a wide range of the inducing signal (Fig. 1-1).

Regulated degradation of a transmembrane anti-sigma factor

The transcriptional activity of σ^E is permanently dampened down by the inner-membrane spanning anti-sigma factor, RseA [26, 27]. The cytoplasmic domain of RseA (RseA cyto) binds to σ^E and masks its binding determinants to RNA polymerase. As revealed in a crystal structure of the σ^E / RseA cyto complex, their binding interface is very extensive [28]. σ^E binds to RseA cyto very tightly *in vitro* (K_d < 10 pM), consistent with the extensive interface between the two proteins (I.Grigorova, unpublished results). Due to tight binding and a probable excess of

RseA over σ^E (I.Grigorova, unpublished results), the anti-sigma factor can drastically downregulate σ^E activity.

The signal generated by unassembled porins leads to the regulated degradation of RseA by a proteolytic cascade [29] (Fig. 1-2A). DegS initiates this cascade and is the only identified sensor of the porin signal [23, 25]. DegS is present at the inner membrane in a proteolytically inactive conformation. The C-termini of porins bind to the PDZ domain of DegS and convert it into proteolytically active form [23, 30]. As porin C-termini are usually masked in the trimer interface, this signal faithfully reports on the buildup of unassembled porin monomers [31, 32]. Activated DegS cleaves RseA in the C-terminal periplasmic domain ~ 30 aa above the inner membrane. The membrane localized RseA fragment is then recognized by a membrane-spanning RIP protease, RseP, which cleaves RseA in the membrane close to the cytoplasm. Following release to the cytoplasm, ClpXP and other cytoplasmic proteases dissociate the RseA cyto/σ^E complex and degrade RseA cyto, thereby releasing free σ^E that is competent for transcription [33], (R. Chaba, unpublished).

Regulated degradation of RseA enables rapid activation and shut off of σ^E activity on a time scale that is much shorter than the RseA turnover rate [34]. Fast response is possible because of a very tight binding between σ^E and RseA. The slow dissociation of σ^E from RseA cyto *in vitro* ($k_{off} << 10^{-4}$ sec^{-1}; I.Grigorova, unpublished results) suggests that σ^E is released from RseA predominantly by RseA degradation *in vivo*. Because of this, changes in the rate of RseA degradation immediately change the rate of σ^E release from RseA, and therefore the activity of σ^E [35]. σ^E activity is also modulated by alterations in the relative levels of σ^E and RseA [29]. Since these

changes occur on the time scale of RseA half life they should contribute to the delayed phase of the σ^E response.

Proposed mechanism for graded activation of σ^E

Graded activation of σ^E in response to accumulation of porin monomers is wired into the properties of the proteolytic cascade [25]. DegS cleavage of RseA is believed to be the rate-limiting step in RseA degradation. This proposition is based on the low accumulation of RseA cleavage intermediates, and the insensitivity of the pathway to variations in the levels of RseP and cytoplasmic proteases [25, 36, 37] (R. Chaba, unpublished). Since RseA cleavage by DegS is the rate-limiting step in the proteolytic cascade, the rate of RseA degradation is determined by the extent of DegS activation. Activation of DegS, in turn, is limited by the periplasmic porin signal. Therefore, porins directly regulate the rate-limiting step in RseA degradation, enabling the pathway to vary its rate of RseA degradation and thus σ^E activity in accordance with the magnitude of inducing signal.

Sensing a broad range of OMPs signals imposes three important constraints on the players in the proteolytic pathway, each of which is discussed below:

(i) DegS must be in excess over the physiologically relevant range of the unassembled OMPs that can bind to its PDZ domain.

(ii) Activated, DegS initiates degradation of full-length RseA faster than any other protease.

(iii) RseP and cytoplasmic proteases must degrade proteolytic intermediates of RseA faster than the rate of RseA cleavage by activated DegS.

(i) Excess of DegS over periplasmic OMP signal was inferred from the fact that σ^E activity is insensitive to variations in DegS levels, but very sensitive to variations in porin expression [22, 25, 36]. Together these data suggest that DegS activation is limited by the OMP signal.

(ii) Two independent pathways inhibit RseP from cleaving RseA prior to DegS cleavage. First, RseB, a periplasmic protein that binds to the periplasmic domain of RseA (RseA-peri), the gln-rich region of RseA-peri and the PDZ domain of RseP function in a pathway that inhibits RseP activity [25, 38, 39]. Second, DegS independently inhibits RseP [25]. At the moment, complete interactions between all of these players and the two mechanisms that underlie inhibition remain to be determined. The importance of downregulating RseP activity is illustrated by the phenotype resulting from removal of RseB. In cells that lack OmpR, a transcriptional activator of the OmpC and OmpF porin expression, the OMP periplasmic signal is very low. Therefore, in an *ompR* background, σ^E activity is downregulated 20-fold compared to the wt cells. However, removal of *rseB* in an *ompR* background results in over a 4-fold increase in σ^E activity compared to *ompR* cells [25]. This increase in σ^E activity is explained by an increase in the OMP - independent cleavage activity of RseP, which is normally inhibited by RseB.

(iii) Rapid unfolding and degradation of RseA cyto is a challenging task for cytoplasmic proteases, because they are presented with a very tightly bound RseA cyto/σ^E complex. Nevertheless, cytoplasmic proteases can dissociate this complex, and degrade RseA cyto with a half life less than 20 seconds, which is at least 20-fold faster than the rate of full-length RseA cleavage by DegS in wt cells at 30°C (R.

Chaba, unpublished results). ClpXP is the major cytoplasmic protease that degrades RseA-cyto [33], but multiple proteases are involved (R. Chaba, unpublished results).

Decoupling σ^E activation from other pathways

The properties of the proteolytic cascade make σ^E activity sensitive to the OMP signal and simultaneously robust against variations in the availability of RseP and cytoplasmic proteases. RseP has a potential ability to cleave a wide range of membrane proteins [40], although at the moment other substrates in *E. coli* are not known. Likewise, the main cytoplasmic protease that degrades RseA cyto, ClpXP, is known to degrade a number of regulatory substrates, including the general stress sigma, σ^S [41]. However, degradation of other substrates by RseP and ClpX should not perturb σ^E activity as long as RseA cleavage by DegS remains the slowest step in the proteolytic cascade. The rapid degradation of RseA cyto should buffer σ^E activity from the substrate load of ClpXP and other ATP-dependent proteases. Possibly, there are some conditions of extreme stress where rapid degradation of RseA fragments is prevented. In that case, the σ^E induction range controlled by the proteolytic cascade will decrease. However, in general, this transmembrane signaling pathway should be largely uncoupled from the state of other intracellular processes that utilize cytoplasmic proteases (such as degradation of σ^S) or RseP.

Other stresses in the periplasmic space

In addition to controlling outer membrane integrity, the σ^E regulon is believed to diminish general stress in cell envelope. Indeed, cells that lack certain periplasmic

folding catalysts, produce abnormal LPS, or are subjected to high temperatures or ethanol further induce σ^E activity [22, 42-47]. However, although the transmembrane pathway that regulates σ^E in accord to the OMPs folding state is largely understood, much less is known about other possible signals that induce σ^E. One of the possibilities is that various envelope stresses either directly perturb OMP maturation or titrate away OMP folding catalysts thus increasing the flux of unassembled OMPs in the envelope. Alternatively (or in addition), unfolded proteins could activate σ^E via OMPs –independent pathway that does not require activation of DegS. Since RseP possesses inherent ability to cleave full-length RseA without prior cleavage by DegS [40], unidentified periplasmic signals could possibly upregulate RseP-dependent initiation of RseA degradation, for example, by titrating away RseB [25]. In that case OMPs and other periplasmic signals would converge on RseA degradation, resulting in additive σ^E activity. Even if not present in *E. coli*, this proposed mechanism could be exploited by other evolutionarily related bacteria that use similar RIP signaling pathways.

Summary of σ^E pathway in E. coli

In *E. coli*, the transmembrane signaling pathway that activates σ^E in response to unassembled porins in the envelope implements a graded σ^E response to a wide range of OMP signal. The key to this mechanism is (i) sequential proteolysis of the anti-sigma factor by DegS, RseP and the cytoplasmic proteases with the rate-limiting step proportional to amount of DegS, activated by the periplasmic OMP signal, and (ii)

correlation between transcriptional activity of σ^E and the rate of RseA degradation (Fig. 1-1).

The AlgU(T) pathway in *Pseudomonas aeruginosa* (*P. aeruginosa*)

The transmembrane signaling pathway that activates σ^E in *E. coli* is highly conserved in members of gamma (γ) subdivision of proteobacteria: orthologues of σ^E and its regulators, RseA, RseB and RseC (a protein whose function in the pathway is still unknown), are usually transcribed in a single operon as they are in *E. coli*. In addition, orthologues of DegS/HtrA and RseP are present [47]. However, very few studies have examined either the organization of the signal-transduction pathway or the functions regulated by σ^E orthologues in other γ-proteobacteria. The notable exception is *P. aeruginosa*, where overexpression of AlgU (T), its σ^E orthologue, is of profound medical importance. Cystic fibrosis (CF) is the most common lethal genetic disease in Caucasians. Lethality is usually caused by chronic colonization of the lungs by mucoid *P. aeruginosa* [48, 49]. Mucoidy results from upregulation of AlgU and the consequent overexpression of the enzymes that produce alginate, a thick mucopolysaccaride layer that surrounds the organism and leads to the formation of biofilms [50-57]. Interestingly, comparison of the *algU* and σ^E pathways suggests that the two may differ significantly both in function and in regulation.

Analysis of the σ^E regulon in *E. coli* K12 and its very close relatives indicated that the conserved function of the regulon is to ensure the synthesis, assembly and homeostasis of two important outer membrane constituents, porins and LPS. Interestingly, there was also a variable, organism-specific component of the regulon

with possibly pathogenesis related functions [24, 58]. Although most AlgU genes function in the envelope, the AlgU regulon does not appear to be involved in OMP or LPS maintenance. Instead, the theme of virulence related functions appears to dominate the AlgU regulon [59-61]. The most notable AlgU virulence determinant is a large operon of 11 genes devoted to alginate biosynthesis, which aids in colonization of the lung [57, 61, 62]. In addition, the AlgU regulon encodes several proinflammatory lipoproteins and adhesins, and directly or indirectly regulates elastase and a metalloprotease important in extracting iron [59, 60]. AlgU does maintain two transcriptional regulatory connections characteristic of the σ^E regulon: it transcribes itself and its negative regulators as a single operon: *algU*, *mucA* (*rseA*), *mucB* (*rseB*), *mucC* (*rseC*) and *mucD* (*htrA*) and it transcribes the gene encoding σ^{32}, which carries out the cytoplasmic heat shock response [63-65]. In conclusion, although the AlgU and σ^E signaling pathways are related, there are almost no genes in common between the two regulons and the key functions of their regulons seem to be different [24, 58-61].

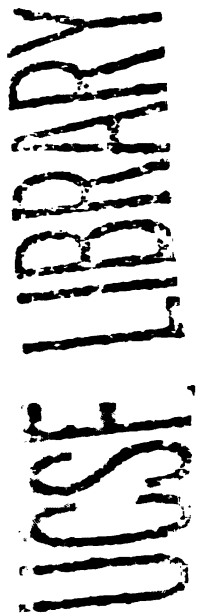

Are the signals that induce σ^E and AlgU related? AlgU is induced in response to extreme temperature, as is σ^E. Since σ^E is the main sigma factor transcribing σ^{32} under these conditions in *E. coli*, and it is known that AlgU also transcribes σ^{32}, a similar role might be suggested for AlgU [42, 43, 46, 65, 66]. In contrast, induction of AlgU by unassembled *P. aeruginosa* porins is unlikely, as the AlgU response does not appear to maintain porin homeostasis. Reactive oxygen species or their products may be among the unidentified inducers of the AlgU pathway, since strains lacking AlgU are sensitive to oxidative stress [67-69].

The signal inducing AlgU during colonization of the lungs of CF patients has been carefully studied. Most *P. aeruginosa* strains isolated from CF lungs have mutations in the periplasmic domain of transmembrane anti-sigma factor, MucA [70-72]. Truncations in MucA periplasmic domain activate AlgU by increasing the rate of degradation of MucA [73]. Importantly, these mutations are induced by high H_2O_2, a condition that mimics conditions encountered during growth in the lung. This high mutation rate is encoded in the sequence of MucA itself. The periplasmic domain of MucA has a stretch of 5 G's located between positions 429 and 433 followed immediately by a CGCC sequence. The most frequent MucA mutation is a deletion within this G stretch. Two features of this sequence promote mutation. First, homopolymeric stretches lead to slipped strand mispairing [74]. Second, the CGCC sequence following the G-tract results in a GGCGCC sequence. This is the recognition sequence of the NaqI restriction enzyme, and is a well-known hot spot for frameshift mutations in *E. coli* [75]. Therefore it is tempting to suggest that this region of the periplasmic site of MucA have evolved into a "hot spot" that increases probability of inducing mutations in MucA in response to conditions found in lungs. Induction of AlgU in the lung, resulting from mutational alterations of MucA, appears to be irreversible [71], although during passage of the isolates in the laboratory it is frequently downregulated by accumulating suppressors [76]. Perhaps, when *P. aeruginosa* transitions into biofilm growth mode in the lungs, it does not require graded, reversible induction of the response, the very properties which are essential for *E. coli* to maintain economical homeostasis of OMPs.

How is the signal from the MucA mutants transmitted? The available evidence suggests that this signal is transmitted by a proteolytic cascade, as is true for induction of σ^E, although the proteases have not been identified [76]. The primary evidence for protease involvement comes from the phenotype of the MucA mutants [53-55, 71] and from the identity of one of the common mutations that suppresses mucoidy by inactivating Prc, a periplasmic protease [76]. Interestingly, this suppressor only affects mucoidy resulting from a MucA truncation but not that due to a *mucB* mutation. Taken together, the phenotype of these mutants leads us to suggest that they work by increasing the activity of the *P. aeruginosa* RIP homologue, by analogy to changes that activate the RIP protease, RseP, in degradation of RseA in *E. coli* [36, 37]. In *E. coli,* removal of the Gln-rich periplasmic region of RseA or deletion of RseB allows RseP to function without prior cleavage by DegS [25, 38, 39]. The periplasmic truncations of MucA and inactivation of MucB that increase AlgU activity could have similar effects on the *P. aeruginosa* RIP homologue [54, 71]. In this regard, the suppressor phenotype of Prc deletion suggests that at least some MucA truncations may need to be processed further by Prc to remove all inhibitory effects of MucA on the RIP protease [76]. This effectively allows high expression immediately after the initial mutation so that the biofilm is formed rapidly, with potential for down regulation by mutation later on. Why haven't mutations inactivating the RIP protease been identified among suppressor mutations? So far, the search for suppressor mutations was carried out only in the strains where alginate production was eliminated under some growth conditions [76, 77]. However, RIP suppressor mutations might shut off AlgU activity under the most conditions, as is the

case with inactivation of RseP in *E. coli* [36, 37]. It is currently unclear whether a signaling event, analogous to activation of DegS, induces this cascade under other circumstances. However, should this aspect of the *E. coli* signal-transduction pathway be preserved, the signal does not activate either of the degS/htrA orthologues in *P. aeruginosa*. Deletion of a*lgW* or *mucD increases* rather than suppresses AlgU activity [63]. These two proteases might directly inhibit the activity of the *P. aeruginosa* RIPs protease [25] or they may be required for elimination of periplasmic signals that induce AlgU activity.

In summary, *P. aeruginosa* σ^E regulates different functions in the cell envelope than *E. coli* σ^E and is probably activated by different kinds of signals. Although we suggest that this transmembrane pathway also exploits RIPs to transmit the signal, its signaling properties are very different, at least under well studied conditions of lung colonization in CF patients.

P. aeruginosa is not the only example where a σ^E orthologue plays a role in pathogenesis. Transcriptional activity of extracytoplasmic function sigma factors (ECFs) related to σ^E have been implicated in aiding virulence in an number of other gram negative and gram positive bacterium, including *Salmonellae typhimurium*, *Vibrio cholerae*, *Mycobacterium tuberculosis*, *nontypeable Haemophilus influenzae*, *Actinobacillus pleuropneumoniae, and Burkholderia pseudomallei* [78, 79].

RseP in *Vibrio cholerae* (*V. cholerae*)

V. cholerae contains the RIP protease YaeL (RseP) [80]. Interestingly, this protease may be involved in two distinct signal transduction cascades in this

organism. First, both DegS and YaeL have been implicated in the σ^E response in that organism [80], which is similar to the response in *E.* coli [36, 37]. Second, YaeL, but not DegS, is implicated in regulating one of the transcriptional activators that initiates virulence gene expression [80]. In this latter case, YaeL participates in the degradation of TcpP, one of two membrane spanning transcriptional activators that collaborate to transcribe ToxT, which is the direct transcriptional activator of the cholera toxin and the toxin co-regulated pilus [81-88] (Fig. 1-3). TcpP is an intrinsically unstable protein, which is stabilized by association of its periplasmic domain with TcpH [85]. Cells lacking TcpH have little TcpP and low ToxT activity. However, when cells lack YaeL in addition to TcpH, a transcriptionally active, smaller TcpP protein accumulates, which is still membrane localized. By analogy to the σ^E protease cascade, this finding suggests that TcpH protects TcpP from another protease that cleaves TcpP prior to YaeL. However, the initial protease in the pathway is not a DegS orthologue [80]. The YaeL pathway mediating degradation of TcpH may be active under conditions requiring a rapid switch to non-virulent gene expression. This is the only case to date where a single RIP protease is thought to participate in two distinct signal-transduction pathways. Cross-talk between the two pathways is prevented by utilizing distinct upstream proteases to receive the signal.

Since this RIP pathway is involved in the switch to virulence, TcpP activation is likely to be a threshold type of response. In agreement with this hypothesis under experimental conditions tested a product of TcpP transcriptional activity, TcpA, accumulated to an approximately the same amount independently of variation in

TcpP levels, but was completely absent in the absence of detectable amounts of TcpP [80].

Rυ2869c in *Mycobacterium tuberculosis* (*M. tuberculosis*)

In M. tuberculosis, a facultative intracellular pathogen that grows inside macrophages, the RseP orthologue, Rυ2869c, appears to be involved in regulation of cell envelope virulence determinants [89]. An emerging model is that the extractable lipids of the cell envelope of M. tuberculosis modulate the host immune response or alter intracellular trafficking, thereby being direct effectors of pathogenesis [90-95]. Rυ2869c was shown to affect some of these lipids, by controlling the extractable mycolic acid composition in the cell envelope and by regulating transcription of various lipid biosynthetic and lipid-degrading genes [89]. However, the downstream transcription factors that are regulated by Rυ2869c still remain to be determined.

The YluC and SpoIVFB pathways in *Bacillus subtilis* (*B. subtilis*)

YluC

YluC functions in the signal transduction pathway that regulates σ^W activity [96]. σ^W controls transport processes and detoxification, and is induced by a variety of stresses, including alkaline shock, salt shock, phage infection and antibiotics that affect cell wall biosynthesis [97-101]. σ^W activity is controlled by the regulated degradation of its membrane spanning antisigma factor RsiW, in response to stress [96]. Analogously to the mechanism of RseA degradation, RsiW is cleaved sequentially by at least two proteases. Full length RsiW (21 kDa) is first cleaved by

an unidentified protease to generate a 14 kDa fragment. The smaller fragment is then cleaved by the RIP protease, YluC. Most likely, the cytoplasmic domain of RsiW generated by YluC cleavage is degraded by cytoplasmic proteases, leading to σ^W release, as is the case in *E. coli*. This system retains two salient features of the *E. coli* σ^E signal-transduction pathway: 1) As in *E. coli*, the first cleavage event is the one that is stress signal-dependent. This is based on evidence that alkaline shock results in the accumulation of the initial 14kD fragment when YluC is absent. Interestingly this cleavage is not performed by an HtrA/DegS orthologue. 2) As in *E. coli*, efficient cleavage of RsiW by the RIP protease requires removal of the extracytoplasmic domain by the initial cleavage event. It remains to be established which inhibitory interactions prevent YluC cleavage of full length RsiW. It will be of great interest to examine the performance features of this system to see if they continue to conform to the paradigm set up by the *E. coli* σ^E signal-transduction pathway.

SpoIVFB

SpoIVFB regulates a late step in sporulation, a complex developmental pathway triggered jointly by high density of the culture and starvation conditions leading to a drop in intracellular GTP concentrations. During sporulation, two specialized cells, the larger mother cell and the smaller forespore are generated by unequal cell division (reviewed in Errington, 2003 [102]). These cells initially lay side-by-side; subsequently the forespore is engulfed by the mother cell. Successful spore formation requires tight coordination of the gene expression programs of the mother cell and forespore (reviewed in Kroos, 2000[103]; Piggot, 2002). This task is

accomplished by a cascade of cell type-specific σ factors: σ^F, σ^E, σ^G and σ^K triggered sequentially in the mother cell and the forespore by signals from the other cell type. σ^K, the final σ factor in this cascade, is a mother cell specific transcription factor, which controls expression of the spore coat proteins deposited around the engulfed forespore. σ^K is synthesized as an inactive protein with a 20 amino acid N-terminal prosequence that facilitates association of pro-σ^K with the membranes [104-106]. SpoIVFB removes the prosequence, thereby releasing active σ^K into the cytoplasm of the mother cell [6, 107-109]. The appearance of active σ^K is approximately coincident with completion of engulfment. Timing is critical, as premature activation of σ^K has a detrimental effect on sporulation [104]; tight control by two mechanisms accomplishes this task (Fig. 1-4).

In the first mechanism, the catalytic activity of SpoIVFB is controlled by 2 transmembrane proteins that form a complex with SpoIVFB: BofA and SpoIVFA. BofA directly inhibits SpoIVFB; SpoIVFA stabilizes and positions BofA; it is currently unclear whether SpoIVFA itself contributes directly to SpoIVFB inhibition [7, 109-115] (Fig. 1-4, left). At least one, and possibly two proteolytic events remove these inhibitory interactions thereby releasing the RIP protease, SpoIVFB, so that it can activate σ^K. The serine protease SpoIVB, which is delivered from the forespore, cleaves SpoIVFA, based on cleavage studies performed on proteins expressed in an E. coli transcription-translation extract [116-118]. This cleavage event is thought to disrupt the inhibitory complex. In addition, the mother cell serine protease, CtpB, which fine-tunes this event, may degrade BofA [119, 120]. The proteolytic event(s) preceding RIPs seem to act as a checkpoint that coordinates gene expression in both

the mother cell and the forespore with engulfment. The protease CtpB is expressed only after initiation of sporulation upon activation of σ^E in the mother cell [119]. In turn, the forespore SpoIVB serine protease is produced in high amounts only when σ^G is active in the forespore [104, 116, 121]. As σ^G activity is dependent on activity of σ^E and engulfment, removal of the inhibitory complex that prevents σ^K activation is indirectly coupled to engulfment.

This complex mechanism of SpoIVFB inhibition in *B. subtilis* contrasts with the simpler mechanism of RseP inhibition in E. coli. For RseP, the signal comes only from the periplasmic compartment, rather than from two different cells. RseP requires only a single cleavage event to remove inhibition, whereas it is proposed that two cleavages are necessary to activate SpoIVFB [36, 37, 120]. Also, DegS cleavage of the anti-sigma factor simultaneously abolishes all inhibition of RseP [38, 39], whereas inhibition of SpoIVFB appears to be removed sequentially. In addition to these differences, both the nature of developmental process and the importance of its proper timing suggest that σ^K activation should take place in "all or none" fashion, rather than be graded as in E. coli. From this perspective, it is interesting that DegS is always present in the cell, waiting for the OMP signal, while SpoIVB and CtpB are expressed only during sporulation prior to induction of σ^K.

Recent evidence suggests that SpoIVFB is also inhibited by a second mechanism, which is directly coupled to the engulfment process [122] (Fig. 1-4, right). When cells lack BofA, the inhibitory complex is inoperative [104, 112]. Hence, the need for σ^G activity and the forespore serine protease SpoIVB is bypassed. However, mutants defective in engulfment still lack σ^K activity, indicating that the RIP protease

SpoIVFB is still unable to cleave pro-σ^K even in the absence of the known inhibitory complex. The mechanism for this inhibition is unknown. A molecular understanding of the complex machine that allows irreversible activation of σ^K will be an important contribution to our understanding of how the activity of RIP proteases is controlled.

MmpA in *Caulobacter crescentus* (*C. crescentus*)

MmpA is involved in the sequential degradation of PodJ, a transmembrane protein that aids in the localization of several polar organelles [123]. Interestingly, PodJ has two functional forms: $PodJ_L$ (full-length PodJ), and $PodJ_S$, (a smaller cleavage product lacking most of the periplasmic domain of the protein), each controlling distinct aspects of polar organelle development at different times during the cell cycle [124, 125]. $PodJ_L$ is produced in predivisional cells and $PodJ_S$ appears near division, generated by an unknown protease that is not an orthologue of DegS [123] (Fig. 1-5). The protease or the activating signal that induces first cleavage must appear in a cell-cycle dependent way. MmpA then cleaves $PodJ_S$ to initiate its degradation at the swarmer to stalked cell transition [123]. As MmpA is present constitutively throughout the cell cycle, it coexists with $PodJ_S$ until a particular point in the cell cycle. Therefore, in this case, cleavage at the periplasmic face of the protein is not sufficient to allow efficient cleavage by the RIPs protease. Instead, MmpA cleavage of $PodJ_S$ must be prevented by inhibitory mechanisms that are removed in a cell-cycle dependent manner. Both MmpA and the unidentified protease involved in $PodJ_L$ cleavage, control the availability and particular domain structure of the protein at certain points of the cell cycle. That is different from the role of DegS

and RseP proteases in *E. coli*, which together control the rate of RseA degradation rather than its availability in the cell.

Concluding remarks

In this review, we have performed two different comparisons of systems in diverse bacteria that utilize transmembrane signaling. First, we examined a particular transmembrane signaling pathway, the *E. coli* σ^E pathway to ask whether the components of the pathway and its organization are likely to be conserved in other organisms using this pathway. Second, we examined pathways that utilize RIPs in their transmembrane signaling, to assess the commonalities and differences in regulating the activity of such proteases. Where sufficient mechanistic information exists, these comparisons reveal a divergence in mechanism that can be rationalized in light of the functions of the regulons.

Although various players of the σ^E activation pathway are conserved in many γ-proteobacteria, and orthologous σ's often regulate cell envelope functions, the inducing signals and signal implementation could be quite different. For example, in *P. aeruginosa*, the σ^E orthologue, AlgU does not appear to regulate OMP homeostasis. In the lungs of CF patients AlgU promotes virulence by aiding the bacterial switch into a biofilm growth mode. At least under those conditions, AlgU is activated irreversibly. Since many ECF sigma factors are involved in establishing virulence, a developmental decision, the induction of these pathways may be much less graded compared to that in *E. coli*. In those pathways, the role played by DegS in E. coli as a gradual sensor of OMPs signal, could possibly be omitted. It will be well

worthwhile to examine this issue in pathogenic organisms more closely related to *E. coli*.

Bacterial RIP proteases are largely used for proteolysis of transmembrane proteins. Regulation of these RIP proteases is correlated with the purpose of the response. For example, whereas in *E. coli*, RIP proteolysis of RseA increases gradually in concert with an increase in the unassembled porin signal and is reversible (Fig. 1-1), in *B. subtilis* RIP of pro-σ^K is likely to be turned on irreversibly in an all or none fashion at a desired point during sporulation (Fig. 1-4).

Many RIP proteases appear to require preliminary cleavage of a transmembrane protein by another protease, as was first demonstrated for S2P in eukaryotic cells. Likewise, in *E. coli*, prior cleavage by DegS is normally required for RseA degradation by RseP. Inhibition of RseP cleavage is mediated in part by the periplasmic domain of RseA and by RseB. If either is removed, RseP can cleave RseA in an unregulated, DegS-independent fashion. These experiments indicate that preliminary cleavage of a transmembrane protein by another protease is not prerequisite for intramembrane proteolysis and that additional mechanisms of controlling that cleavage might exist. Indeed, this has been demonstrated for SpoIVFB in *B. subtilis*, whose activity is inhibited by a complex of transmembrane proteins, removed in a signal-specific manner. In this case, upstream proteolytic events targeted the inhibitory proteins rather than the one cleaved by RIPs. Indeed, one could imagine scenarios in which inhibitory proteins are removed by mechanisms other than proteolysis, although such cases have not yet been identified experimentally. None-the-less, preliminary cleavage within the extracytplasmic

domain of the same protein cleaved by a RIPs protease is common and is most likely exploited for regulation. However, even when sequential proteolysis occurs, cleavage by the first protease is not necessarily rate-limiting as it is in *E. coli* as demonstrated by the sequential degradation of PodJ in *C. crescentus* (Fig. 1-5). Therefore it appears as if sequential cleavage of transmembrane proteins may be adapted to a variety of different regulatory scenarios.

We expect that accumulation of knowledge about RIPs signaling pathways and cellular functions that they affect will help cross-comparison between various organisms, and shed new light on the evolutionary adaptation of the existing functional blocks for implementing new pathways and functions.

Figure Legends:

Figure 1-1. σ^E pathway in *E. coli* and homeostasis of OMPs in the periplasm.

The rate limiting step in degradation of RseA is controlled by the unassembled monomers of OMPs in the periplasm. RseA proteolysis results into release of σ^E, which afterwards either rebinds to RseA or forms a complex with RNA polymerase ($E\sigma^E$). $E\sigma^E$ promotes transcription of the target genes; the products of those assist OMPs maturation in the periplasm and insertion into the outer membrane.

Figure 1-2. Proteolysis of RseA by a protease cascade.

In wild type cells in the absence of the OMP signal RseA is not degraded. OMP monomers bind to the PDZ domain of DegS and convert it into the proteolytically active conformation. Activated DegS cleaves RseA in the periplasmic domain. RseP then cleaves a fragment generated by DegS from the membrane/cytoplasmic side. A complex of RseA cyto/σ^E is released from the membrane into the cytoplasm, dissociated, and RseA cyto is degraded by ClpXP and other cytoplasmic proteases.

Figure 1-3. Current model of YaeL (RseP) signaling pathway in *V. cholerae*.

YaeL mediates degradation of TcpP, transcriptional activator of *toxT* gene. Under virulence inducing conditions TcpP proteolysis is inhibited by TcpH. Membrane-localized TcpP turns on transcription of ToxT. Under virulence noninducing conditions unidentified protease cleaves TcpP. The fragment is then cleaved by YaeL. A cytoplasmic fragment of TcpP can not activate transcription of ToxT. ToxT synthesis is turned off.

Figure 1-4. Current model of SpoIVFB signaling pathway in *B. subtilis*.

Proteolytic activity of SpoIVFB is inhibited by a protein complex that consists of BofA and SpoIVFA. During sporulation a cascade of cell type-specific σ factors: σ^F, σ^E, σ^G and σ^K is triggered sequentially in the mother cell and the forespore by signals from the other cell type. σ^K is synthesized as an inactive protein with prosequence that localizes it to membrane. After initiation of sporulation σ^E turns on transcription of protease CtpB in the mother cell. CtpB fine-tunes activation of SpoIVFB, possibly via degradation of BofA. The forespore SpoIVB protease is produced in high amounts when σ^G is active in the forespore. SpoIVB is then delivered from the forespore to cleave SpoIVFA. As σ^G activity is dependent on activity of σ^E and engulfment, removal of the inhibitory complex of SpoIVFB that prevents σ^K activation is indirectly coupled to engulfment. SpoIVFB is also inhibited by a second mechanism, which is directly coupled to the engulfment process. After all inhibitory mechanisms are removed, SpoIVFB cleaves the prosequence, thereby releasing active σ^K into the cytoplasm of the mother cell.

Figure 1-5. Current model of MmpA signaling pathway in *C. crescentus*.

Protein PodJ is MmpA is a transmembrane protein that aids in the localization of several polar organelles during the cell cycle of *C. crescentus*. $PodJ_L$ (full-length PodJ) is produced in predivisional cells (PD). $PodJ_L$ plays a role in pili biogenesis. During cell division $PodJ_L$ is cleaved by unidentified protease. A smaller cleavage product lacking most of the periplasmic domain of the protein, $PodJ_S$, plays a role in chemotaxis and holdfast formation in the swarmer cell (SW). MmpA then cleaves

$PodJ_S$ to initiate its degradation at the swarmer to stalked cell (ST) transition. MmpA is present constitutively throughout the cell cycle. MmpA cleavage of $PodJ_S$ must be prevented by inhibitory mechanisms that are removed in a cell-cycle dependent manner.

Figure 1-1

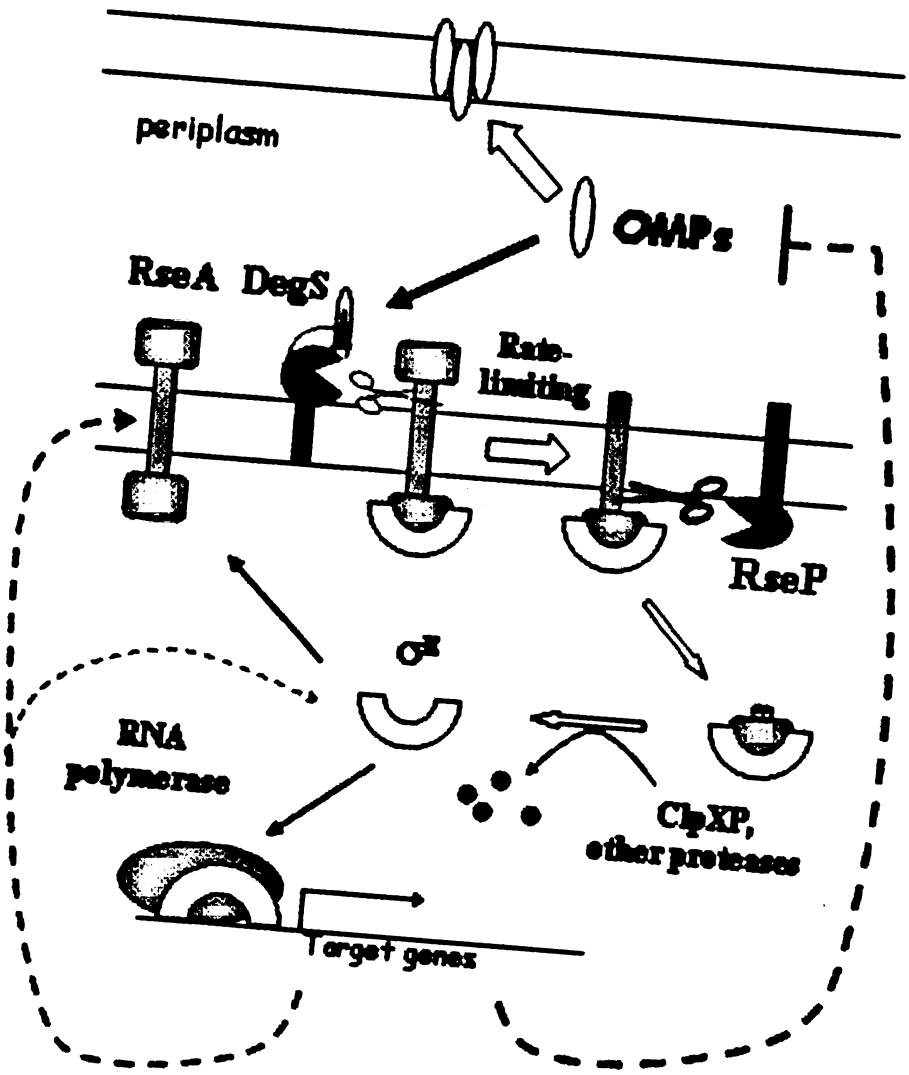
periplasm
OMPs
RseA
DegS
Rate-limiting
RseP
σE
RNA polymerase
ClpXP, other proteases
Target genes

Figure 1-2

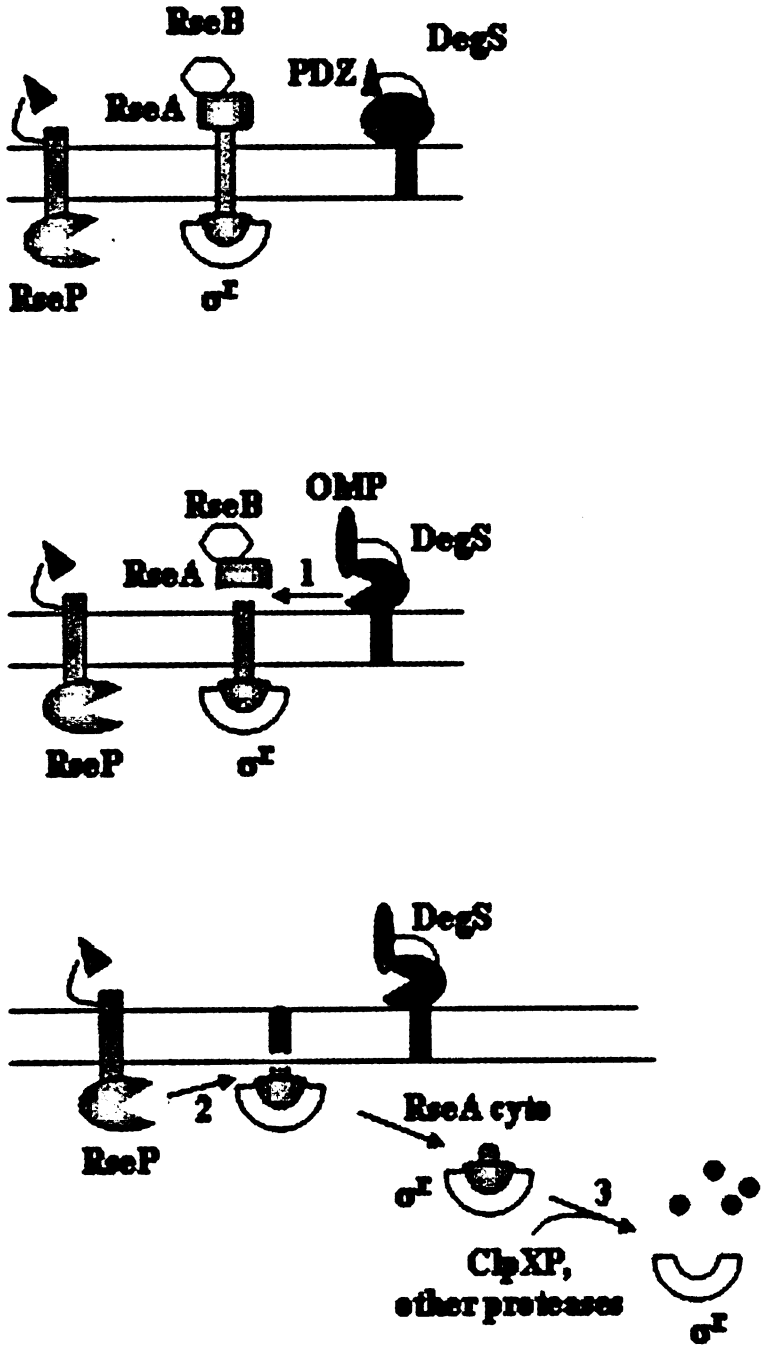

Figure 1-3.

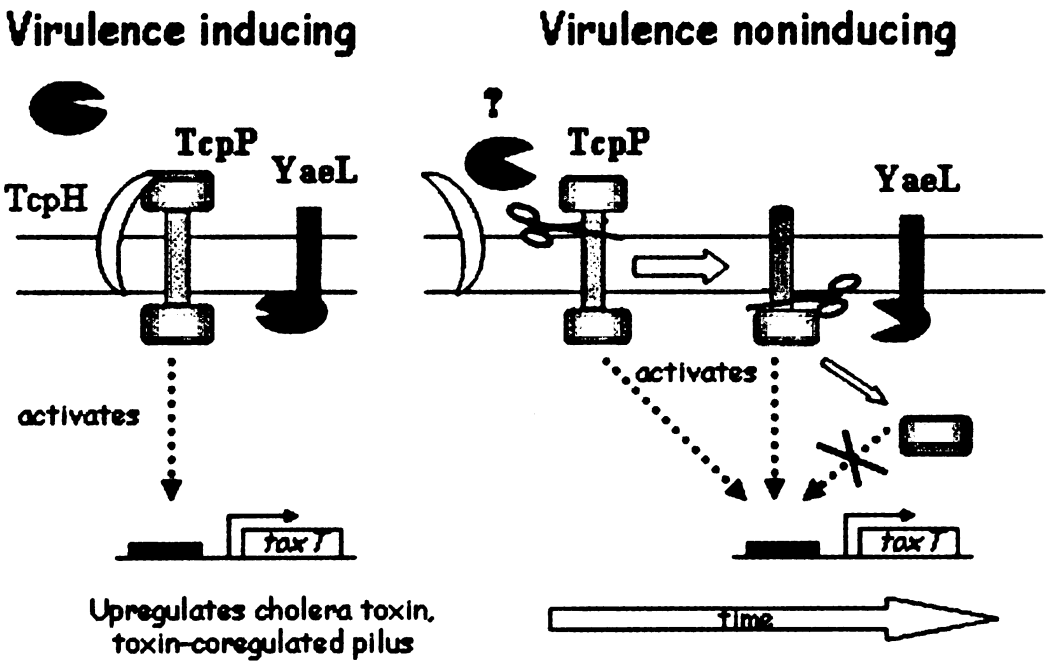

Figure 1-4.

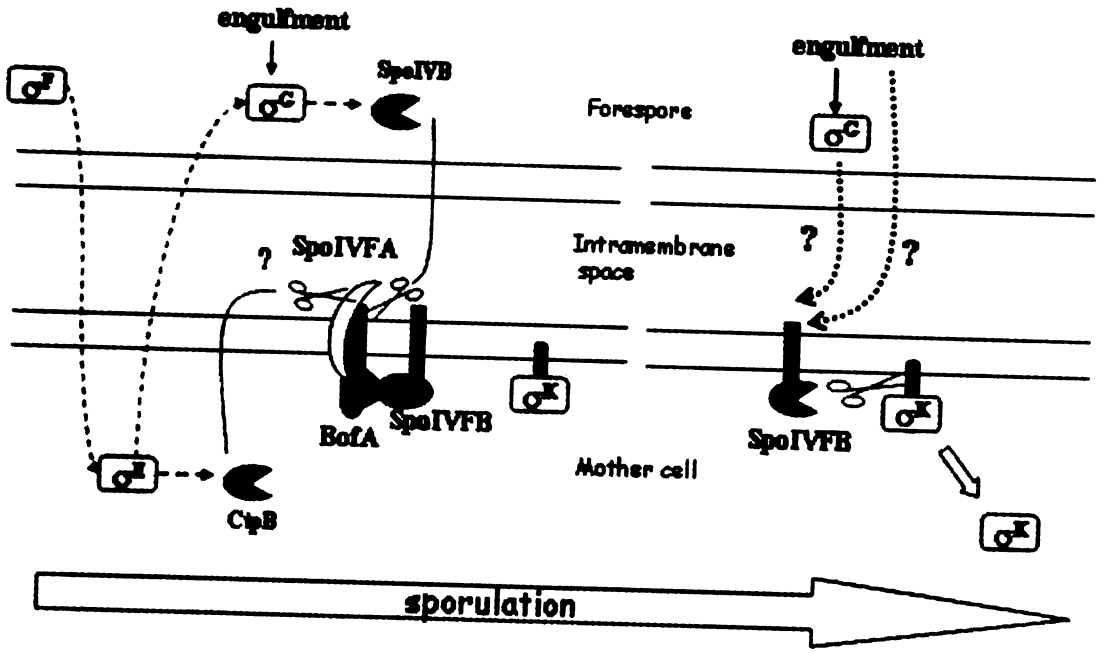
engulfment
SpoIVB
Forespore
engulfment
?
SpoIVFA
Intramembrane space
?
?
BofA
SpoIVFB
SpoIVFB
Mother cell
CtpB
sporulation

Figure 1-5.

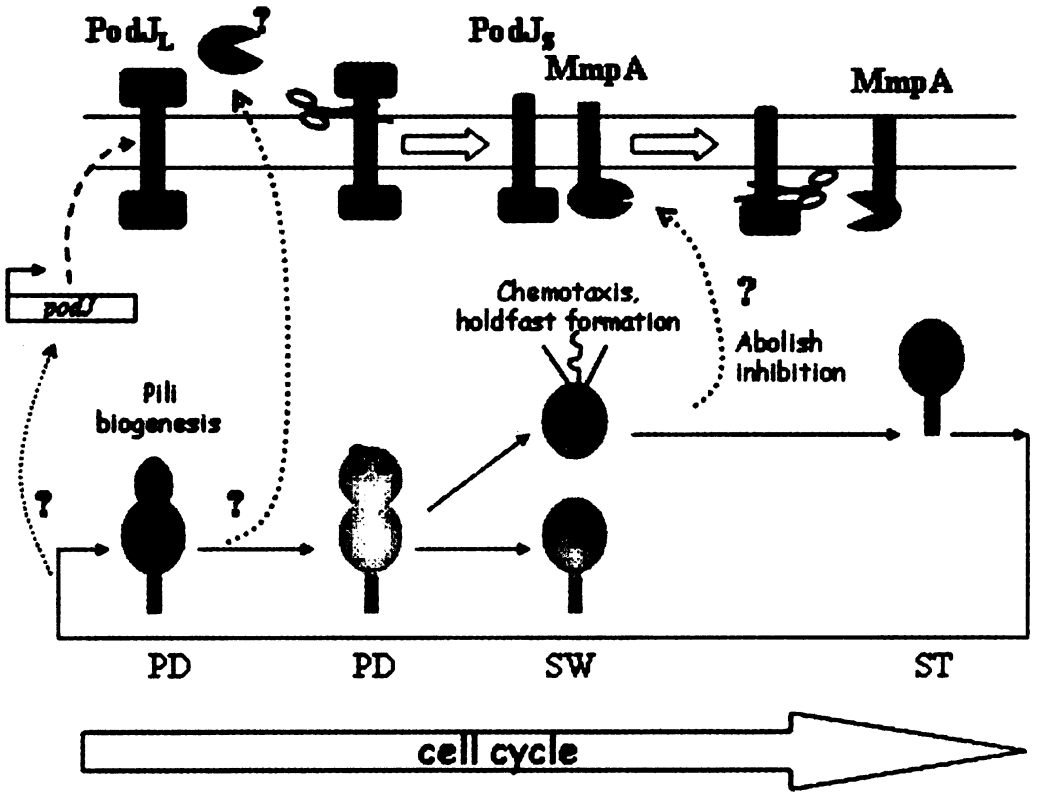

Chapter Two

Regulation of the alternative sigma factor, σ^E, during initiation, adaptation, and shut-off phases of the extracytoplasmic heat shock response in *Escherichia coli*.

Summary

The alternative sigma factor, σ^E, is activated in response to stress in the extracytoplasmic compartment of *Escherichia coli*. Here we show that σ^E activity increases upon initiation of the stress response by a shift to elevated temperature (43 °C) and remains at that level for the duration of the stress. When the stress is removed, by a temperature downshift, σ^E activity is strongly repressed and then slowly returns to levels seen in unstressed cells. We provide evidence that information about the state of the cell envelope is communicated to σ^E primarily through the regulated proteolysis of the inner membrane antisigma factor RseA, as the degradation rate of RseA is correlated with the changes in σ^E activity throughout the stress response. However, the relationship between σ^E activity and the rate of degradation of RseA is complex, indicating that other factors may cooperate with RseA and serve to fine-tune the response.

Introduction

Protein denaturation and aggregation resulting from exposure to elevated temperature or other stresses present a severe problem for cells. However, the detrimental effects of these stresses are combated by highly conserved responses that increase the synthesis of the heat shock proteins, whose function is to remove or refold damaged cellular proteins [126, 127]. The transcription factors that control heat shock gene expression are subject to complex regulatory mechanisms to ensure that the response is rapidly induced following exposure to stress, is maintained when the cells are subject to continuous stress, and is down-regulated when cells are returned to the unstressed state [126-131] .

In the bacterium *Escherichia coli*, individual stress responses exist to maintain homeostasis in the cytoplasm and the cell envelope. The alternative sigma factors σ^E and σ^{32} control the cell envelope and cytoplasmic heat shock responses, respectively [42, 43, 45, 132-135]. The σ^{32}-dependent stress response has been extensively characterized. The stability, activity, and rate of translation of σ^{32} are all subject to regulation depending upon the circumstance [127, 136-142]. This complex network of regulatory interactions modulates the amount and activity of σ^{32} so that the amount of active σ^{32} is optimal for the needs of the cell.

The cell envelope plays an essential role for the bacterium providing a barrier between the cell and the environment, determining cellular morphology, and maintaining the structural integrity of the cell. Although σ^E is crucial for maintaining the integrity of the cell envelope during the stress response, little is known about its regulation. σ^E is activated both by general stress inducers, such as a heat shock, which

lead to protein unfolding in both cellular compartments and by specific inducers, such as overexpression of porins, which lead to accumulation of unfolded proteins solely in the cell envelope [22, 42-44, 64, 143]. Once activated, σ^E transcribes a set of genes primarily targeted to the cell envelope that encode periplasmic proteases, folding catalysts, several key enzymes in the biosynthetic pathways of cell envelope constituents and a number of lipoproteins [24, 58].

Since σ^E resides in the cytoplasm, it cannot directly sense damage in the cell envelope. The key protein responsible for directly communicating damage in the envelope to σ^E is the antisigma factor RseA. RseA is an inner membrane protein with a single transmembrane spanning segment. The N-terminal cytoplasmic domain of RseA binds to σ^E and inhibits the activity of σ^E and its C-terminal periplasmic domain binds RseB, a weak inhibitor of σ^E activity [26, 27]. The interaction between RseA and σ^E must be disrupted for σ^E to bind to RNA polymerase and initiate transcription. σ^E, RseA and RseB are all members of an operon that is transcribed by σ^E itself [26, 27, 42]. This autoregulatory loop allows the cell to tightly control σ^E activity since upon activation both σ^E and its inhibitors are transcribed together.

Previous studies on the regulation of σ^E activity focused solely on the initiation phase of the stress response [29]. These studies indicated that the major pathway for releasing σ^E from RseA is through the regulated proteolysis of RseA carried out by the inner membrane proteases DegS and YaeL [29, 36, 37]. Here we investigate the regulation of σ^E activity during all phases of the stress response: initiation, adaptation, and shut-off. We find that σ^E activity increases during the initiation of the stress response and remains elevated as cells are maintained under stress during the

adaptation phase of the response. During the shut-off phase of the response when the stress is removed, σ^E activity drops to a level below that observed under normal conditions and then slowly recovers. Our earlier experiments indicated that increased proteolysis of RseA is responsible for the increase in σ^E activity upon initiation of the stress response [29, 36, 37]. Therefore, we examined whether alterations in the proteolysis of RseA can account for the changes in σ^E activity during the other phases of the response or if additional modes of regulation are utilized. We find that σ^E activity is correlated with the degradation rate of RseA during all phases of the response indicating that RseA degradation is the primary means by which information about the state of the cell envelope is communicated to σ^E in the cytoplasm. However, changes in the rate of RseA degradation are not sufficient to account for all of the observed changes in σ^E activity, indicating that other regulatory mechanisms are likely to be involved.

Results

In this paper, we explore the relationship between the activity of σ^E and the degradation of RseA during the different phases of the stress response: the initiation phase, after a change in the growth temperature from 30 °C (no stress) to 43 °C (stress); the adaptation phase, as cells are maintained at 43 °C for longer periods of time; and the shut-off phase, after a change in growth temperature back to 30 °C from 43 °C. During each phase we measure the changes in σ^E activity by determining the rate of synthesis of two members of the σ^E regulon, DegP and RseA. We then analyze the contribution of RseA degradation to the regulation of σ^E by measuring changes in the degradation rate of RseA throughout the stress response. We performed these experiments in the MG1655 strain of E. coli, which grows more reproducibly at 43 °C than the MC1061strain used in our earlier work [29].

σ^E activity during initiation and adaptation

σ^E activity increases rapidly after a growing culture is shifted from 30 °C to 43 °C. Within 10 minutes, the synthesis rates of both DegP and RseA are 2 to 2.5-fold higher than at 30 °C (Fig. 2-1) and the kinetics of induction for both proteins are similar within the error of the experiment. As cells continue growing at 43 °C, the synthesis rates of both proteins remain 2 to 2.5-fold higher than those during steady state growth at 30 °C. Our results are consistent with the approximately 3-fold increase in σ^E -dependent transcription previously observed for these genes following a heat shock [42]. These elevated rates are maintained even after 18 hours of growth at 43 °C in cells that have been grown overnight and subcultured at high temperature (Fig.

2-1). DegP expression can also be induced by the Cpx two-component regulatory system [144, 145]. However, σ^E, not Cpx, is responsible for the induction of DegP synthesis observed after temperature shift as a strain lacking Cpx shows the same 2.0 –2.5 fold induction of DegP as the wild-type strain (data not shown). Taken together, these data show that σ^E is indeed activated rapidly in response to a shift to 43 °C. However, the magnitude of the activation is less than the approximately 5-fold increase observed after overproduction of the outer membrane porin, OmpC [22, 29]. This implies that the σ^E-dependent stress response can be activated to different extents and that the requirement for σ^E regulon members may be lower following a temperature shift than during overproduction of OmpC. In addition, the σ^E response appears to lack a classic "adaptation" phase in which a response is downregulated after a strong initiation phase. Instead, σ^E activity increases within the first 5-10 minutes of the response and remains at that level as long as the cells are kept at 43 °C (see discussion).

σ^E activity during the shut-off phase of the stress response

After cells that had been growing at 43 °C are returned to 30 °C, the synthesis rates of both RseA and DegP drop rapidly to levels below those normally observed during steady state growth at 30 °C (Fig. 2-2, Table 2-1). By 15 minutes after the temperature downshift, RseA synthesis has declined 8-fold (Fig. 2-2A) and DegP synthesis has declined 20-fold compared to the 43 °C synthesis rates (Fig. 2-2B). The rates of synthesis of both proteins remain low for another 10 minutes then slowly increase to approximately the level observed in unstressed cells within 60 minutes for

RseA (Fig. 2-2A) and 75 minutes for DegP (Fig. 2-2B). These results show that the production of σ^E regulon members drops sharply and significantly immediately following a return to normal growth temperatures when elevated levels of chaperones and proteases are no longer necessary.

RseA stability in unstressed cells

For σ^E activity to increase, the interaction between RseA and σ^E must be disrupted. Previous work indicated that one mechanism to disrupt the complex is through the regulated proteolysis of RseA [29, 36, 37, 146, 147]. If proteolysis of RseA is the primary mechanism controlling σ^E activity, then changes in RseA stability should correlate with changes in σ^E activity during the different phases of the stress response. To test this hypothesis we first measured the stability of RseA in unstressed cells growing at 30 °C. Newly synthesized RseA is stable for approximately 5 minutes following synthesis and is subsequently degraded with a half-life of 7.8 ± 0.8 minutes (Fig. 2-3). These results confirm our previous observations that RseA is a relatively unstable protein [29]. However, our current results differ from our previous measurements performed in MC1061 (Fig. 2-3) in two respects: in the earlier work, we did not observe a lag before the onset of proteolysis and the half-life of RseA was longer than that measured here [29]. These differences are due to changes in the protocol, adopted to minimize growth perturbations and not to differences between the strains. In the course of the current work, we found that the addition of excess cysteine during the chase step of the pulse-chase protocol caused the cells to stop growing for a short period of time. Therefore,

we modified the protocol by including cysteine in the growth media and labeling proteins with methionine alone, which eliminated the growth arrest (see Materials and Methods for details). The stability of RseA in MC1061 measured with this optimized protocol is nearly identical to that in MG1655. Under the optimized conditions, RseA in MC1061 is stable for 5 minutes and is then degraded with a half-life of 8.8 ± 0.9 minutes (Fig 2-3).

RseA stability during initiation and adaptation

The rapid increase in σ^E activity during the initiation phase of the stress response (Fig. 2-1) is correlated with a decrease in RseA stability (Fig 2-4, Table 2-1). Within 5 minutes following a shift to 43 °C, RseA is degraded with a half-life of 2.2 ± 0.1 minutes following a 5 minute lag (Fig. 2-4, Table 2-1). This degradation rate is 3.5-fold faster than that in unstressed cells. Surprisingly, RseA is not degraded as rapidly during the adaptation phase of the stress response as during the initiation phase, even though σ^E activity is the same during both phases. In cells that are grown continually at 43 °C, RseA is degraded with a half-life of 4.5 ± 0.2 minutes following a 5 minute lag, or 2-fold more slowly than during the initiation phase (Fig. 2-4, Table 2-1). Although RseA is stabilized during the adaptation phase relative to the initiation phase, it is still degraded faster than in unstressed cells. These results are surprising as the activity of σ^E is the same during initiation and adaptation suggesting that the rate of RseA degradation may not be the sole determinant of σ^E activity (see discussion). In addition, the observation that newly synthesized RseA is stable for 5

minutes in both stressed and unstressed cells indicates that a time-dependent but stress-independent event occurs before RseA degradation commences.

RseA stability during shut-off

The decrease in σ^E activity during the shut-off phase of the response (Fig. 2-2, Table 2-1) is correlated with stabilization of RseA. Within 5 minutes after cells that were grown at 43 °C are returned to 30 °C, the half-life of RseA increases dramatically to >50 minutes, which is considerably longer than the approximately 8 minute half-life exhibited by unstressed cells (Fig 2-5A, Table 2-1). The half-life of RseA slowly returns to that observed in unstressed cells concurrent with the recovery of σ^E activity to normal levels. By 40 minutes following the downshift, the half-life of RseA is 13.5 ± 1.8 minutes and by 65 minutes it is the same as in unstressed cells (Fig. 2-5B, Table 2-1).

Stabilization of RseA during the shut-off phase of the response should result in an increase in the amount of RseA in the cell. However, upon temperature downshift, synthesis of RseA decreases (Fig. 2-2). To determine the net effect of these opposing processes, we measured the steady state level of both RseA and σ^E in cells growing at 43 °C and at various times following a temperature downshift. The steady state levels of RseA and σ^E do not change (Fig. 2-5C). Therefore, any gain in the level of RseA in the cell due to stabilization is offset by the decrease in new synthesis of the protein.

Discussion

The work presented here examines the relationship between σ^E activity and the stability of its inner-membrane antisigma factor, RseA, during the initiation, adaptation and shut-off phases of the heat shock response. We find that, in general, σ^E activity is inversely correlated with RseA stability (Table 2-1, summarized in Figure 2-6), leading us to suggest that regulated proteolysis of RseA is a major pathway for communicating information about protein unfolding in the cell envelope to σ^E in the cytoplasm. How might changes in the degradation rate of RseA alter σ^E activity? σ^E activity is determined by the number of σ^E molecules that are free (not bound to RseA) and therefore available to bind to RNA polymerase and direct transcription. Changing the degradation rate of RseA could alter σ^E activity by changing the relative levels of σ^E and RseA in the cell, and also by altering the effective dissociation constant of σ^E from RseA. These mechanisms can explain the change of σ^E activity in each phase of the heat shock response. However, the fact that the relationship between σ^E activity and RseA degradation is not simple raises the possibility that other, as yet unknown, mechanisms may also play a role in regulating σ^E.

The initiation phase of the response

After shift to high temperature, both σ^E activity and RseA degradation increase. Increased degradation of RseA would be expected to increase the ratio of σ^E to RseA in the cell, thereby increasing the free pool of σ^E and σ^E activity. Preliminary computer modeling of the σ^E-dependent stress response shows that only a small (<2

fold) change in the ratio of σ^E to RseA is needed to give a 2.5-fold increase in σ^E activity (I. Grigorova, unpublished results). Although we have not been able to reproducibly measure such a small change in steady-state levels by western blotting analysis, our measurements of RseA production and stability are consistent with this expectation. The net amount of RseA should decrease during initiation of the stress response, as its half-life drops 4-fold, while its production increases only 2.0 to 2.5-fold. Since σ^E is stable, the steady-state ratio of σ^E to RseA should increase. This would lead to an increase in the free pool of σ^E in the cell and increased σ^E activity. Indeed, we previously showed that this mechanism was sufficient to explain the induction of σ^E activity after overexpression of the outer membrane porin OmpC [29].

The adaptation phase of the response

Although σ^E activity is the same during the initiation and adaptation phases of the heat shock response, the degradation rate of RseA is different. RseA is twice as unstable during initiation as during adaptation. This suggests that the degradation rate of RseA is not the sole determinant of σ^E activity during adaptation.

Several additional factors could contribute to the observed level of σ^E activity during adaptation. First, the synthesis rate of σ^E is greater at high temperature and should result in a higher concentration of σ^E in cells grown for long periods of time at 43 °C. Since more σ^E will be available to bind to RNA polymerase and direct transcription, the rate of degradation of RseA during adaptation may not need to be as high as that during initiation to maintain comparable levels of σ^E activity. Second, the affinity of the σ^E-RseA complex could be lower during the adaptation phase

leading to an increase in the amount of free σ^E available to bind RNA polymerase and initiate transcription. Collinet et al. observed that binding of the periplasmic protein RseB to RseA enhances the affinity of the σ^E-RseA complex [148]. In addition, RseB has been shown to copurify with periplasmic inclusion bodies [148]. During the adaptation phase of the response, unfolded proteins may accumulate in the periplasm. RseB could be titrated away from RseA by these aggregated, unfolded proteins resulting in a lowered affinity of the σ^E-RseA complex and an increase in the free pool of σ^E in the cell. Finally, other mechanisms may modulate the activity of σ^E including chemical modification or conformational changes in σ^E. Any additional regulatory mechanisms may work alongside the degradation of RseA and serve to fine-tune the response.

The shut-off phase of the response

Following a shift to low temperature after growth at 43 °C, the activity of σ^E decreases 8 to 15-fold relative to that at 43 °C. Paradoxically, shut-off occurs without altering the steady-state ratio of σ^E to RseA. Clearly, the change in σ^E activity during the shut-off phase of the response is not due to a change in this ratio. It is possible that an unknown factor collaborates with RseA to decrease σ^E activity. However, it is also possible to explain the data with the existing players.

The fact that RseA is stabilized 10 to 20-fold during the shut-off phase suggests the possibility that σ^E activity is controlled by the rate of RseA degradation. If the dissociation rate (k_{off}) of RseA from σ^E is slower than its degradation rate, σ^E will predominantly be released from RseA when RseA is degraded and the amount of free

σ^E in the cell will primarily depend on the degradation rate of RseA. The magnitude of the drop in the degradation rate of RseA after downshift can account for the large decrease in σ^E activity that we observe. In addition, the affinity of the σ^E-RseA complex is sufficiently high to entertain this model. Even in the presence of the high concentrations of detergent required to maintain full-length RseA in a soluble form, RseA binds to σ^E with a K_d of 50-100 nM [148]. The isolated cytoplasmic domain of RseA ($RseA_{cyto}$) may be a better model than the full-length protein as it is fully soluble and inhibits σ^E-directed transcription both *in vivo* and *in vitro* [26, 27]. Transcription experiments suggest that the K_d for interaction between $RseA_{cyto}$ and σ^E is $\leq$ 1 nM (L. Connolly, unpublished results). Moreover, the interaction of these two proteins is remarkably stable. They can be purified as a complex from crude cell lysates and remain associated even in 650 mM NaCl and at 50 °C (J. Tupy, unpublished observations). The magnitude of the drop in the rate of RseA degradation observed after downshift is sufficient to account for the large decrease in σ^E activity that we observe.

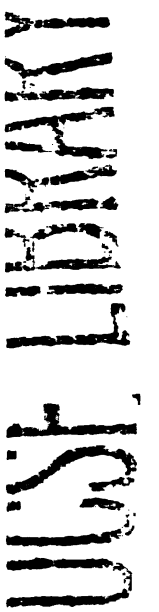

An alternative model is based on our demonstration that newly synthesized RseA is insensitive to proteases (Figures 2-3 and 2-4) indicating that a time-dependent event triggers RseA proteolysis. If the protease-resistant, newly synthesized RseA also has a low affinity for σ^E, then this time-dependent process converts RseA from a form that binds σ^E weakly to a form that binds σ^E tightly. This scenario is sufficient to explain the observed differences in σ^E activity during the adaptation and shut-off phases of the response. At elevated temperatures, the low affinity form predominates as rapid degradation of RseA depletes the high affinity form and new synthesis

replenishes the cell with low affinity RseA. In contrast, during the shut-off phase, degradation of RseA is slow and new synthesis of RseA is low, therefore the high affinity form will accumulate and repress σ^E activity efficiently. As the two forms are indistinguishable on SDS-PAGE, the level of RseA and the ratio of RseA to σ^E will appear unchanged as observed (Fig. 2-5C). The change in the affinity of RseA for σ^E and its susceptibility to proteolysis could result from conformational changes in RseA itself or binding of an accessory factor that alters the affinity of RseA for σ^E. Further experiments are clearly necessary to understand exactly how the degradation of RseA determines σ^E activity.

Regulation of the Proteolysis of RseA

The degradation rates of RseA vary considerably in response to changes in the growth temperature, indicating that its proteolysis is not controlled by a simple on-off switch. Upon induction of the stress response, the initial cleavage of RseA is carried out by the inner membrane protease, DegS [36, 37]. A second inner membrane protease, YaeL, then cleaves RseA further, releasing it from the membrane after which the remaining fragments are degraded to completion by cytoplasmic proteases including ClpXP [33, 36, 37]. Changes in the rate of degradation of RseA are dependent on a signal and are not controlled by alterations in the levels of DegS and YaeL since the overexpression both DegS and/or YaeL in unstressed cells does not lead to increased σ^E activity [36]. The amount of RseA in the cell does not appear to influence its proteolysis either, as different rates of proteolysis are realized without changes in the overall amount of RseA in the cell (Fig. 2-5). Preliminary results also

indicate that σ^E does not protect RseA from proteolysis as RseA is not degraded faster in the absence of σ^E (data not shown) Therefore, the inducing signal either influences the activity of the proteases or alters the susceptibility of RseA to proteolysis. Furthermore, the activity or amount of the signal must vary in response to changes in the growth temperature.

Another unusual aspect of the proteolysis of RseA is our observation that newly synthesized RseA is resistant to proteolysis. As discussed above, one possibility is that the lag represents a time-dependent conformational change in RseA. Although the insertion of RseA into the membrane has not been measured, we believe that any conformational change occurs in the membrane, as insertion is rapid for most proteins. The lag may have been masked by the longer half-life for RseA in unstressed cells measured in our previous work with MC1061 using the old experimental protocol, although a lag was not seen when RseA was rapidly degraded following a shift to 43 °C in that work [29]. It is also possible that the lag is caused by the sudden change in the level of methionine in the chase step of our experimental protocol. Since most unstable proteins do not demonstrate such a lag, this may represent a specific response by the σ^E system to the either amount of methionine or a physiological effect caused by the change in methionine levels.

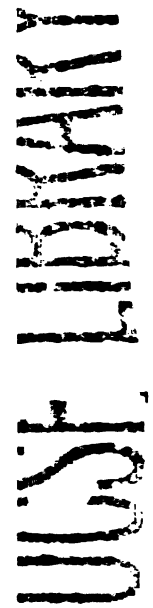

Comparison of periplasmic and cytoplasmic stress responses

Like the σ^E response, the σ^{32} cytoplasmic stress response also exhibits initiation, adaptation, and shut-off phases. During the shut-off phase, the activities of both σ^{32} and σ^E decrease rapidly and then slowly recover to the level seen in unstressed cells

after 1-2 generations of growth [141]. This allows regulon members to return to their unstressed levels by dilution of existing proteins through cell division and protein turnover. However, the initiation and adaptation phases of the two responses differ significantly. One of the hallmarks of σ^{32} response is a strong (10-fold) but transient increase in the transcription of heat shock genes during the first 5-10 minutes after a shift to high temperature, followed by repression to a rate somewhat (2 to 3-fold) higher that that in unstressed cells [137, 142]. In contrast, the small (2.5-fold) increase in σ^{E} activity is maintained for the duration of the heat shock response. The lack of a transient initial burst of σ^{E} activity appears to be a hallmark of the response, as it was not observed even with a more potent inducer, overexpression of OmpC [29]. The initial burst of heat shock gene synthesis is thought to be a mechanism to rapidly increase the level of proteases and chaperones in the cell immediately following a stress. The fact that σ^{E} does not display such an increase indicates that the steady-state level of periplasmic chaperones and proteases will increase more slowly than those in the cytoplasm. Why might this be the case? We suggest that a large burst of synthesis of σ^{E}-dependent genes could actually be detrimental to the cell. As many σ^{E} regulon members are located in the cell envelope, they must be translocated across the inner membrane. A large increase in their synthesis could overwhelm the translocation machinery and actually increase the number of unfolded proteins emerging from translocons into the periplasm thereby exacerbating the folding problem.

Materials and Methods

Media and strains

M9 minimal medium was prepared as described [149]. M9 was supplemented with 0.2% glucose, 1mM MgSO4, 2 μg/ml thiamine, and all amino acids (40 μg/ml) except for media used in the pulse-label and pulse-chase experiments in which methionine was omitted. The bacterial strains used in this work were CAG45114 (MG1655 Φλ[rpoHP3-lacZ] *ΔlacX74*), CAG16037 (MC1061 Φλ[rpoHP3-lacZ] *araD* Δ(*ara-leu*)7697 Δ(*codB-lacI*) *galK*16 *galE*15 *mcrA*0 *relA*1 *rpsL*150 *spoT*1 *mcrB*9999 *hsdR*2, (20)), and CAG33149 (BL21(DE3) pLC234, Km^R, [26]). pLC234 encodes the periplasmic domain of RseA fused to the N-terminal Histidine tag in pET28b [26].

Determination of synthesis rates by pulse-labeling immunoprecipitation

Cells were grown in supplemented M9 minimal media lacking methionine to an OD450=0.2-0.4. Proteins were labeled at indicated times by adding a 900 μl aliquot of the culture to 2 μl of L-[^{35}S]Methionine in a pre-warmed 50 ml conical tube shaking at the desired temperature. The samples were incubated for 45 seconds then further incorporation of radioactive methionine was blocked by adding 100 μl of a 1% solution of unlabeled methinonine. After 30 seconds, the entire sample was added to an eppendorf tube containing 100 μl of ice-cold TCA. Samples were incubated on ice for at least 15 minutes then precipitated proteins were collected by centrifugation. The pellets were resuspended by vortexing and boiling in 50 μl of 20

mM $NaPO_4$ pH 7.5, 10 mM EDTA, 2% SDS, 1 mM AEBSS after which 750 µl of PO_4 Ripa (20 mM $NaPO_4$ pH 7.5, 0.5 M NaCl, 0.5% sodium deoxycholate, 1% IGEPAL, 0.1% SDS) was added. The radioactivity in each sample was counted in duplicate in a scintillation counter. DegP and RseA were immunoprecipitated to determine the amount of each protein synthesized during the 45 second pulse as a fraction of total protein synthesis. Samples were normalized to the overall amount of protein synthesis by adding equal counts per minute of each sample to the immunoprecipitation reactions. The final volume of the immunoprecipitation reactions was 500 µl and they contained the sample, polyclonal antibody raised to the periplasmic domain of RseA, polyclonal antibody raised to DegP, and 20 µl of a1:1 slurry of UltraLink Immobilized Protein A beads (Pierce) in PO_4 Ripa. As an internal standard, a culture overexpressing the periplasmic domain of RseA (strain CAG33149) was pulse-labeled and an aliquot was added to each sample before immunoprecipitation. The samples were rocked at 4 °C for one hour, then immune complexes were collected by centrifugation. The beads were washed three times with PO_4 Ripa followed by one wash with 1X PBS. Proteins were eluted from the beads by boiling for five minutes in 30 µl of Lamelli sample buffer. The samples were loaded onto 15% Tris-glycine gels and proteins were visualized with the Molecular Dynamics Storm 560 PhosphorImager scanning system. Bands were quantified using the program ImageQuant 1.2 and the intensity of band for full-length RseA or DegP in each lane was normalized, after background correction, to the intensity of the band for the internal standard, the periplasmic domain of RseA, in that lane.

Determination of the half-life of RseA by pulse-chase immunoprecipitation

Cells were grown in supplemented M9 minimal media lacking methionine to an OD450 of 0.2-0.4 at the specified growth temperature. In experiments to measure the half-life of RseA after a shift in growth temperature, the entire culture was shifted to the new temperature rather than splitting the culture by placing an aliquot a new flask. We found that moving the entire flask gave the most reliable and reproducible measurements of RseA stability. Proteins were pulse-labeled for 1 minute by the addition of L-[^{35}S]Methionine to the growing culture after which a chase of cold methionine was added to a final concentration of 1% to block further incorporation of radioactive methionine. A 900 µl sample was removed immediately (t=0) after the chase and additional 900 µl samples were removed at the indicated times. Samples were added to 100 µl of ice-cold TCA, incubated on ice for >15 minutes, processed, and immunoprecipitated with polyclonal antibodies directed against the periplasmic domain of RseA as described above for the determination of synthesis rates. The intensity of the full length RseA band in each lane was normalized, after background correction, to the intensity of the band in that lane corresponding to the periplasmic domain of RseA, the internal standard described above. RseA remaining at each time point was determined by dividing the normalized intensity of full length RseA at that time to the normalized intensity at t=0. Half-lives were determined by fitting the data to the exponential decay equation.

The method used for pulse-labeling proteins was modified for the work presented here. Previously we omitted both methionine and cysteine from the growth media,

labeled proteins with both amino acids, and blocked further incorporation by adding an excess of both amino acids [29]. In our current protocol cells are grown in media lacking only methionine, proteins are labeled with radioactive methionine, and then further incorporation of the radioactive amino acid is blocked by the addition of excess unlabeled methionine. We modified our protocol because we found that the cells stopped growing briefly following the addition of excess cysteine in the latter protocol and we were concerned that this would lead to experimental artifacts.

Western blot detection of σ^E and RseA

Cells were grown 43 °C in supplemented M9 minimal media to an OD450 = 0.3-0.4. Duplicate samples of 900 µl each were taken (t=0) then the culture was shifted to 30 °C and additional samples of 900 µl were taken at the indicated times. All samples were added to 100 µl ice-cold TCA and incubated on ice for >15 minutes. Precipitated proteins were collected by centrifugation and resuspended by boiling in Lamelli sample buffer at pH 9.0. Samples were loaded onto 15% Tris-glycine SDS gels such that extracts from an equal number of cells were loaded in each lane. Western transfer was performed using standard methods. The blots were probed with polyclonal antibodies directed against the periplasmic domain of RseA, the cytoplasmic domain of RseA, σ^E, and either σ^{70} or maltose binding protein as controls. The corresponding bands were detected by probing with anti-rabbit immunoglobulin radiolabeled with ^{35}S (Amersham Biosciences). Bands were visualized using the Molecular Dynamics Storm 560 PhosphorImager scanning system and quantified using the program ImageQuant 1.2. The intensity of the band

at each time point was normalized to the intensity of the average of the two t=0 bands. The changes in the steady state levels of RseA and σ^E over the course of the experiment were similar to the changes in the steady state levels of maltose binding protein or σ^{70}.

ACKNOWLEDGEMENTS:

The authors would like to thank Benjamin Alba, Joyce West, and Ken Keiler for critical reading of the manuscript. This work was supported by U. S. Public Health Service Grant GM36278-18 from the NIH. I. Grigorova was supported by the NIH Training Grant GM08284.

Figure Legends:

Figure 2-1. $E\sigma^E$ activity increases during the initiation and adaptation phases of the stress response. Cells were grown to early exponential phase at 30 °C then shifted to 43 °C. $E\sigma^E$ activity was determined by measuring the rate of synthesis of RseA **(A)** and DegP **(B)** using the pulse-label protocol described in Materials and Methods. The synthesis rates shown for each protein are normalized to the synthesis rate of that protein at 30 °C before the shift to 43 °C (t=0). Error bars are shown for data points representing the average of at least 2 independent determinations.

Figure 2-2. $E\sigma^E$ activity decreases during the shut-off phase of the stress response then slowly returns to normal levels. Cells were grown overnight at 43 °C, diluted and regrown into early exponential phase at 43 °C, and then shifted to 30 °C. $E\sigma^E$ activity was determined by measuring the rate of synthesis of RseA **(A)** and DegP **(B)** using the pulse-label protocol described in Materials and Methods. The synthesis rates shown for each protein are normalized to the synthesis rate of that protein at 43 °C, before the downshift to 30 °C (t=0). The dotted line indicates the average synthesis rate in unstressed cells at 30 °C. Data points from several experiments are shown.

Figure 2-3. RseA is degraded in unstressed cells. Cells of strain MG1655 (◆) and MC1061 (□) were grown to early exponential phase at 30 °C and RseA stability was measured using the optimized protocol described in Materials and Methods. The stability of MC1061 (■) measured using the old protocol (1) is shown for reference.

The data points and error bars shown are the averages and standard deviations, respectively, from four independent experiments.

Figure 2-4. RseA is degraded faster during the initiation and adaptation phases of the stress response than in unstressed cells. Cells were grown to early exponential phase and left at 30 °C (no stress, ◆), shifted to 43 °C (initiation, O) or grown to early exponential phase at 43 °C (adaptation, Δ). RseA stability was measured by a pulse-chase protocol as described in Materials and Methods. The stability of RseA during the initiation phase was measured 5-10 minutes after the shift to 43 °C. The data points and error bars shown are the averages and standard deviations, respectively, from a minimum of three independent experiments.

Figure 2-5. RseA is stabilized but the steady state levels of RseA and σ^E do not change during the shut-off phase of the stress response. **(A)** RseA degradation is significantly slower following a shift from 43 °C to 30 °C than during steady state growth at 43 °C or 30 °C. Cells were grown to early exponential phase at 30 °C (no stress, ◆), grown to early exponential phase and left at 43 °C (adaptation, Δ) or grown to early exponential phase at 43 °C then shifted to 30 °C (shut-off, ●). RseA stability was measured by a pulse-chase protocol as described in Materials and Methods. The stability of RseA during the shut-off phase was measured 10 minutes after the shift to 30 °C. The data points and error bars shown are the averages and standard deviations, respectively, from a minimum of three independent experiments. **(B)** RseA is stabilized immediately following a shift from 43 °C to 30 °C, then

becomes progressively less stable as the cells remain at 30 °C. Cells were grown to early exponential phase at 43 °C and shifted to 30 °C (shut-off) or grown to early exponential phase at 30 °C (no stress, ◆). RseA stability was measured 10 minutes (shut-off 10 min., ●), 40 minutes (shut-off 40 min., □), and 65 minutes (shut-off 65min., ✕) following the temperature shift. Data points with error bars are the averages and standard deviations, respectively, from a minimum of two independent experiments. A representative data set is shown for the shut-off 65 min. experiment. **(C)** The steady state levels of RseA and σ^E do not change following a shift from 43 °C to 30 °C. Cells were grown to early exponential phase at 43 °C then shifted to 30 °C. The levels of RseA (◆) and σ^E (□) were determined before the temperature shift (t=0) and at various times after the shift by western blot analysis as described in Materials and Methods. The amount of each protein at a given time is normalized to the amount of that protein at t=0. Data from two independent experiments are shown.

Figure 2-6. Changes in σ^E activity (black stippled bars) are inversely correlated with changes in RseA stability (white stippled bars). σ^E activity (the synthesis rate of RseA) and the half-life of RseA during the initiation, adaptation, shut-off and recovery from shut-off (40' after the temperature downshift) were normalized those values measured in unstressed cells at 30 °C. The $\log_2$ values of the fold changes are plotted such that no change gives a value of 0, a 2-fold increase gives a value of 1, and 2-fold decrease gives a value of –1, etc.

Figure 2-1.

A

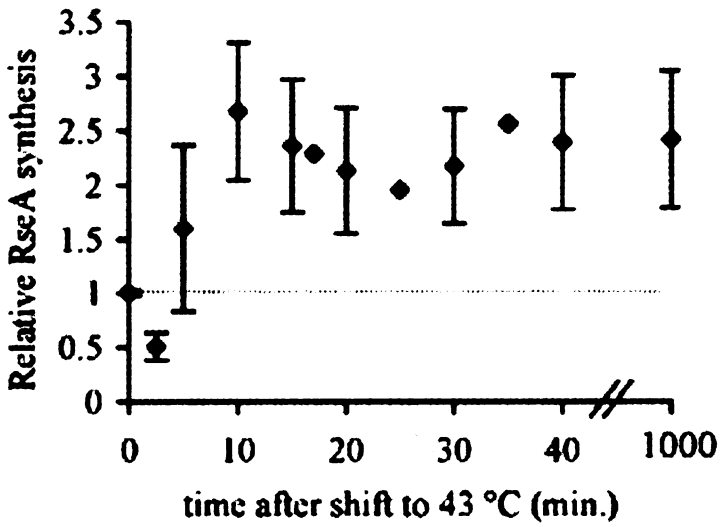
Relative RseA synthesis
3.5
3
2.5
2
1.5
1
0.5
0
0
10
20
30
40
1000
time after shift to 43 °C (min.)

B

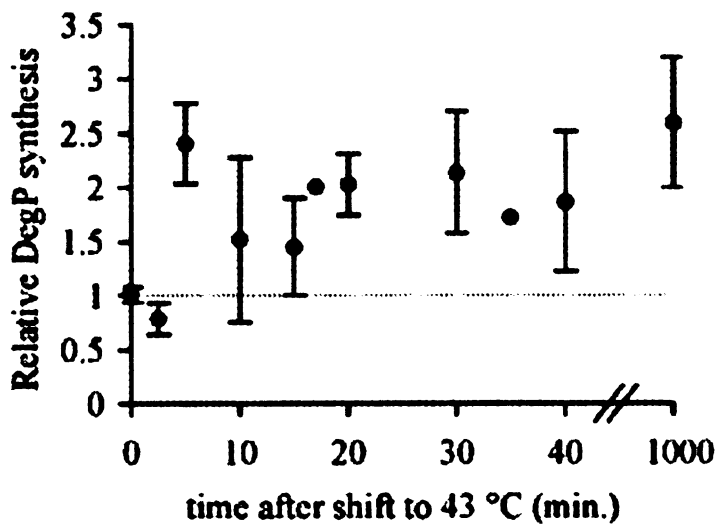
Relative DegP synthesis
3.5
3
2.5
2
1.5
1
0.5
0
0
10
20
30
40
1000
time after shift to 43 °C (min.)

Figure 2-2.

A

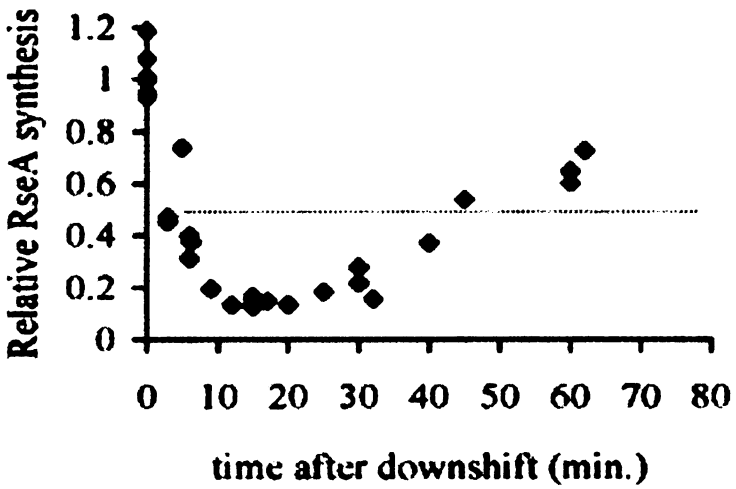
Relative RseA synthesis
1.2
1
0.8
0.6
0.4
0.2
0
0 10 20 30 40 50 60 70 80
time after downshift (min.)

B

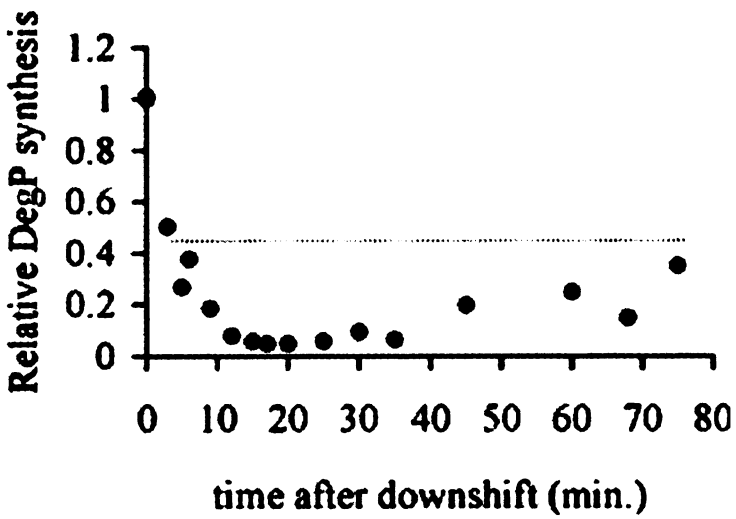
Relative DegP synthesis
1.2
1
0.8
0.6
0.4
0.2
0
0 10 20 30 40 50 60 70 80
time after downshift (min.)

Figure 2-3.

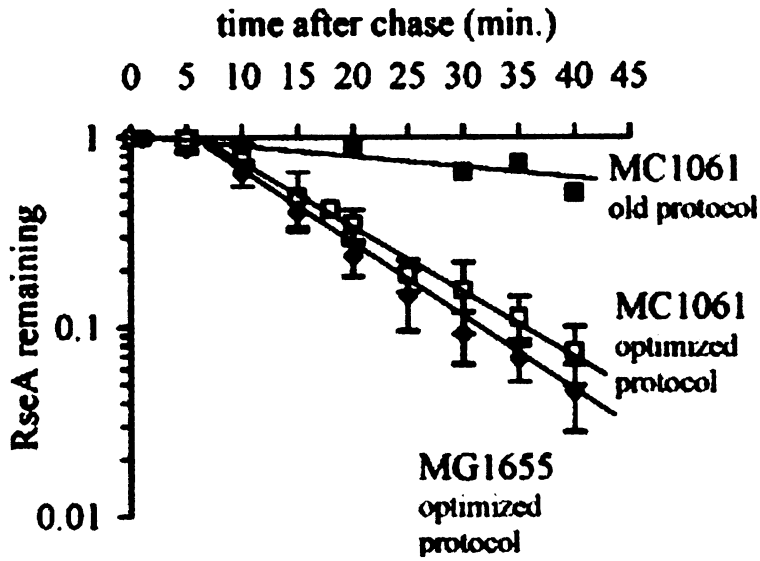

Figure 2-4

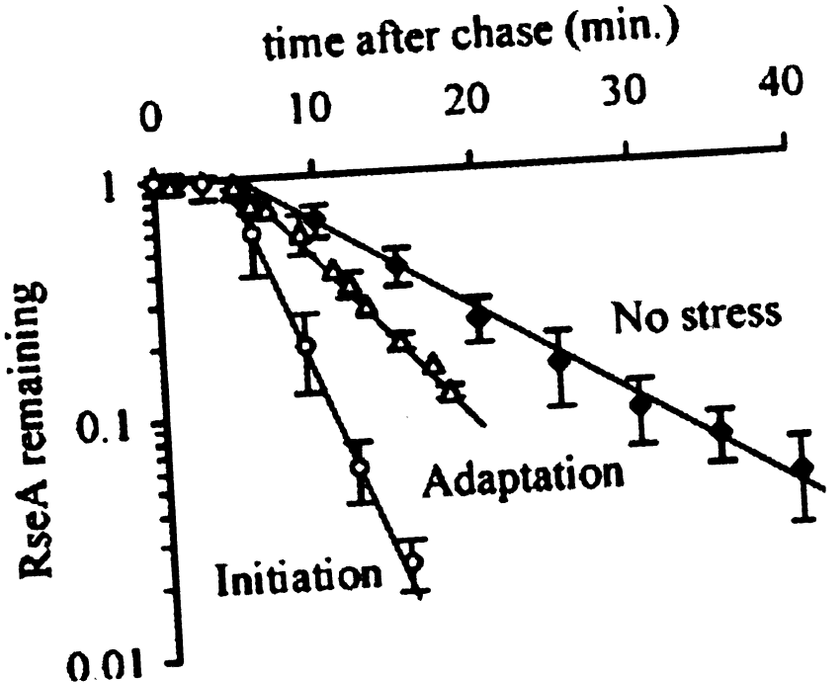

Figure 2-5.

A

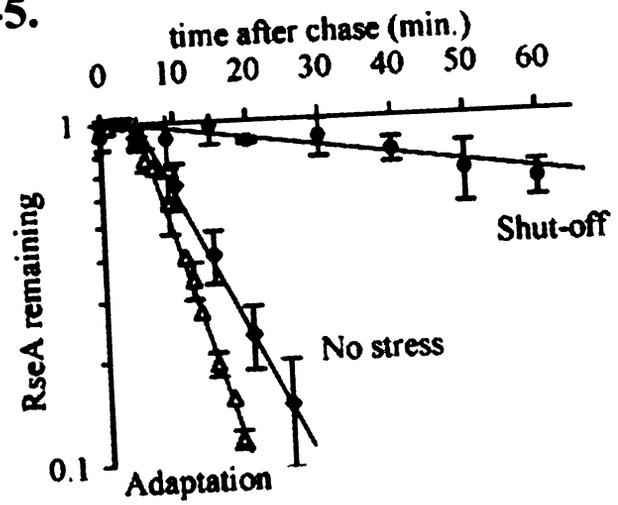

B

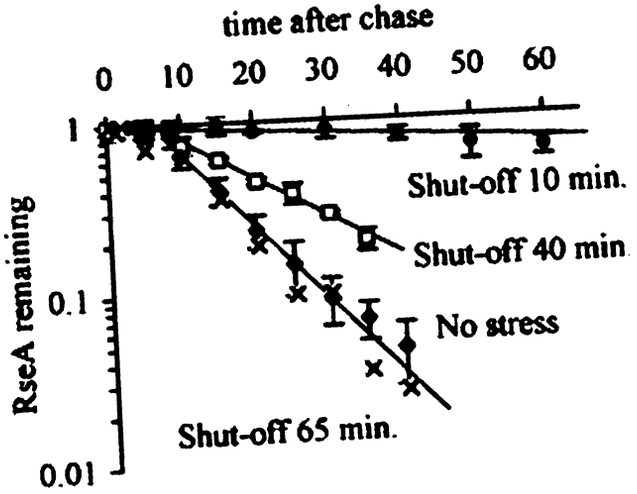

C

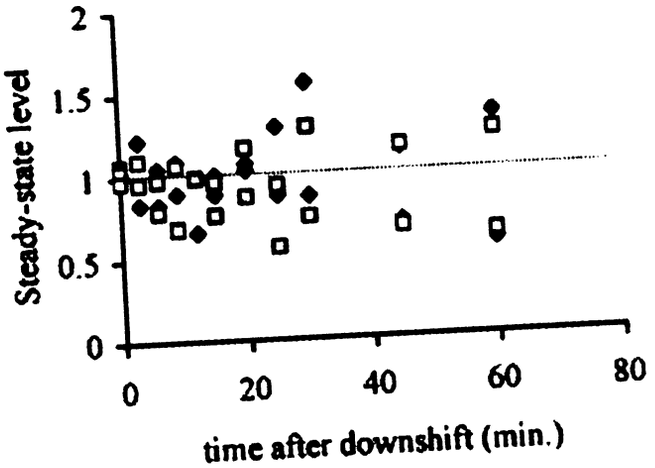

Figure 2-6.

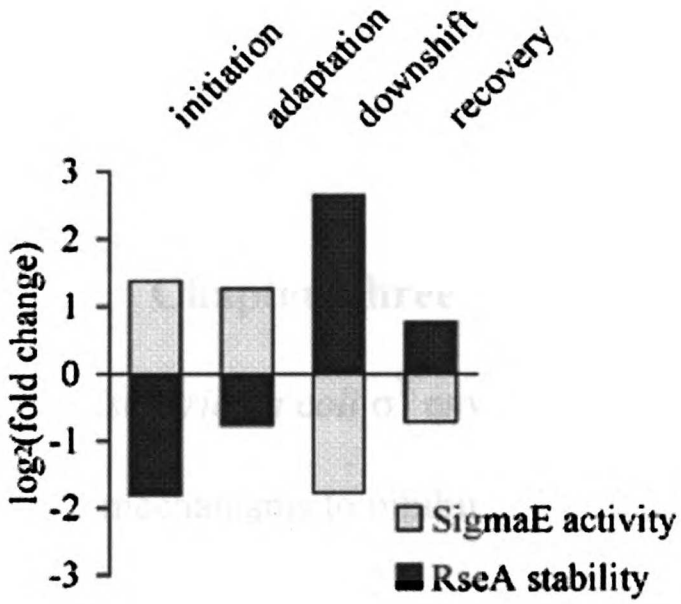

Chapter Three

Fine-tuning of the *Escherichia coli* σ^E envelope stress response relies on multiple mechanisms to inhibit signal-independent proteolysis of the transmembrane anti-sigma factor, RseA.

Summary

Proteolytic cascades are widely implicated in signaling between cellular compartments. In *Escherichia coli*, accumulation of unassembled outer membrane porins (OMPs) in the envelope leads to expression of σ^E-dependent genes in the cytoplasmic cellular compartment. A proteolytic cascade conveys the OMP signal by regulated proteolysis of RseA, a membrane-spanning anti-sigma factor whose cytoplasmic domain inhibits σ^E-dependent transcription. Upon activation by OMP C-termini, the membrane localized DegS protease cleaves RseA in its periplasmic domain, the membrane embedded protease RseP (YaeL) cleaves RseA near the inner membrane, and the released cytoplasmic RseA fragment is further degraded. Initiation of RseA degradation by activated DegS makes the system sensitive to a wide range of OMP concentrations and unresponsive to variations in the levels of DegS and RseP proteases. These features rely on the inability of RseP to cleave intact RseA. In the present report, we demonstrate that RseB, which binds to the periplasmic face of RseA, and DegS each independently inhibit RseP cleavage of intact RseA. Thus, the function of RseB, widely conserved among bacteria utilizing the σ^E pathway, and the second role of DegS (in addition to RseA proteolysis initiation) is to improve the performance characteristics of this signal-transduction system.

Introduction

Intracellular communication is an essential feature of living cells, permitting them to mount a coordinated cellular response to changing conditions. In *Escherichia Coli* (*E. coli*), physiological stress in the envelope compartment induced either by overproduction of outer membrane porins (OMPs) or by temperature upshift, is communicated through the inner membrane to the cytoplasmic compartment of the cell [22, 42, 43, 133]. The stress signal originates from accumulation of immature OMP species and possibly from other unfolded proteins in the extracytoplasmic space [22, 23, 44, 143] and is transduced to the cytoplasm to activate σ^E, the bacterial transcription initiation factor that governs the response to envelope stress. The gene encoding σ^E, *rpoE*, is essential for viability under all conditions tested, indicating that σ^E transcriptional activity is required during normal growth as well as under stress [150]. In this work, we dissect the elements of the transmembrane signaling pathway that contribute to the sensitivity of the pathway to inducing signals and make the pathway unresponsive to noise.

The signal transduction cascade conveys envelope stress signals to the cytoplasmic compartment by altering the stability of RseA, a negative regulator of σ^E activity [29, 34]. RseA is a membrane spanning anti-sigma factor that binds to σ^E with its cytoplasmic domain, preventing σ^E from interacting with RNA Polymerase [26-28]. In response to stress signals generated in the envelope, a protease cascade, consisting of DegS, RseP (YaeL) and cytoplasmic proteases including ClpX, is activated to degrade RseA, thereby releasing σ^E from its inhibitory interaction with RseA and thus transmitting the signal through the inner membrane [29, 36, 37], (J.

Flynn, T. Baker, G&D, in press.; R. Chaba, unpublished). Both the DegS and RseP proteases are essential for *E. coli* viability; their essential function is to provide *E. coli* with active σ^E via proper proteolysis of the anti-sigma factor [36, 37, 146].

The inner membrane-anchored DegS protease initiates degradation by cleaving RseA in its periplasmic domain ~30 aa C-terminal to the transmembrane domain of RseA (Fig. 3- 7A) [29, 36, 37]. Until DegS receives an activating signal it exists in proteolytically inactive conformation (that we call here unactivated) [23, 30]. Both *in vivo* and *in vitro* evidence is consistent with the idea that DegS is activated when OMP C-termini bind to its PDZ domain (Fig. 3-7A,C) [23, 30-32]. The build-up of exposed OMP C-termini signals that the normal OMP folding pathway is impaired, as OMP C-termini are likely to be buried in the trimer interface in the native protein [31, 32]. RseP then cleaves the DegS generated membrane-localized fragment of RseA to release the cytoplasmic domain of RseA (Figure 3-7A) [29, 36, 37]. This cleavage is supported by genetic, physiological and biochemical evidence [36-38] and has been shown to occur within the transmembrane sequence of RseA *in vivo* and *in vitro* (Y. Akiyama, K. Kanehara, K. Ito, pers. comm.). Two Gln-rich regions (Q1 and Q2) in the periplasmic domain of RseA inhibit RseP from cleaving the intact protein [38]. When DegS cleaves RseA, it removes these Gln-rich regions thereby creating an attractive substrate for RseP [23, 36, 37]. The periplasmically located PDZ domain of RseP is required for the inhibitory reaction that prevents RseP cleavage of intact RseA because RsePΔPDZ can perform that reaction [38, 39].

The transmembrane σ^E activation pathway has two principal design features. First, σ^E activity is very sensitive to the periplasmic OMP signal, varying greatly from cells expressing low OMPs to those expressing high OMPs [22]. Second, σ^E activity is relatively unresponsive to variations in the levels of the DegS and RseP proteases themselves [36]. We have investigated construction features of this pathway that contribute to these characteristics. We find that the OMP signal is sensed only by DegS. Thus, coordination of the magnitude of the σ^E response to the extent of the OMP inducing signal requires that RseA cleavage be initiated only by activated DegS and not by RseP. We show here that two additional players reinforce the inability of RseP to cleave intact RseA: RseB, a periplasmic protein that binds to the periplasmic domain of RseA, and DegS itself. Whereas in the absence of DegS, the transmembrane signal transduction pathway completely loses its sensitivity to the OMP signal, in the absence of RseB, sensitivity is suboptimal in that it does not respond to the full range of OMP signals and is affected by the levels of the proteases. Sequential proteolytic cascades are employed for transmembrane signal transduction by a number of organisms [2, 47]. We suggest that the regulatory and construction principles that we describe here are likely to be general design features for these signal transduction circuits.

Results:

RseB inhibits DegS-independent proteolysis of RseA

Previous work indicated that RseA degradation increased 1.5 to 2.0-fold in the absence of RseB [29] (Fig. 3-1B). This result could be explained if RseB partially shields RseA from cleavage either by DegS and/or other proteases. If other proteases are able to degrade RseA, cells lacking both DegS and RseB should have increased σ^E activity relative to a strain lacking only DegS. We tested this prediction by comparing the activity of a chromosomal *lacZ* reporter under σ^E control in the two strains (see Materials and Methods). As DegS is essential, these experiments were performed in a strain that suppressed the requirement for DegS (Δ*degSsup*$^+$) [146]. To our surprise, σ^E activity was 6.5-fold higher in a Δ*degSsup*$^+$Δ*rseB* derivative than in the original Δ*degSsup*$^+$ strain (Fig. 3-1A), suggesting the possibility that other proteases do degrade RseA when RseB was missing.

As the essential function of DegS is to provide active σ^E [146], we considered the possibility that DegS would no longer be essential in Δ*rseB* strains. We therefore transduced Δ*degS* into a Δ*rseB* strain by selecting for the closely linked *argR:Tn5* (Kan^R) marker. When tested by PCR, approximately 50% of the Kan^R transductants in the Δ*rseB* strain had acquired the Δ*degS* marker indicating that DegS is no longer essential in a Δ*rseB* strain (Table 3-1). As previously reported, Δ*degS* could not be cotransduced with this Kan^R marker in the wt strain (Table 3-1) [146]. The σ^E activity of the Δ*degS*Δ*rseB* strain was 6.5-fold higher than that of the Δ*degSsup*$^+$ strain and was equivalent to that exhibited by Δ*degSsup*$^+$Δ*rseB* strain (Fig. 3-1A),

indicating that the elevation in σ^E activity was not caused by the suppressor mutation. We directly tested whether elevated σ^E activity resulted from DegS-independent proteolysis of RseA by measuring RseA stability using a pulse-chase immunoprecipitation protocol. Whereas RseA was completely stable in a $\Delta degSsup^+$ strain [29], it was unstable in the *ΔdegSΔrseB* strain, exhibiting a half-life several-fold slower than that of RseA in the wild type (wt) strain (Fig. 3-1B). A rate of RseA degradation slower than wt was expected because the σ^E activity of the *ΔdegSΔrseB* strain was lower than wt (Fig. 3-1A, data not shown). In conclusion, in the absence of RseB, DegS is no longer essential to cellular viability, and both σ^E activity and RseA degradation are significantly increased in the *ΔdegSΔrseB* strain relative to the $\Delta degSsup^+$ strain. These observations are consistent with the idea that other proteases can degrade RseA in the absence of RseB.

RseP is essential in the ΔrseB and $\Delta degSsup^+$ΔrseB strains

Our finding that RseA degradation is initiated in a DegS independent manner in the *ΔdegSΔrseB* strain raised the possibility that RseA was degraded by an alternative pathway that bypassed RseP as well as DegS. To test this, we asked whether *rseP* was dispensable in strains lacking RseB. The essential function of RseP is to provide active σ^E [36, 37], therefore RseP should not be essential if it is not required for RseA degradation in Δ*rseB* strains. Contrary to this expectation, we could not transduce *rseP::kan* either into a *ΔrseB* strain, or a $\Delta degSsup^+\Delta rseB$ strain, although control experiments indicated that these strains were fully transducible (Table 3-1). {We had previously reported that *rseP::kan* could be transduced into $\Delta degSsup^+$ [36], however

further investigation of that strain indicated that *rseP* was still present and the DegS suppressor could not itself substitute for RseP function (I. Grigorova, unpublished). Thus, *rseP* is still essential in strains lacking both DegS and RseB. We verified that *rseP* was required to generate active σ^E in this background by depleting plasmid-borne RseP under P_{ara} control carried in a $\Delta degSsup^+\Delta rseB\Delta rseP$ strain. Upon transfer from inducing medium (arabinose) to non-inducing (glucose) medium, the RseP protein was diluted out by cell growth and division, σ^E activity decreased and growth ceased after 3 dilutions (data not shown). This phenotype is essentially the same as that observed after depletion of RseP from wt strains [36], indicating that RseP is required for RseA degradation in the $\Delta degSsup^+\Delta rseB$ strain background, just as it is in wt cells.

RseP can cleave full-length RseA in a ΔdegSΔrseB strain

There are two potential alternative routes for the degradation of RseA observed in cells lacking both DegS and RseB. First, other periplasmic proteases could substitute for DegS, thereby creating an attractive substrate for RseP cleavage. Second, RseP itself might recognize and cleave full-length RseA. As RseP does not cleave intact RseA in wt cells, this finding would imply that RseB and/or DegS actively inhibit that cleavage. The idea that RseP initiates cleavage of full length RseA in the *ΔdegSΔrseB* cells makes several explicit predictions. First, an increased level of RseP should result in increased σ^E activity. Second, altering the proteolytic activity of RseP should alter the capacity of overexpressed RseP to increase σ^E activity. Finally, the proteolytic

target of RseP should be full length RseA rather than an RseA fragment generated by other proteases. We tested these predictions.

A moderate 2-fold increase in RseP level (as estimated from quantitative Westerns) caused a 2-fold increase in σ^E activity in the *ΔdegSΔrseB* strain but did not change σ^E activity in the wt background (data not shown). Overproduction of RseP from a pTrc promoter gave a 60-fold increase in σ^E activity in the *ΔdegSΔrseB* background but less than a two-fold increase in wild type cells (Fig. 3-2A). The increase in RseP level was roughly comparable in both cases (~20 to 40-fold) indicating that the dramatic difference in σ^E activity cannot be explained by differential induction (Fig. 3-2B). Finally, comparable overexpression of RseP-E23D (Fig. 3-2B), a RseP active site mutant, which cleaves the DegS generated RseA fragment significantly slower than wt RseP [36], gave an 8-fold increase in σ^E activity in *ΔdegSΔrseB* cells, only 13% as much as overproducing wt RseP (Fig. 3-2A). These experiments show that the level and catalytic activity of RseP are directly reflected in altered σ^E activity, thereby providing evidence that RseP is rate limiting for RseA degradation in the *ΔdegSΔrseB* background.

We next tested whether the increased σ^E activity of *ΔdegSΔrseB* cells overexpressing RseP (Fig. 3-2A,B) was accompanied by very rapid disappearance of full-length RseA using a pulse-chase immunoprecipitation protocol. Indeed, full-length RseA disappears much faster (~20-fold) in cells overexpressing RseP than in the vector control (Fig. 3- 2C,D). Thus, the substrate of RseP is full-length RseA, rather than a smaller RseA fragment, generated by some periplasmic protease. Taken

together, these experiments strongly support the idea that RseP is able to cleave full-length RseA in the absence of RseB and DegS (Fig. 3-7B). The small (≤ 2-fold) increase in σ^E activity in wt cells upon dramatic overproduction of RseP (Fig. 3-2A,B) could indicate the normal, very low rate of RseP cleavage of intact RseA in wt cells or could indicate escape from RseB and/or DegS inhibition as a consequence of massive overproduction of RseP.

RseP missing its PDZ domain is able to cleave full-length RseA [38, 39]. We asked whether RseB inhibits cleavage of intact RseA by RsePΔPDZ, just as it inhibits cleavage by wt RseP. Removing RseB from a Δ*degSsup*$^+$ strain with wt RseP increased σ^E activity at least 6-fold (Fig. 3-1A), as a consequence of impaired inhibition of RseP cleavage of intact RseA. In sharp contrast, removing RseB from Δ*degSsup*$^+$ strain with RsePΔPDZ gave little or no increase in σ^E activity over the isogenic strain containing RseB (Fig. 3-3A, compare lanes 2, 3). The inability of RseB to inhibit RsePΔPDZ cleavage of intact RseA does not result from the fact that the rate of RseA degradation is already maximal in this strain: increasing the amount of RsePΔPDZ present in the cell leads to a significant increase in σ^E activity (Fig. 3-3B). We conclude that the ability of RseB to inhibit RseP cleavage of intact RseA is significantly impaired by the absence of the PDZ domain of RseP.

DegS itself inhibits DegS-independent proteolysis of RseA by RseP

The above experiments were performed in the absence of both DegS and RseB, raising the possibility that DegS also contributes to the inability of RseP to cleave full length RseA in wt cells. We tested this idea by measuring the inhibitory effect of

DegS in the absence of its contribution to RseA proteolysis using a catalytically dead DegS mutant DegS-S201A [23, 29]. Simultaneous overexpression of DegS-S201A and RseP decreases σ^E activity 3 to 4-fold in a *ΔdegSΔrseB* strain compared to overexpression of RseP alone, indicating that DegS inhibits RseP cleavage of full length RseA independently from RseB (Fig. 3-3C). Importantly, the RseP PDZ domain is unnecessary for this inhibitory mechanism as overexpression of DegS-S201A inhibited cleavage of RseA by RsePΔPDZ as well as wt RseP (Fig. 3-3A, compare lanes 2, 4). DegS-S201A inhibits RsePΔPDZ whether or not RseB is present (Fig. 3-3A, compare lanes 3, 5). DegS-mediated inhibition is not an artifact of using the catalytically dead mutant as we can demonstrate inhibition by wt DegS in a circumstance where constitutive cleavage by RseP is likely to contribute to σ^E activity. In Δ*rseB* cells, RseA degradation will be initiated by RseP as well as by activated DegS. This may be the reason why Δ*rseB* cells exhibit a 1.6-fold increase in σ^E activity. Interestingly, overexpression of wt DegS decreased σ^E activity of Δ*rseB* cells to that of wt cells (about 1.6-fold) but did not affect σ^E activity in wt cells (data not shown), consistent with the idea that DegS can inhibit constitutive cleavage of RseA by RseP.

The alternative degradation pathway is not induced by OmpC

In the usual RseA degradation pathway, OMPs directly activate DegS, thereby initiating RseA proteolysis and activating σ^E [23, 29]. We tested whether OMP overproduction also induces σ^E activity via the DegS-independent pathway, either by titrating RseB from RseA or by directly activating RseP cleavage of intact RseA. In

ΔdegSsup$^+$ cells, removal of RseB increased σ^E activity about 6-fold (Fig. 3-1A). Therefore, if OmpC removed RseB from RseA, overexpression of OmpC would significantly increase σ^E activity. It was previously observed [29] and we show here that OmpC overexpression did not increase σ^E activity in *ΔdegSsup*$^+$ cells (Fig. 3-4, compare lanes 5, 6), indicating that OMPs cannot remove RseB from RseA. We then tested whether OmpC overexpression activated RseP. OmpC overexpression did not increase σ^E activity in the *ΔdegSΔrseB* background, where σ^E activity is dependent on the rate of RseP cleavage (Fig. 3-4, compare lanes 7, 8). Therefore OmpC does not activate RseP. Control experiments demonstrated appropriate induction when OmpC overexpression was performed in wt or Δ*rseB* cells (Fig. 3-4, lanes 1-4). In addition, overexpression of OmpC in the *ΔdegSsup*$^+$ and *ΔdegSΔrseB* backgrounds was confirmed by monitoring OmpC levels in the outer membranes of the cells, as described in Mecsas et al. 1993 (data not shown). We conclude that DegS remains the only identified sensor of the OMP signal.

Appropriate downregulation of σ^E activity requires RseB

Removal of OmpR, an activator of *ompC* and *ompF* transcription, decreases OMP expression [151, 152]. This results in fewer OMP intermediates to bind to the PDZ domain of DegS and activate the initiating protease, thereby downregulating σ^E activity [22]. As cells lacking RseB have lost one mechanism for inhibiting RseP cleavage of intact RseA, we suspected that RseP would make a significant contribution to initiating RseA cleavage in such cells. As RseP cleavage does not depend on the OMP signal, it should not be downregulated in response to decreased

concentration of OMP intermediates. We therefore tested whether a Δ*rseB* strain was partially defective in downregulating σ^E activity in response to decreased OMP expression. Whereas deletion of *ompR* in wt cells resulted in about a 20-fold drop in σ^E activity, only a 4-fold decrease in σ^E activity was observed in *ΔrseB* cells (Fig. 3-5A). The Δ*ompR* derivatives have not lost their sensitivity to the OMP signal as overexpressing OmpC from a plasmid strongly induced σ^E activity in both strains (Fig. 3- 5B). These results indicate that RseB is required for appropriate downregulation of σ^E activity in the absence of the OMP inducing signal, and thus is necessary for the full range of response of the system.

A possible second role for RseB?

Since RseB inhibits DegS-independent proteolysis of RseA by RseP, RseB titration by unfolded proteins could be exploited as an alternative way to induce the σ^E pathway. RseB has been shown to co-localize with the periplasmic inclusion bodies, formed by the MalE31 unstable mutant [148, 153]. We therefore tested whether overexpression of MalE31 would activate σ^E in the *ΔdegSsup*$^+$ background, where complete removal of RseB should result in 6-fold induction. Upon overproduction, σ^E activity increased about 1.7-fold, indicating that MalE31 is likely to titrate a small fraction of RseB (25-30%) from RseA (Fig. 3-6, compare lanes 1, 2 and see inset, which presents these data in an expanded scale). We confirmed that induction resulted from removal of RseB rather than activation of DegS or RseP by showing that no detectable σ^E induction was observed in *ΔrseB* or *ΔdegSΔrseB* backgrounds (Fig. 3-6, lanes 3-6). MalE31 overexpression did not perceptibly induce

wt cells (Fig. 3-6, compare lanes 7, 8). As complete removal of RseB results in only a 1.6-fold increase in σ^E activity in wt cells, the limited RseB titration by MalE31 is not expected to result in significant induction in this strain background. This latter finding is in accord with a recent report, that the previously observed increase in DegP synthesis upon accumulation of MalE31 in wt cells is due to activation of the Cpx pathway, rather than σ^E pathway [154].

Discussion

The signal transduction pathway linking periplasmic stress with σ^E activity converts the accumulation of OMP intermediates into activation of the DegS protease. DegS, RseP and ClpX, together with as yet, unidentified cytoplasmic proteases then degrade RseA, the membrane spanning antisigma factor that inhibits σ^E activity (Fig. 3- 7) [22, 23, 30, 36, 37], (J. Flynn, T. Baker, G&D, in press.). The principal goal of this work was to elucidate design features that make the σ^E pathway sensitive to the OMP signal and unresponsive to variations in the levels of DegS and RseP proteases themselves. We find that only DegS senses the OMP signal. Thus, effective coupling of signal to degradation necessitates that only DegS initiates the proteolytic cascade. We show here that RseB, and to a lesser extent, DegS itself, inhibit RseP-mediated degradation of RseA, thereby contributing to the sensitivity and robustness of the σ^E pathway (Fig. 3-7).

Examples of protease cascades that carry out intercompartmental signaling are common from bacteria to humans [2]. The σ^E signal transduction pathway itself is broadly present in gram-negative bacteria. In addition, similar protease cascades have been identified in gram-positive bacteria [47, 155]. For example, it was recently shown that upon alkaline shock in *Bacillus subtilis*, RsiW (an RseA orthologue) is degraded from the extracytoplasmic side to a 14kDa fragment that is further degraded by YluC, an orthologue of RseP [96]. Finally, the DegS family of proteases is widely distributed among prokaryotic and eukaryotic organisms, where they have been implicated in stress signaling pathways [156]. For example, murine HtrA2 has been suggested to sense mitrochondrial stress [157]. Although the signals inducing these

other responses may be entirely different [2], these cascades will need to utilize mechanisms comparable to those described here to ensure signal-dependent initiation of proteolysis. Strategies similar to those elucidated here may be utilized by many such cascades to block the degradation of intact regulator by proteases meant to function after the initiating event.

RseP is able to cleave intact RseA in cells lacking DegS and RseB

In wt cells, cleavage of RseA is overwhelmingly initiated by DegS, as demonstrated by the fact that in the absence of this protease, σ^E activity is very low and RseA is a stable protein (Fig. 3-7A) [29, 36, 37]. In the present work, we demonstrate that removal of RseB in addition to DegS significantly increases σ^E activity and RseA cleavage. Elimination of RseB could either expose RseA to proteases that substitute for DegS in performing initial cleavage of RseA or allow RseP to cleave intact RseA more efficiently. Our data support the later idea.

DegS cleavage of RseA is the rate-limiting proteolytic step in wt cells. Thus, increasing the amount or altering the activity of RseP has little effect on σ^E activity [36]. It is probably the case because RseP cleavage of intact RseA is effectively inhibited, while DegS cleaved RseA is a very attractive substrate for RseP [38]. In cells lacking RseB and DegS, the situation is very different. We have conclusively demonstrated that σ^E activity correlates with the level and activity of RseP, indicating that RseP cleavage is now the rate-limiting step in generating active σ^E in such cells. This finding rules out the idea that some other protease cleaves in the vicinity of the DegS cleavage site to generate an attractive RseP substrate. In that case, the other

protease, not RseP, would be rate limiting for the reaction. In further validation of the idea that RseP itself performs the initial cleavage event, we show that in *ΔdegSΔrseB* cells, RseP overexpression increases the rate of degradation of full-length RseA rather than an intermediate formed by preliminary cleavage by other proteases. Together these data support the idea that removing both RseB and DegS partially relieves the inhibitory mechanisms that prevent RseP cleavage of intact RseA (Fig. 3-7B).

Our data suggest that at least two independent mechanisms inhibit RseP from cleaving intact RseA. The first mechanism requires the presence of the PDZ domain of RseP. Both the two Gln-rich regions of RseA [38] and RseB inhibit cleavage of intact RseA by RseP but not by RsePΔPDZ. The most parsimonious interpretation of these data is that the RseP PDZ domain, RseB and the Gln-rich RseA region all participate in the same inhibitory reaction. We tested whether RseB binding to the Gln-rich regions of RseA might make RseA refractory to RseP cleavage. As periplasmic RseA variants with amino acid substitutions in one or both Gln-rich regions (Gln to Ala) bind RseB indistinguishably from wt RseA, this idea is not correct (data not shown) [38]. As an alternative, RseB binding to RseA might facilitate a conformational change in RseA that makes its Gln-rich regions more accessible to binding by the PDZ domain of RseP, thereby facilitating the inhibitory reaction. Of course, we cannot eliminate the possibility that RseB binds independently to the RseP PDZ domain to inhibit cleavage. We note that bacterial RseP orthologues all contain PDZ domains. Therefore it is likely that these domains play similar role(s) in other systems.

The second mechanism for inhibiting RseP cleavage of intact RseA involves a reaction mediated by unactivated DegS and is independent of the PDZ domain of RseP. DegS could negatively regulate RseP by forming a complex with RseA, thereby either blocking or altering the RseA recognition sites for RseP. Because overexpression of catalytically dead DegS-S201A does not inhibit σ^E activity in wt cells (data not shown), we believe it is unlikely that DegS-S201A occludes RseA, as this binding should also reduce the ability of wt DegS to initiate cleavage. Alternatively, unactivated DegS could form a complex with RseP thereby reducing its ability to cleave intact RseA. Interestingly, whereas unactivated DegS-S201A inhibits RseP cleavage, DegS-S201A activated by overexpression of OmpC-termini increases the rate of RseP cleavage (data not shown). Together these experiments suggest that complex interactions between DegS and RseP may promote cleavage of RseA in response to the activation signal.

RseB and DegS increase both the sensitivity and robustness of the signal-transduction pathway activating σ^E

To provide adequate response to signals, signal transduction pathways must sense inducing signals over a wide concentration range, and to be unresponsive to variations in the concentrations of the signal transduction molecules themselves. The work reported here documents the roles of RseB and DegS in enhancing these two properties of the σ^E signal transduction pathway.

In wt cells, the signal-transduction pathway activating σ^E is sensitive to a wide range of OMP concentrations. σ^E activity changes more than 40-fold from its low point in a *ΔompR* strain, which should have a very low concentration of unassembled OMPs, to its high point in a wt strain with overproduced OMPs (Fig. 3-5A, B). Cells can modulate σ^E activity over such a broad range because the system is designed so that the rate-limiting step in activation is sensitive to the OMP signal. This is achieved as follows. OMP binding to the PDZ-domain of DegS activates a corresponding fraction of the DegS molecules (Fig. 3-7A). Because DegS-dependent initiation of RseA degradation is the rate-limiting step in proteolysis, the rate of RseA degradation is set to be proportional to the amount of active DegS and thus to the OMP signal. Therefore, a graded σ^E response over a wide range of OMP signals requires initiation of RseA proteolysis via active DegS. In the present work we showed that RseB is required to make RseA proteolysis completely dependent on DegS. In the absence of RseB, RseP, which ordinarily degrades only DegS cleaved RseA, is able to cleave intact RseA (Fig. 3-7B). As RseP is not responsive to the OMP signal, this decreases the extent to which σ^E activity reflects the concentration of OMP intermediates. This deficit is clearly seen in a *ΔompR* strain, where Δ*rseB* cells show a 4-fold higher activity than wt cells. Additionally, DegS plays a second role by reinforcing sequential cleavage. It not only senses the OMP signal but also, in its unactivated form, inhibits RseP cleavage of intact RseA, thereby reinforcing the dependence on activated DegS for initiating proteolysis (Fig. 3-7C). Together, these two mechanisms increase the sensitivity of the system to OMP signal.

In wt cells, σ^E activity is unaffected by variations in the levels of RseP or DegS [36]. This situation results from the fact that the rate of RseA degradation is determined solely by the amount of active DegS, which is defined by the extent of the OMP signal. In contrast, when cells lack RseB, changes in either RseP or DegS levels are translated into changes in σ^E activity. Because RseP can initiate RseA degradation constitutively in cells lacking RseB, σ^E activity increases with increased amounts of RseP. For this same reason, σ^E activity decreases with increased amounts of DegS, as accumulation of DegS inhibits RseP cleavage of intact RseA. The σ^E pathway might be unresponsive to the protease levels in order to suppress the contribution of "noise" in the system, which could arise from stochastic variation, lack of tight control or alteration in the levels of these proteases as part of another physiological pathway. In conclusion, by turning off RseP-initiated proteolysis of RseA, RseB and DegS make the system both sensitive to the OMP signal, and insensitive (robust) to variations in the absolute levels of DegS and RseP.

RseB is a possible sensor of other periplasmic stress signals

It is rather curious that cells employ a separate protein, RseB, in addition to interactions between RseA and RseP to dampen RseP activity and adjust the sensitivity and robustness of the system, and that RseB is not removed by OmpC overexpression. One possibility is that RseB plays an additional role in the signal transduction pathway. The full extent of signals inducing σ^E pathway is currently unknown, as is the essential activity of this system. Based on our indication that overexpression of MalE31 could partially titrate RseB from RseA, we speculate that

in addition to the OMP signal, other signals may exist that activate σ^E by titrating RseB from RseA and thus activate RseP-dependent proteolysis of the anti-sigma factor. In this scenario, RseB would act as a "switch" between the two modes of RseA degradation: DegS-dependent and OMP sensitive vs. RseP-dependent and OMP insensitive. RseB would then be responsible for adjusting the sensitivity of the pathway to these different types of signals. We are currently determining whether physiologically relevant signals of this type exist.

Materials and methods

Media and antibiotics

Luria-Bertani (LB) and M9 minimal medium were prepared as described [149]. M9 was supplemented with 0.2% glucose, 1 mM $MgSO_4$, 2 μg/mL thiamine, and all amino acids (40 μg/mL), except methionine. When required, the media was supplemented with 30 μg/mL kanamycin (Kan), 20 μg/mL chloramphenicol (Cm), and/or 100 μg/mL ampicillin (Ap). A final concentration of 0.2% L-(+)-arabinose was used to induce the expression of *rseP* and *ompC* from the arabinose-inducible promoter P_{ara}. 0.2% glucose was used to repress expression of *rseP* from P_{ara}. Isopropyl-β-D-galactoside (IPTG) at a final concentration of 0.1 mM was added to induce the expression of *rseP*, *rseP-E23D*, *malE31*, and *degS* from the P_{Trc} promoter.

Strains

Bacterial strains used in this study are described in Table 3 2.

Plasmids

pRseP was constructed in two steps. The *rseP* gene was amplified from *E. coli* MG1655 DNA with primers 5'-ccggaattcatgctgagttttctctgggatttggc-3' and 5'-gcgggatcctcataaccgagagaaatcattgaaaagtgcaag-3'. The product was then digested with restriction enzymes *Bam*HI/*Eco*RI and cloned at the corresponding sites of vector pTrc99a.

pRseP-E23D (glutamic acid 23 changed to aspartic acid) was constructed by quick change mutagenesis with primers 5'yaeLig02: 5'-cttatcaccgtgcatgattttggtcatttctgg-3' and 3'yaeLig02: 5'-ccagaaatgaccaaaatcatgcacggtgataag-3' using pRseP as the template.

pRsePΔPDZ was obtained from pRseP by deleting the PDZ domain of RseP (glutamic acid E203 through glutamine Q279) by quick change mutagenesis with primers 5'yaeLig04: 5'-gtaaagctcgatttacgtcactgggcgtttgggagtcccttgtctttgacattaatcccg-3'and 3'yaeLig04: 5'-cgggattaatgtcaaagacaagggactcccaaacgcccagtgacgtaaatcgagctttac-3'.

For the construction of pIG02, *malE* was PCR amplified from *E. coli* MG1655 DNA with primers malE1: 5'- ggggtaccaggaccatagattatgaaaataaaaacaggtgca-3' and malE2, 5'-ggaagcttttacttggtgatacgagtc-3' followed by digestion at *Kpn*I/*Hind*III and ligation at the corresponding sites of pBA169. The *malE* double mutant (glycine 32 changed to aspartic acid and isoleucine 33 changed to proline) was generated by quick-change mutagenesis using primers malE3 5'-ttcgagaaagataccgatccgaaagtcaccgttgag-3'and malE4 5'-ctcaacggtgactttcggatcggtatctttctcgaa-3'.

β-galactosidase assays

Overnight cultures were diluted to an OD_{600} ~ 0.03 (in LB) or OD_{450} ~ 0.02 (in supplemented M9 minimal medium) and grown at 30°C. In experiments with *rseP*,

rseP-E23D, *rseP*ΔPDZ, *degS*, *degS*-S201A, *ompC*, *and malE31* overproduction, arabinose or IPTG was added immediately after dilution to turn on transcription from P_{ara} or P_{Trc} promoters respectively. σ^E activity was measured by monitoring β-galactosidase expression from a single-copy σ^E dependent *lacZ* reporter gene. β-galactosidase activity/0.5 ml cells was plotted versus OD_{600} of the culture. The observed plots showed two linear regions: the first linear region, at OD_{600} less than 0.25 - 0.3 had a smaller slope, and the second, at OD_{600} between 0.3 and 0.6 had a bigger slope (data not shown). Existence of the two phases implied that there was a growth-phase dependent increase in σ^E activity at OD_{600} around 0.3. Interestingly, in the cells lacking wild type *degS* the second slope was not observed. β-galactosidase activity/0.5 mL of cells was plotted against $OD_{600}(OD_{450})$ ranging from 0.3 to 0.6. The slope of the data, representing the differential rate of β-galactosidase synthesis and a measure of σ^E activity, was calculated. All assays were performed at least twice reproducibly and data from a single experiment is shown. In some cases, where differences were small, assays were performed ≥3X and data from all samples with error are shown. Assays were performed as described [22, 29, 158].

Determination of RseA stability by pulse-chase immunoprecipitation

Cells were grown in supplemented M9 minimal medium lacking methionine (with added antibiotics and arabinose/IPTG when necessary) at 30°C. At OD_{450} ~ 0.3 the cells were pulse-labeled for 1 min by L-[^{35}S]methionine, followed by a chase of 0.1% cold methionine and samples processed as described [34].

RseP depletion in vivo

CAG43509 and CAG51036 were grown at 30°C in LB/Cm/arabinose to an OD_{600} ~ 0.3. The culture was poured onto a 0.45 μm Millipore filter (Millipore) in a Nalgene filtering system and washed with 10 mL of 30°C LB. The cells were resuspended in 30°C LB/Cm containing glucose to an OD_{600} ~ 0.03. The culture was maintained in exponential growth phase by periodically diluting the culture (to OD_{600} ~ 0.03) into a flask with fresh, prewarmed media. Aliquots were sampled for western blots.

Western blotting (RseP, cyto-RseA)

Western blotting of RseP and RseA was performed as described [36]. The Western blots were developed with the SuperSignal West Dura Extended Duration Substrate from Pierce. Epi Chemi II Darkroom (UVP Laboratory Products) was used to capture the light emitted from the blots. The band's intensity was quantified using associated software (Labworks).

Acknowledgements

We thank Tania Baker and Akiyama Yoshinori for communicating unpublished results. We also thank Eric Guisbert and Svetlana Makovets for critically reading the manuscript. This work was supported by U.S. Public Health Service Grant GM36278-18 from the NIH to C.A.G. and a Burroughs Wellcome Predoctoral Fellowship awarded to I.L.G.

Table 3-1. *P1 transduction experiments demonstrate that DegS is dispensable in ΔrseB cells whereas RseP is essential in all backgrounds tested*

		Donor P1 strain			
		ΔdegS argR::Tn5 (CAG43081)			*rseP::kan* (CAG43445)
Recipient	Strain	Number of Kan^R colonies	Number tested by colony PCR	% linkage	Number of Kan^R colonies
ΔrseB	(CAG22951)	~70[a] ~35[b]	9 11	67 36	0 n/d
wt	(CAG16037)	~10	9	0	0
ΔdegSs up⁺ ΔrseB	(CAG51021)	n/d n/d	n/d n/d	n/d n/d	0[a] 0[b]

[a],[b] stand for two separate experiments. Control transductions showed that each recipient strain is transducible (data not shown).
n/d – not determined

Table 3-2 *Strains and plasmids used in this study*

Strains/plasmids	Relevant genotype	Source/reference/P1 transduction donor strains
Strains		
MC1061	*araD Δ(ara-leu)7697 Δ(codB-lacI) galK16 galE15 mcrA0 relA1 rpsL150 spoT1 mcrB9999 hsdR2*	(Casadaban and Cohen 1980); *E. coli* Genetic Stock Center
CAG16037	MC1061 Φλ[*rpoH P3::lacZ*]	(Mecsas et al. 1993)
CAG22951	16037 *ΔrseB nadB-3140::Tn10*, Tet^R	(De Las Penas et al. 1997)
CAG22955	WT *ΔrseB nadB::Tn10*, Kan^R	(De Las Penas, unpublished)
CAG33315	MC1061 *ΔdegS* Φλ[*rpoH P3::lacZ*]	(Ades et al. 1999)
CAG41001	MC1061 *rpoE+* with supressor of *rpoE*::ΩCm	(Alba et al. 2001)
CAG43081	MC1061 *ΔdegS arg::Tn5*, Kan^R	(Alba et al. 2001)
CAG43216	16037 pBA114, Cm^R	(Walsh et al. 2003)
CAG43217	16037 *ompR::Tn10*, Tet^R	(this work)
CAG43256	16037 pBAD33, Cm^R	(this work)
CAG43263	33315 pTrc99a, Ap^R	(this work)
CAG43278	33315 pBAD33, Cm^R	(this work)
CAG43341	22951 pTrc99a, Ap^R, Tet^R	(this work)
CAG43445	*rseP::kanR* pJAH184, Kan^R, Cm^R	Jennifer Leeds
CAG43509	16037 *rseP::kanR* pJAH184, Kan^R, Cm^R	(Alba et al. 2002)
CAG43586	16037 pBA191, Ap^R	(this work)
CAG43604	16037 pBA169, Ap^R	(Walsh et al. 2003)
CAG43605	33315 pBA169, Ap^R	(Walsh et al. 2003)

CAG43629	33315 pBA114, Cm^R	(this work)
CAG51021	33315 *ΔrseB nadB::Tn10*, Tet^R	(this work, P1 donor CAG22951)
CAG51025	22951 *ΔdegS arg::Tn5*, Km^R, Tet^R	(this work, P1 donor CAG43081)
CAG51032	22951 pBA114, Cm^R, Tet^R	(this work)
CAG51033	22951 pBAD33, Cm^R, Tet^R	(this work)
CAG51034	51021 pJAH184, Cm^R, Tet^R	(this work)
CAG51035	51021 pBAD45, Cm^R, Tet^R	(this work)
CAG51036	51034 *rseP::kanR* pJAH184, Kan^R, Cm^R, Tet^R	(this work, P1 donor CAG43445)
CAG51050	16037 *ΔrseB nadB::Tn10*, Km^R	(this work, P1 donor CAG22955)
CAG51055	51050 *ompR::Tn10*, Tet^R, Km^R	(this work, P1 donor CAG43217)
CAG51057	43217 pBAD33, Cm^R,Tet^R	(this work)
CAG51058	43217 pBA114, Cm^R,Tet^R	(this work)
CAG51059	51055 pBAD33, Cm^R,Tet^R, Km^R	(this work)
CAG51060	51055 pBA114, Cm^R,Tet^R, Km^R	(this work)
CAG51070	16037 pIG02, Ap^R	(this work)
CAG51072	51050 pIG02, Ap^R. Km^R	(this work)
CAG51074	33315 pIG02, Ap^R	(this work)
CAG51076	16037 pJAH184, Cm^R	(this work)
CAG51077	51025 pJAH184, Cm^R, Km^R, Tet^R	(this work)
CAG51079	51025 pIG02, Ap^R. Km^R,Tet^R	(this work)
CAG51083	51025 pBAD33, Cm^R, Km^R, Tet^R	(this work)
CAG51084	51025 pBAD45, Cm^R, Km^R, Tet^R	(this work)
CAG51085	16037 pBAD45, Cm^R	(this work)
CAG51091	16037 pRseP, Ap^R	(this work)
CAG51092	51025 pRseP, Ap^R, Km^R, Tet^R	(this work)
CAG51093	51025 pBA169, Ap^R, Km^R, Tet^R	(this work)
CAG51098	22951 pBA191, Ap^R, Tet^R	(this work)
CAG51108	51025 pBA114, Cm^R, Km^R, Tet^R	(this work)
CAG51115	51092 pRseP, pSU21, Ap^R, Cm^R, Km^R, Tet^R	(this work)
CAG51116	51092 pRseP, pLC261, Ap^R, Cm^R, Km^R, Tet^R	(this work)
CAG51120	51093 pBA169, pSU21, Ap^R, Cm^R, Km^R, Tet^R	(this work)
CAG51122	51025 pRseP-E23D, Ap^R, Km^R, Tet^R	(this work)
CAG51138	51091 *rseP::kanR* Kan^R, Ap^R	(this work, P1 donor CAG43445)
CAG51139	16037 *rseP::kanR* pRsePΔPDZ, Ap^R, Kan^R	(this work, P1 donor CAG43445)
CAG51140	22951 *rseP::kanR* pRsePΔPDZ, Ap^R, Tet^R, Kan^R	(this work, P1 donor CAG43445)
CAG51143	33315 *rseP::kanR* pRseP, Ap^R, Kan^R	(this work, P1 donor CAG43445)
CAG51144	51021 *rseP::kanR* pRsePΔPDZ, Ap^R, Tet^R, Kan^R	(this work, P1 donor CAG43445)
CAG51146	33315 *rseP::kanR* pRsePΔPDZ, Ap^R, Kan^R	(this work, P1 donor CAG43445)
CAG51147	51144 pSU21, Cm^R, Ap^R, Tet^R, Kan^R	(this work)
CAG51148	51144 pLC261, Cm^R, Ap^R, Tet^R, Kan^R	(this work)
CAG51149	51146 pSU21, Cm^R, Ap^R, Kan^R	(this work)
CAG51150	51146 pLC261, Cm^R, Ap^R, Kan^R	(this work)

Plasmids

pLC261	*degS*-S201A and *degS* promoter in pSU21, Cm^R	(Ades et al. 1999)
pJAH184	*rseP* in pBAD45, Cm^R	(Alba et al. 2002)
pBA169	pTrc99A ΔNcoI, Ap^R	(Walsh et al. 2003)
pBA191	DegS-6His in pBA169, Ap^R	(Walsh et al. 2003)
pBA114	*ompC* in pBAD33, Cm^R	(Alba et al. 2002)
pBAD33	Vector, pACYC ori, Para, Cm^R	(Guzman et al. 1995)
pSU21	Vector, p15a ori, *lac* promoter, Cm^R	(Bartolome et al. 1991)
pTrc99a	Vector, pBR322 ori, Ap^R	(Amersham Pharmacia Biotech)
pBAD45	Vector, p15A ori, Para, Cm^R	(Beckwith lab)
pRseP	*rseP* in pTrc99a, Ap^R	(this work)
PRseP-E23D	*rseP-E23D* in pTrc99a, Ap^R	(this work)
pRsePΔPDZ	*rsePΔPDZ* in pTrc99a, Ap^R	(this work)
pIG02	*malE31* in pBA169, Ap^R	(this work)

Figure Legends:

Figure 3-1. σ^E activity and RseA degradation in *ΔrseB* strains.

A. Relative σ^E activity in the wild-type (CAG16037), *ΔrseB* (CAG22951), *ΔdegSsup*$^+$ (CAG33315), *ΔdegSsup*$^+$*ΔrseB* (CAG51021), and *ΔdegSΔrseB* (CAG51025) strains grown in LB at 30°C. Samples were assayed for σ^E activity by monitoring β-galactosidase activity produced from a single-copy [Φ*λrpoH* P3::*lacZ*] fusion. The differential rate of *lacZ* synthesis was quantified as described in Materials and Methods.

B. RseA stability in the wild-type (■), *ΔrseB* (○), and *ΔdegSΔrseB* (▲) strains. Cells were grown in supplemented M9 media at 30°C to OD_{450} ~ 0.3, pulse-labeled with [^{35}S]methionine followed by chase of cold methionine. The stability of RseA was determined as described in Materials and Methods.

Figure 3-2. Effects of RseP overexpression on σ^E activity and RseA stability in the wild-type and *ΔdegSΔrseB* strain backgrounds. Wild-type cells containing the plasmid pRseP (CAG51091) or vector alone (CAG43604) and *ΔdegSΔrseB* cells with vector (CAG51093), pRseP (CAG51092) and pRseP-E23D (CAG51122) were grown in supplemented M9 media in the presence of IPTG at 30°C.

A. Relative σ^E activity in the wild-type and *ΔdegSΔrseB* cells with vector alone (white bar), with overexpressed RseP (grey bar) and with overexpressed RseP-E23D (lined bar) was assayed by monitoring β-galactosidase activity produced from a

single-copy [Φλ*rpoH* P3::*lacZ*] fusion. The differential rate of *lacZ* synthesis was quantified as described in Materials and Methods.

B. Relative RseP levels in the wild-type and *ΔdegSΔrseB* cells with vector alone (white bar), with overexpressed RseP (grey bar) and with overexpressed RseP-E23D (lined bar). At OD_{450} ~ 0.3 cells were collected and TCA-precipitated. RseP levels were determined by Western blot analysis as described in Material and Methodes with polyclonal antibodies to RseP.

C.D. RseA stability in *ΔrseBΔdegS* cells with overexpressed RseP from pRseP plasmid, or with vector alone. Cells were grown to OD_{450} ~ 0.3, pulse-labeled with [^{35}S]methionine and chased with cold methionine. At various time points after the chase cells were collected and TCA precipitated. Equal amounts of [^{35}S]methionine labeled periplasmic domain of RseA, used as the standard (RseA*), were added to the samples, and then intracellular RseA and the standard were immunoprecipitated with antibodies against peri-RseA. The stability of RseA was determined as described in Materials and Methods. Representative data is shown in Fig. 3-2C and plotted in Fig. 3-2D.

Figure 3-3. The role of the RseP PDZ domain and DegS in inhibiting σ^E activity.

A. Effects of the presence of RseB and overexpression of a catalytically dead DegS mutant DegS-S201A on σ^E activity in cells with RseP ΔPDZ. σ^E activity in various strains grown in LB at 30°C was determined as described in Fig. 2. White bar: *ΔdegS*sup$^+$*ΔrseP* cells carrying pRseP plasmid (CAG51143, white bar); Grey bars: *ΔdegS*sup$^+$*ΔrseP* (CAG51149) and *ΔdegS*sup$^+$*ΔrsePΔrseB* (CAG51147) cells

carrying pRsePΔPDZ plasmid and pSU21 vector; lined bars: *ΔdegS*sup$^+$*ΔrseP* (CAG51150) and *ΔdegS*sup$^+$*ΔrsePΔrseB* (CAG51148) cells carrying pRsePΔPDZ and pLC261 plasmids.

B. σ^E activity increases when RsePΔPDZ is induced. σ^E activity in the *ΔdegS*sup$^+$ *ΔrseP* strain carrying pRsePΔPDZ plasmid and pSU21 vector (CAG51149) grown in LB at 30°C determined as described in Fig. 3-2A, with (+IPTG) or without (-IPTG) overexpression of RsePΔPDZ.

C. Effect of overexpression of DegS-S201A on σ^E activity induced by overexpression of RseP. σ^E activity in cells grown in supplemented M9 medium in the presence of IPTG at 30°C was determined as described in Fig. 3-2A. White bar: *ΔdegSΔrseB* cells carrying pTrc99a and pSU21 vectors (CAG51120); grey bar: *ΔdegSΔrseB* cells carrying the pRseP plasmid and pSU21 vector (CAG51115); lined bar: *ΔdegSΔrseB* cells carrying pRseP and pLC261 encoding DegS-S201A (CAG 51116)

Figure 3-4. Induction of σ^E activity by overexpression of OmpC in various strains. Relative σ^E activity in cells grown in LB with arabinose at 30°C, determined as described in Fig. 3-2A. White bar: cells carrying vector; Grey bar: cells carrying pOmpC in the following backgrounds: wild-type (CAG43256 and CAG43216), *ΔrseB* (CAG51033 and CAG51032), *ΔdegS*sup$^+$ (CAG43278 and CAG43629), and *ΔdegSΔrseB* (CAG51083 and CAG51108).

Figure 3-5. Downregulation of σ^E activity by deletion of *ompR*. Relative σ^E activity was assayed as described in Fig. 3-1A.

A. Downregulation of σ^E activity upon deletion of *ompR* in the wild-type and *ΔrseB* strains. Wild-type and *ΔrseB* cells with wild-type *ompR* (CAG16037 and CAG51050, white bar) or with deleted *ompR* (CAG43217 and CAG 51055, lined bar) were grown in LB at 30°C.

B. Induction of σ^E activity in the *ΔompR* and *ΔompRΔrseB* strains by overexpression of OmpC. *ΔompR* and *ΔompRΔrseB* cells carrying vector alone (CAG51057 and CAG51059, lined bar) and pOmpC plasmid (CAG51058 and CAG51060, grey bar) were grown in LB with arabinose at 30°C.

Figure 3-6. Induction of σ^E activity by overexpression of MalE31 in various strains. Relative σ^E activity of cells grown in LB with IPTG at 30°C, determined as described in Fig. 3-2A. Shown are the average values from three experiments. White bar: cells carrying vector alone; grey bar: cells carrying pMalE31 in the following strain backgrounds: wild-type (CAG43604 and CAG51070), *ΔrseB* (CAG43341 and CAG51072), *ΔdegS*sup$^+$ (CAG43605 and CAG51074), and *ΔdegSΔrseB* (CAG51080 and CAG51079). The inset shows data for the *ΔdegS*sup$^+$ background on an expanded scale.

Figure 3-7. Various modes of RseA degradation.

A. Wild type: DegS-dependent proteolysis of RseA. OMP monomers activate DegS by binding to the PDZ domain of DegS. DegS initiates proteolysis of RseA. RseP can cleave RseA fragment generated by DegS cleavage.

B. *ΔdegSΔrseB*: RseP can initiate cleavage of the full-length RseA in the absence of RseB and DegS, that block RseP from cleaving RseA in wt cells.

C. *ΔompR*: In the absence of the OMP signal, DegS is catalytically inactive and therefore does not initiate degradation of RseA. RseA is not degraded.

Figure 3-1.

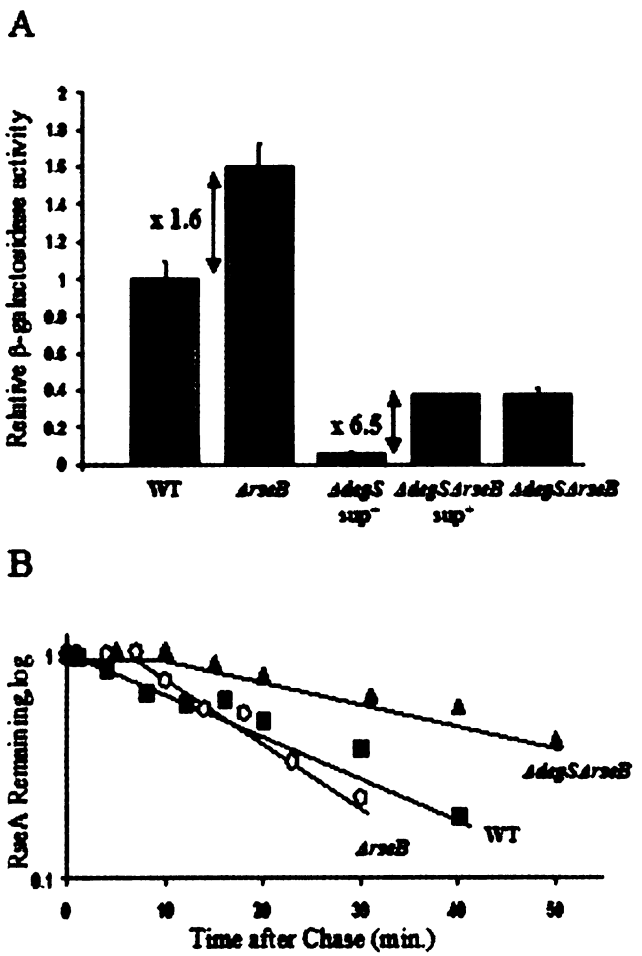
A
Relative β-galactosidase activity
x 1.6
x 6.5
WT
ΔrseB
ΔdegS sup⁻
ΔdegSΔrseB sup⁺
ΔdegSΔrseB
B
RseA Remaining, log
ΔdegSΔrseB
WT
ΔrseB
Time after Chase (min.)

Figure 3-2.

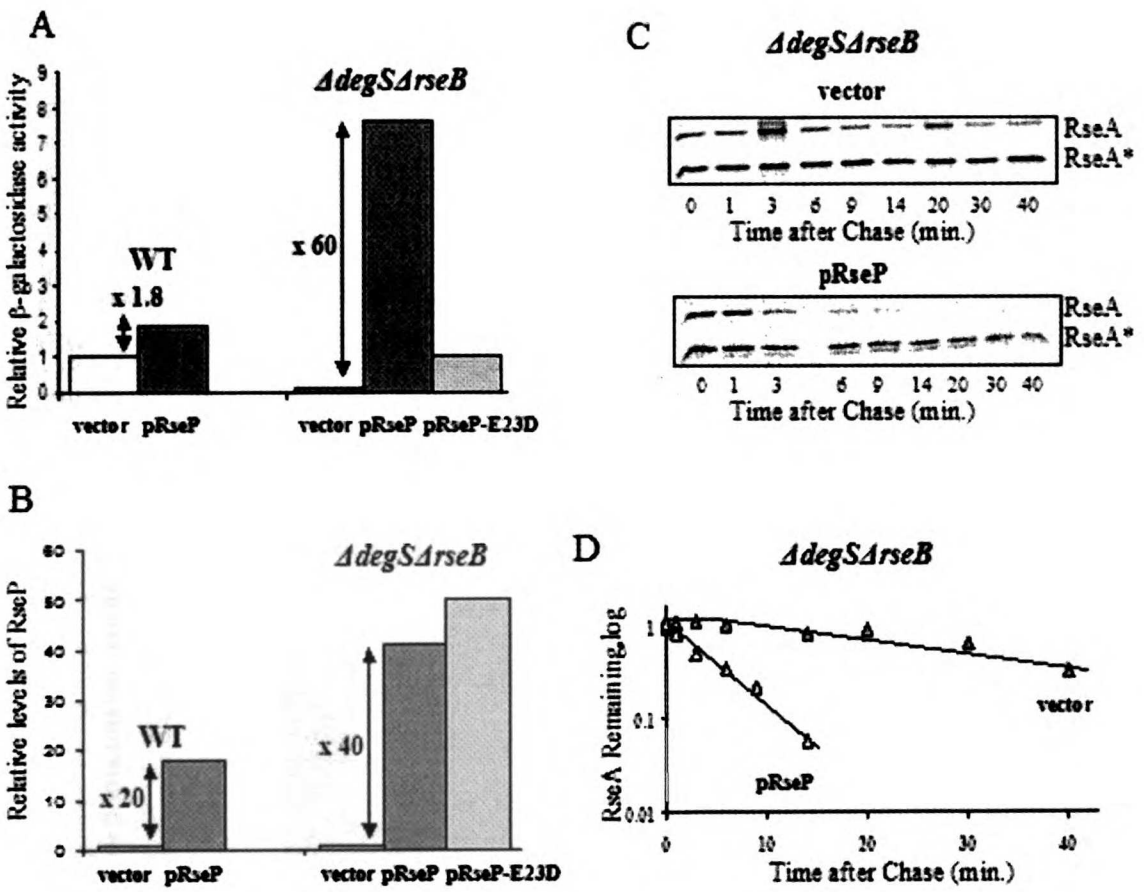
A
ΔdegSΔrseB
Relative β-galactosidase activity
WT
x 1.8
x 60
vector pRseP
vector pRseP pRseP-E23D
B
ΔdegSΔrseB
Relative levels of RseP
WT
x 20
x 40
vector pRseP
vector pRseP pRseP-E23D
C
ΔdegSΔrseB
vector
RseA
RseA*
0 1 3 6 9 14 20 30 40
Time after Chase (min.)
pRseP
RseA
RseA*
0 1 3 6 9 14 20 30 40
Time after Chase (min.)
D
ΔdegSΔrseB
RseA Remaining,log
vector
pRseP
0 10 20 30 40
Time after Chase (min.)

Figure 3-3.

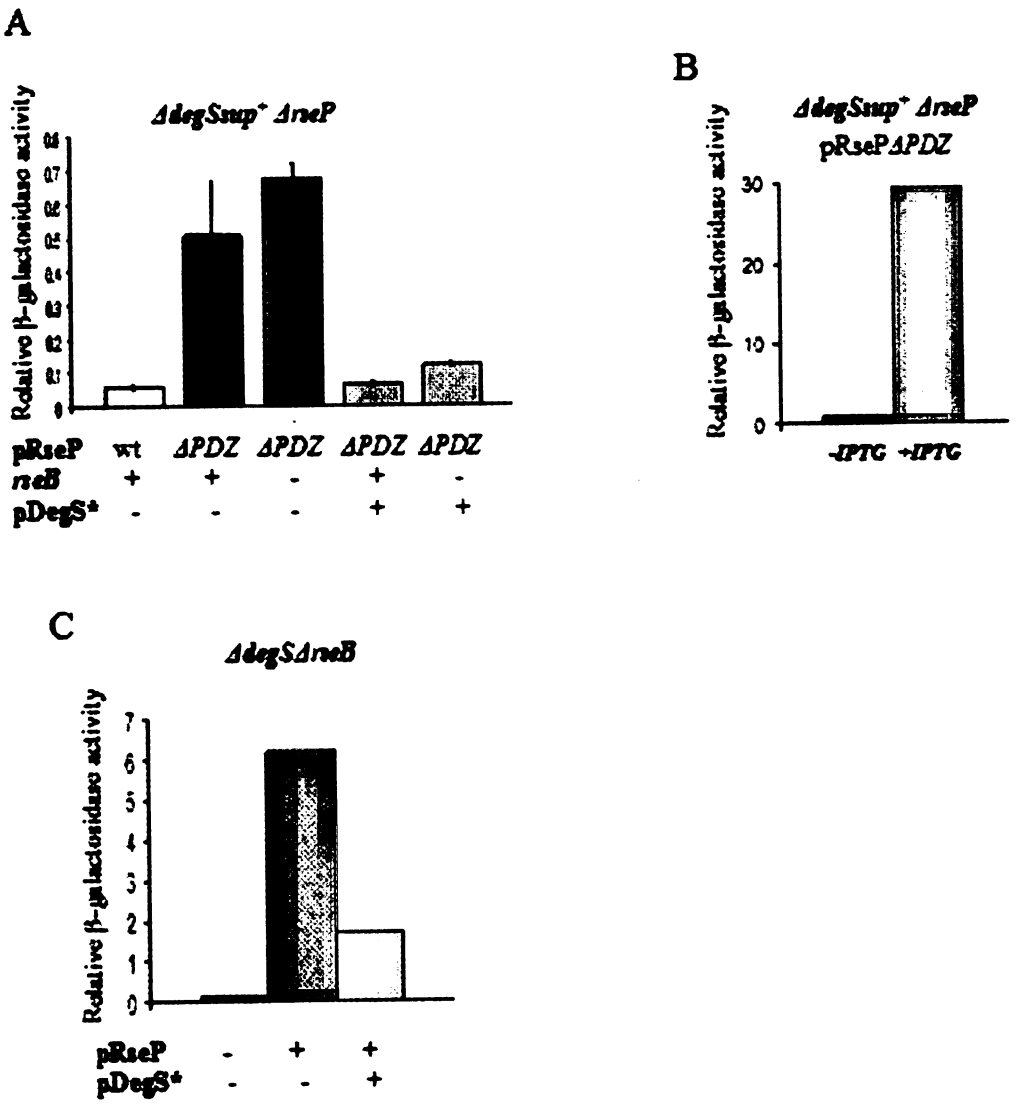
A
ΔdegSΔrseP+ ΔrseP
Relative β-galactosidase activity
pRseP wt ΔPDZ ΔPDZ ΔPDZ ΔPDZ
rseB + + - + -
pDegS* - - - + +
B
ΔdegSΔrseP+ ΔrseP
pRsePΔPDZ
Relative β-galactosidase activity
30
20
10
0
-IPTG +IPTG
C
ΔdegSΔrseB
Relative β-galactosidase activity
7
6
5
4
3
2
1
0
pRseP - + +
pDegS* - - +

Figure 3-4.

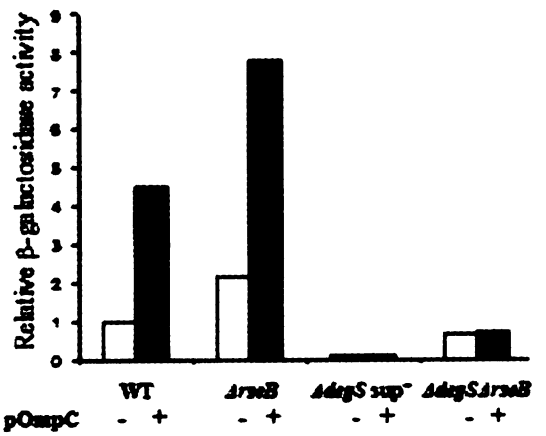
Relative β-galactosidase activity
0
1
2
3
4
5
6
7
8
9
WT
ΔrseB
ΔdegS sup⁻
ΔdegSΔrseB
pOmpC
- +
- +
- +
- +

Figure 3-5.

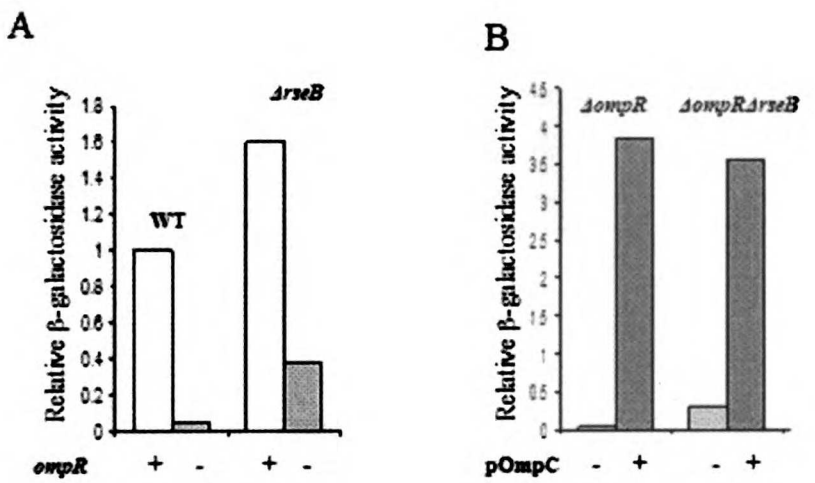
A
ΔrseB
WT
Relative β-galactosidase activity
1.8
1.6
1.4
1.2
1
0.8
0.6
0.4
0.2
0
ompR + - + -
B
ΔompR
ΔompRΔrseB
Relative β-galactosidase activity
4.5
4
3.5
3
2.5
2
1.5
1
0.5
0
pOmpC - + - +

Figure 3-6.

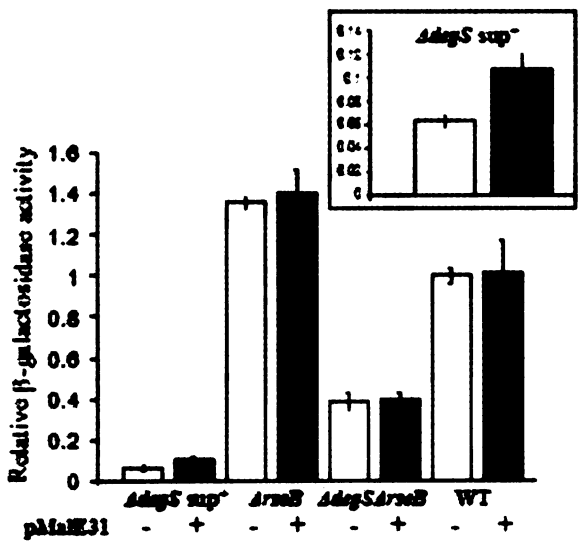
ΔdegS supˢ
Relative β-galactosidase activity
1.6
1.4
1.2
1
0.8
0.6
0.4
0.2
0
ΔdegS supˢ
ΔrnaE
ΔdegSΔrnaE
WT
pMiniR31
-
+
-
+
-
+
-
+

Figure 3-7.

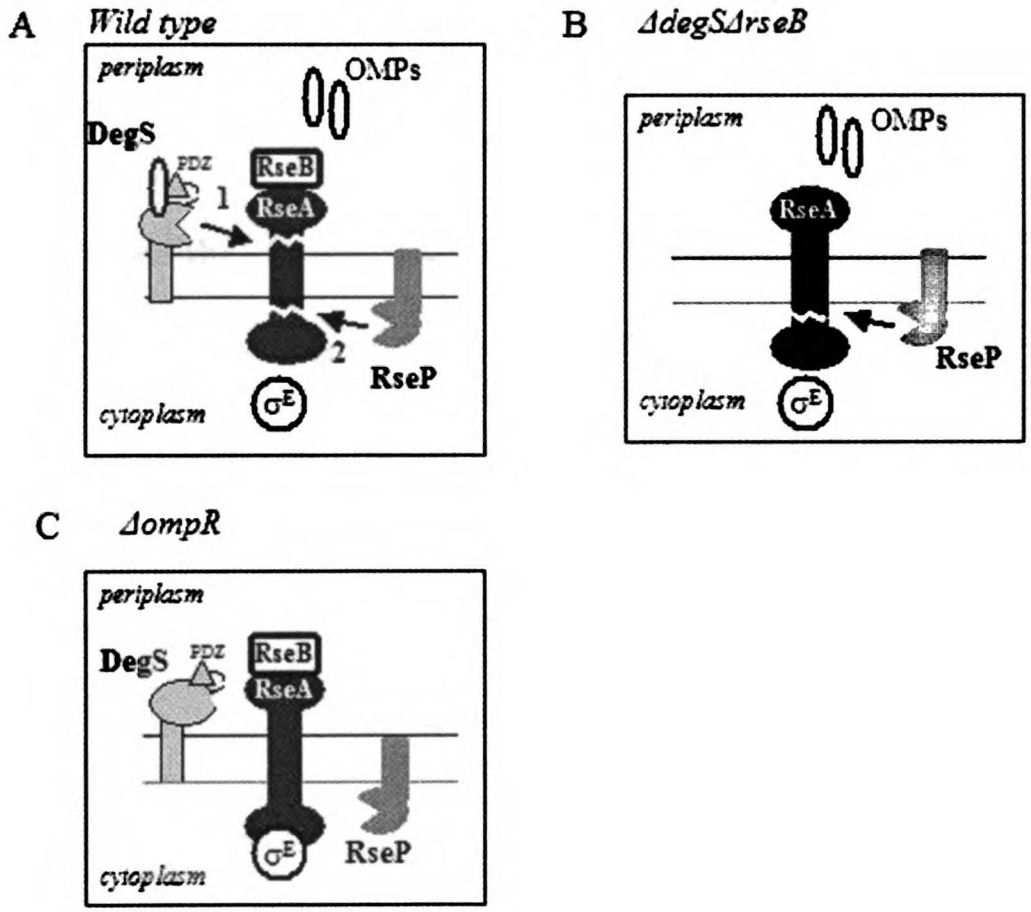
A
Wild type
periplasm
OMPs
DegS
PDZ
1
RseB
RseA
2
RseP
cytoplasm
σE
B
ΔdegSΔrseB
periplasm
OMPs
RseA
RseP
cytoplasm
σE
C
ΔompR
periplasm
DegS
PDZ
RseB
RseA
σE
RseP
cytoplasm

Chapter Four

Insights into nonspecific binding of RNA polymerase to DNA

and σ competition for Core

from an equilibrium model of RNA polymerase binding to DNA.

Summary

In this work we remeasured the levels of E, σ^{70}, σ^{E} and σ^{32} in *E. coli* and developed an equilibrium model that describes the partitioning of RNAP between promoters, nonspecific DNA binding sites and the cytoplasm. By exploring how critical parameters of the model affect promoter saturation with $E\sigma^{70}$ and σ competition, we have obtained important insights on into each of these processes.

Our model suggests that nonspecific binding of holoenzyme to DNA plays a critical role in the extent of promoter saturation. It predicts that strong nonspecific DNA binding is required to keep promoters far from saturation. Weak promoters must be relatively free of holoenzyme *in vivo*, for their binding affinities to contribute to variation in promoter strength, and for activators to function at such promoters by recruiting holoenzyme.. Thus, strong nonspecific DNA binding is predicted to be required for both processes. Additionally, we note that the large pool of $E\sigma$ bound to DNA nonspecifically effectively buffers weak promoters against changes in transcription by the strongest promoters in the cell. For example, if nonsaturating occupancy of promoters were achieved in the absence of significant nonspecific binding by having "just enough" $E\sigma$ to bind to promoters, decreased expression of the strongest promoters (e.g. rRNA promoters) would lead to huge increases in expression of weaker promoters. However, because much of the released $E\sigma^{E}$ will bind nonspecifically to DNA, the increase in transcription at weaker promoters is more modest, which may be necessary to allow appropriate regulation at such promoters.

Our model demonstrates that for σ competition to occur, σs must be in excess over all E not involved in elongation (rather than in excess of only free E). Previously, the number of σ^{70}[159] was thought to be lower than the number of non-elongating E [160], although there was a great deal of evidence for σ competition [161-165]. Our new estimates indicate that σ^{70} and thus total σs exceed non-elongating E and our model rationalizes this finding: this condition is necessary for σ competition. Moreover, the model predicts that σ competition preferentially affects promoters that are far from saturation. This seems to be a sensible strategy. Promoters can be far from saturation because they have been designed to be intrinsically weak as only small amounts of their product are necessary for growth. Alternatively, under the particular conditions tested, the activator for that promoter may be non-functional. In either case, when remodeling transcription, it makes sense to shut off such promoters first. This has been experimentally validated in one case (Shingler, pers. comm.). The generality of this idea can now be subjected to experimental test.

Introduction

In bacteria, transcription is initiated by RNA polymerase holoenzyme (Eσ), which is formed when core RNA polymerase (E) binds the transcription initiation factor sigma (σ)[166]. Eσ initially binds to promoter sites in a closed complex, which then transits to an open complex, competent for transcription. The number of intermediates between the closed and open complex is variable and promoter dependent; each step may be subject to regulation *in vivo* [167, 168]. At least for some promoters, Eσ binding to promoters is thought to be reversible on the time scale of transcription initiation– *in vivo* [168]; reversibility has also been demonstrated *in vitro* for several promoters. [168-171]. Even binding to the strong *lac* UV5 promoter is reversible *in vitro* when tested under conditions that approximate the *in vivo* situation [171].

Recruitment of Eσ to promoters *in vivo* is thought to depend on the intrinsic binding affinity of the promoter, and is modulated by repressors that prevent and activators that stabilize interactions between Eσ and the promoter [168]. Based on *in vitro* studies of the mechanism of activator function, it is believed that promoters that bind Eσ weakly require activators to recruit Eσ. In addition, cells contain multiple σs, which direct E to various sets of promoters specific to the sigma factors [166]. These σ's are believed to compete with each other for binding to E [161, 163-165]. By changing the relative levels of the σs, *E. coli* is thought to coordinate its transcriptional program with growth conditions [172-174]. This view is based upon observations indicating that: 1) overexpressing one σ decreases expression of genes controlled by another σ [161]; 2) mutationally altering binding constants of one σ for

E alters expression by another σ [162]; and that 3) physiological effectors such as ppGpp may act by altering relative binding of σs to E [163-165]. In the present work, we use an equilibrium model of RNA polymerase binding to DNA to explore *in vivo* scenarios that permit transcription regulation by activator recruitment of RNA polymerase and σ competition.

Nonspecific binding of E and Eσ to DNA should be an important component of a model that describes RNA polymerase binding to promoters. Nonspecific binding of both species has been demonstrated *in vitro* [175], however the magnitude and extent of nonspecific binding *in vivo* is hard to evaluate experimentally. von Hippel was the first to develop a model that examined the role of nonspecific binding in regulating transcription. Using a simple equilibrium approach, he examined partitioning of the Lac repressor between specific and nonspecific sites in *E.coli* [176]. His results showed that the kinetics of induction of Lac repressor could be understood only when nonspecific DNA binding was considered, suggesting that nonspecific DNA binding may play an important role in the thermodynamics and kinetics of interaction of transcription factors (as well as RNA polymerase) with their specific sites [176, 177].

Estimation of RNA polymerase partitioning between promoters, nonspecific binding sites on DNA and the cytoplasm requires knowledge of the levels of E, σ^{70} (the housekeeping sigma factor) and at least some alternative σ's. However, published values have been measured by different techniques, in different strains and under different physiological conditions (both during exponential phase and during entry into stationary phase) [178-186]. In fact, discrepancies in these numbers have led to the common perceptions that: : (i) as most RNA polymerase is elongating;

only a minor fraction could be bound to DNA nonspecifically; (ii) cellular levels of σ^{70} are much less than that of RNA polymerase; thus, σs compete because of their excess over free RNA polymerase. We have remeasured the levels of E, σ^{70}, σ^{32} and σ^{E} in *E. coli* K12 MG1655. Our data, which is consistent with most of the primary data in the literature, suggests that *in vivo* (i) only a minor fraction of RNA polymerase (< 20%) is involved in elongation; and (ii) σ^{70} is in excess of total E.

Using an equilibrium model based on our new values and relevant data from the literature, we explored the possible partitioning of E and Eσ between promoters, nonspecific DNA sites and the cytoplasm. Our results suggest that even weak promoters will be saturated with $E\sigma^{70}$ *in vivo* unless non-specific DNA binding by $E\sigma^{70}$ is rather significant. Thus, strong nonspecific binding is required for activators to work by recruiting Eσ and for the binding affinity of the promoter to contribute to regulation. In addition, our model predicts that σ's compete for binding to E only when their total number exceeds the total amount of RNA polymerase (excluding those involved in elongation) rather than the amount of free RNA polymerase, and that weak promoters will be preferentially subjected to σ competition.

Results and discussion

Quantifying intracellular levels of σ^E, σ^{32}, σ^{70} and E

Our data for the levels of σ^{70}, σ^E, σ^{32}, and E in cells growing exponentially in M9 glucose and M9 glucose supplemented with amino acids (M9 complete) are summarized in Table 4-3. Determinations of cell number and total protein mass/cell, taken at the same OD_{450} as sampling for intracellular protein concentrations (Table 4-2), were used to convert our measurements to molecules/cell and fmol/μg total cellular protein (Table 4-3).

Our estimate of about 13,000 molecules E/cell (~ 5,000/genome equivalent) for M9 complete is somewhat higher than the value of 5000 molec /cell (2,000 molec/genome equivalent) usually quoted in most reviews [159, 183], but is consistent with the measured fraction of total protein synthesis that is devoted to E (α_p; Table 4-4). Despite strain differences [Table 4-4: *E. coli B*, entries 1-4 vs. *E. coli K12*, entries 5-8], sample preparation differences [Table 4-4: whole cell lysates, entries 1-5 vs. pelleted lysates, entries 6-8]; and quantification differences [Table 4-4: radioactivity, entries 2-4 and 6-8 vs. densitometry, entries 1,5], α_p values for cells growing in glucose + amino acids are 1.5-1.8 % (Table 4-4, entries 2-5, 7, 8). Thus our α_p value of 1.8 ± 0.6 % (entry 5) is within the range of reported values and 13,000 molecules E/cell is a reasonable estimate to use.

Our estimate that σ^{70} is about 60 fmol /μg total protein in M9 complete (Table 4-3) is similar to reports that there are 50-170 fmol σ^{70} /μg total protein values for cells growing in LB [159, 178, 180]. These estimates of σ^{70} are higher than those obtained

previously using less direct methods [183, 187, 188], probably because of loss of the protein due to experimental procedures. To convert to number of molecules/cell, the fmol σ^{70} /μg total protein was multiplied by the amount of total protein per cell (Table 4-2) and Avogadro's number. Thus 60 fmol σ^{70} /μg total protein corresponds to 17,000 molecules per cell or about 7,000 molecules/genome (Tables 4-3, 4-5). This is almost an order of magnitude higher than the generally reported number of 500-1700 σ^{70} molecules either per cell or per genome equivalent [159, 178, 180]. However, since the fmol σ^{70} /μg total protein used to calculate σ^{70} molecules/cell are all in the same range, the inconsistency is simply a result of miscalculation. Thus, all recent data is consistent with a significantly higher number of σ^{70} molecules per cell than previously thought.

σ^{E} is much more abundant (3000-5500 molecules/cell) than previously reported value of <100 molecules/cell [178]. This profound difference is not a media effect, nor an effect of preparation methods (data not shown). Our measurements indicate that total σ^{E} represents a significant fraction of the σ molecules in a cell, almost comparable in abundance to σ^{70}.

Our data reveal two new aspects of global regulation. First, our E α_p = 0.5 % measured in glucose (Table 4-4, entry 5) is lower than previously measured α_p's in glucose (Table 4-4, α_p= 1-1.4 %; entries 3, 4, 7, 8), possibly because MG1655, a partial purine auxotroph [189] has a much slower doubling time (133') than the other strains (40' to 79'). As E expression varies with growth rate [181, 183, 184], the specific growth limitation may have influenced its α_p. Second, slower growing cells have a 1.4-fold increase in the ratio of σ^{70} /E (Table 4-3, 4-5), which might alter σ

competition. A more comprehensive examination of the ratios of these molecules as a function of a wide range of growth rates is required to establish the generality of these observations.

Insights from the equilibrium model on partitioning of RNAP

Preliminary calculations indicated that the dissociation constants for specific (K_S) and nonspecific (K_{NS}) binding of RNA polymerase (RNAP; $E + E\sigma^{70}$) to DNA are the critical parameters that influence partitioning of RNAP between specific and nonspecific sites on DNA. *In vitro* measurements indicate that these constants are very sensitive to ionic conditions and vary from 10^{-6} -10^{-9} M for K_S (for initial closed complex formation) and from 10^{-3}-10^{-6} M for K_{NS} [167, 175]. Neither the precise intracellular ionic conditions, nor the distribution of promoter binding strengths are known *in vivo*. Therefore, to gain insight on the possible partitioning of RNAP *in vivo*, we varied K_S and K_{NS} over a wide range of values and modeled the outcome.

We first determined how varying K_S and K_{NS} would affect the amount of free cytoplasmic RNAP (E and $E\sigma^{70}$), as this parameter has been measured experimentally [190]. Our model predicts that for K_S and K_{NS} within their reported range *in vitro* [167, 175], the majority of RNAP will be bound to DNA and very little RNAP will be free in the cytoplasm (Fig. 4-4A). As determined by examining how the β' subunit of RNAP partitions into minicells (which lack DNA) $\leq$ 1% of RNAP is free in the cytoplasm ([190]). Thus, for reasonable values of K_S and K_{NS}, the equilibrium model recapitulates experimental results.

We then calculated how varying K_S and K_{NS} affects the fraction of σ^{70} promoters occupied by $E\sigma^{70}$ (Fig. 4-4B). When non-specific binding is weak ($K_{NS} \geq 10^{-2}$-10^{-3} M), $E\sigma^{70}$ promoters are predicted to be fairly close to saturation (Fig. 4-4B). This is true even for promoters that bind $E\sigma^{70}$ very weakly ($K_S \sim 10^{-6}$ M); such promoters are usually thought to fire only in the presence of an activator. On the other hand, if non-specific binding is relatively strong ($K_{NS} \sim 10^{-4}$-10^{-6} M), then $E\sigma^{70}$ promoters with $K_S > 10^{-9}$ M are predicted to be far from saturation (Fig. 4-4B). These results indicate that nonspecific binding of RNAP is a critical determinant of promoter occupancy by $E\sigma^{70}$. Thus, activators can function by recruiting RNAP, and binding affinity can contribute to promoter strength, only if K_{NS} is tight enough *in vivo* to prevent complete promoter occupancy by $E\sigma^{70}$.

The above calculation results were obtained by assuming an equivalent K_{NS} for both E and $E\sigma^{70}$. However, K_{NS} of E and $E\sigma^{70}$ may not be equivalent. We therefore tested whether promoter occupancy by $E\sigma^{70}$ is sensitive to K_{NS} of E. Because E binds much more tightly to σ^{70} ($K_\sigma \sim$ nM) than to non-specific DNA ($K_{NS} \sim 10^{-2}$ - 10^{-6} M), any free E preferentially binds to σ^{70} rather than to DNA. Thus, $E\sigma^{70}$, not E, is the predominant species binding nonspecifically to DNA. As a consequence, K_{NS} of E can be varied over three orders of magnitude relative to K_{NS} of $E\sigma^{70}$ without affecting promoter saturation with $E\sigma^{70}$ (data not shown). The model becomes sensitive to K_{NS} of E only if the binding constant of E to σ^{70} were very weak ($K_\sigma >> 10^{-6}$ M; data not shown). These results indicate that K_{NS} of E has no significant influence on promoter

occupancy by $E\sigma^{70}$. Therefore, we propose that the extent of promoter saturation *in vivo* is determined primarily by K_{NS} and K_S of $E\sigma^{70}$.

Although in the above calculations we did not take into account the alternative σs, the occupancy of σ^A promoters with $E\sigma^A$ would also depend on the tradeoff between the specific and nonspecific binding of $E\sigma^A$ to DNA.

Technically, the above predictions of the model would not apply to promoters for which Eσ – promoter binding is irreversible on the time scale of transcription initiation. Occupancy of the latter promoters is determined by the rate of Eσ association with promoter and the rate of transcription initiation, limited by promoter clearance (~1 sec^{-1}). To keep such promoters unsaturated in the absence of nonspecific binding of Eσ to DNA, their association rate constant must be very slow; on the order of 10^{-4} M^{-1} sec^{-1} or less (data not shown). We therefore suggest that even such promoters require low pool of free Eσ attained through its nonspecific binding to DNA to stay far from saturation.

Insights from the equilibrium model on σ competition

We used our equilibrium model to examine how competition between σ^{70} and σ^A, both assumed to have equal affinity for E, depends on the following three parameters: (i) total number of σs ($\sigma_t = \sigma^{70} + \sigma^A$); (ii) promoter saturation by $E\sigma^{70}$ (in the absence of σ^A); and (iii) the amount of free RNAP (both E and $E\sigma^{70}$).

We determined whether competition between σ's depends on the absolute number of σs by varying the number of σ^A /cell at different numbers of σ^{70} /cell. When σ's

compete, an increase in σ^A /cell decreases promoter occupancy by $E\sigma^{70}$ (Fig. 4-5A). Simulations showed that competition occurs only when total σ exceeds the total number of E (compare solid and dashed line, Fig. 4-5A). This result reflects the fact that $E\sigma^{70}$ complex (K_σ ~ nM) that is additionally involved into interactions with specific and nonspecific sites on DNA is much more stable than the complex of E bound to nonspecific DNA. Thus, σ^A first titrates nonspecifically bound E to form holoenzyme ($E\sigma^A$), and only then competes with σ^{70} for E. Additional simulations of the model indicate that total σ must be in excess over E regardless of variations in the number of free RNAP or the number of promoters saturated with $E\sigma^{70}$ at $\sigma^A = 0$ (data not shown). It is noteworthy that σ^A competes more weakly than an equivalent amount of σ^{70} (Fig. 4-5A, "perfect competition" line). This asymmetry is due to our assumption that $E\sigma^{70}$ binds a large number of promoters, whereas $E\sigma^A$ has no specific binding sites. As a result, equilibrium is shifted so that E has a preferential binding to σ^{70} over σ^A. That the total number of σs must be higher than the number of nonelongating E for σ competition *in vivo* rationalizes the higher number of σ^{70}/cell estimated in this work (Table 4-3). In this regard, it is interesting that at low growth rates, the ratio of σ^{70}/E is greater than at high growth rates (Tables 4-3, 4-5). Thus, the competition among σ's may be more prevalent at low than high growth rates.

We next explored whether extent of promoter occupancy affects competition between σ's. In these simulations, we (i) fixed $\sigma^{70}_t > E_t$, (ii) fixed the concentration of free RNAP to 1% [190], and (iii) varied K_S and K_{NS} to achieve initial $E\sigma^{70}$ promoter occupancies (at $\sigma^A = 0$) of 99%, 48% or 5%. Simulations of σ^A competition

for each initial condition indicate that the σ's always compete (Fig. 4-5B, see a decrease in promoter occupancy with $E\sigma^{70}$ upon an increase in σ^A). However, the extent of competition depends inversely on the promoter saturation: promoters close to saturation are weakly competed, whereas promoters far from saturation show profound competition (Fig. 4-5B). These results can be understood by considering how the assumed K_S and K_{NS} of $E\sigma^{70}$ affect the ability of σ^A to pull $E\sigma^{70}$ from its promoters. High promoter saturation by $E\sigma^{70}$ requires strong affinity for promoters ($K_S << K_{NS}$; see Fig. 4-4 A,B). In this condition, σ^A primarily pulls $E\sigma^{70}$ from its nonspecific interactions with DNA leading to a very small decrease in the occupancy of strong promoters. In contrast, low promoter saturation is achieved when K_S is weak ($K_S \sim K_{NS}$). Here, σ^A competes with promoter bound $E\sigma^{70}$ almost as readily as with nonspecifically bound $E\sigma^{70}$, accounting for the profound competition observed.

Further simulations indicated that when promoter occupancy (at $\sigma^A = 0$) is fixed, altering the free RNAP concentration (5%, 1% or 0.1%) did not affect competition-induced changes in promoter occupancy (data not shown). Therefore, even if less than 1% of RNA polymerase is free *in vivo*, we predict that the relationship between σ competition-induced changes in promoter saturation and promoter binding strengths (Fig. 4-5B) would not be altered. We therefore propose that only promoters far from saturation with $E\sigma^{70}$ will be efficiently regulated by σ competition *in vivo*. This prediction of the model is consistent with experimental data. Shingler et. al. showed that a weak promoter was more subject to sigma competition than a strong promoter *in vivo* (pers. comm.).

How would variation in the relative affinities of various Eσ's to DNA and σ's for E affect predictions of the model? Our results suggests that stronger nonspecific DNA binding of $E\sigma^A$ relative to $E\sigma^{70}$ would shift the equilibrium towards σ^A binding, thereby decreasing the occupancy of promoters with $E\sigma^{70}$; likewise, higher affinity of σ^A than σ^{70} for E would have the same effect.

An equilibrium model that considers specific binding of $E\sigma^A$ to its promoters predicts that changes in the levels of σ^{70} also will affect promoter occupancy by $E\sigma^A$. However, since some alternative σ's are present in much lower amounts than σ^{70}, their promoter binding must be 10 to 1000 times tighter than that of $E\sigma^{70}$ to achieve comparable promoter saturation (data not shown). Alternatively, the nonspecific binding of $E\sigma^A$ to DNA could be weaker than that of $E\sigma^{70}$ to DNA.

Materials and Methods

Protein Purification and quantification

His-tagged σ^{70} [195], σ^{E} [28], σ^{32} [136], and the periplasmic domain of RseA [28], as well as E [196]and GST-tagged σ^{E} [197], were overproduced and purified as previously described. E was quantified by UV A_{280nm} absorbance ($E_{280nm}^{1\%}$ =5.5 [198]). $\sigma^{70}$was quantified by Coomassie staining because degradation products were visible on the gel. As the degradation products would be included in the UV A_{280nm} measurement, the amount of intact σ^{70} would be overestimated. Indeed, when the calibration curve is based on the UV A_{280nm} measurement ($E_{280nm}^{1\%}$ = 8.07 for his_6-σ^{70}), values of σ^{70} are 1.5-fold higher than those estimated by Coomassie. In the Coomassie staining protocol, purified proteins and known amounts of bovine serum albumin (BSA) were coelectrophoresed on the Tris-glycine SDS gels, and then stained with Coomassie brilliant blue R-250 for 20 min and distained overnight. Protein staining was quantified by densitometric analysis using the Alphaimager 2200. A linear calibration curve, obtained from Coomassie staining of the BSA standards, was used to quantify the concentrations of the purified proteins. His_6 - σ^{E} and his_6 - σ^{32} were also quantified by Coomassie staining.

Strains and Media

The bacterial strains used in this work were *E.coli* CAG51114 (MG1655 Φλ[*rpoHP3-lacZ*] *ΔlacX74*) - wild type cells (wt), CAG19193 (ML 20035 *rpoH::kanR* λP_{HS}-*lacZ*, kan^{R}) – the $\Delta\sigma^{32}$ cells [199], CAG22216 (*ΔlacX74 galK galU*

*Δ(araABC-leu)*7679 *araD*139 *hsdR rpsL* mcrB *rpoE*/Ω λP3-*lacZ*) - the $\Delta\sigma^E$ cells; and RL1120 (W3110 *trpR tnaA2 rpoB5201*) [200]. Cells were grown at 30°C either in M9 glucose medium, prepared as described [149] and supplemented with 0.2% glucose, 1mM $MgSO_4$ and 2 μg/ml thiamine, or in M9 glucose + amino acids, (M9 complete), which contained the previous components and all amino acids (40 μg/ml). Wt, RL1120 and CAG19193 cells were grown in both M9 glucose and M9 complete CAG22216 cells were grown in M9 complete only.

Preparation of whole cell extracts and protein level measurements by quantitative westerns

At OD_{450} ~ 0.16 (for M9 glucose) or OD_{450} ~ 0.275 (for M9 complete), 1 ml of culture was added to 111 μl of ice-cold 50% trichloroacetic acid (TCA) and incubated on ice for >15 min. Samples were centrifuged to pellet the precipitated proteins, which were then resuspended by vortexing and boiling for 5 min in Laemmli sample buffer. These whole cell extracts were used for measuring the intracellular levels of σ^{70}, σ^E, σ^{32}, and E.

We found that the efficiency of protein staining with antibodies after their transfer to the PVDV membrane differed for the purified proteins alone and these same proteins mixed with whole cell extract (Fig. 4-1). To more closely approximate conditions of the protein to be measured, we generated calibration curves by mixing known amounts of purified his_6-σ^{70}, his_6-σ^E, his_6-σ^{32}, or E respectively with cellular extracts from wt, Δ*rpoE* (CAG22216), Δ*rpoH* (CAG19193), or RL1120 (whose β subunit is modified by addition of Protein A so that it runs at a higher MW than

authentic β). Samples with equal amounts of the total cellular protein but different amounts of the purified protein standards were loaded onto Tris-glycine SDS gels. Proteins separated on the gels were directly electroblotted onto PVDV membranes. The blots were probed first with dilutions of polyclonal antibodies specific to σ^{70} (1:5,000), σ^{E} (1:10,000), σ^{32} (1:5000), or the β subunit of E (1:5000) and then incubated with a 1:10,000 dilution of horseradish peroxidase-conjugated anti-mouse antibodies. Blots were developed with the SuperSignal West Dura Extended Duration Substrate from Pierce. The signal was visualized by CCD, which eliminates nonlinearities due to properties of the film.

For σ^{70}, intracellular levels were determined directly from the calibration curve samples, which contained both his_6-σ^{70} and σ^{70} (Fig. 4-2A). For σ^{E} (Fig. 4-2B) and σ^{32}, intracellular levels were determined from extracts of wt cells run on the same gel as the calibration samples (which contained his_6-σ^{E} or his_6-σ^{32} mixed with extracts of strain lacking respectively σ^{E} and σ^{32}). For the β subunit of E, intracellular levels were determined from extracts of wt cells run on the same gel as the calibration samples (which contained E mixed with extracts of RL1120, whose endogenous β subunit runs at a position distinct from that of wt β).

The signals of known amounts of the purified proteins within the linear range were fitted to a straight line. We used this calibration curves to measure intracellular concentrations using an appropriate dilution of the cell extract (for example, see Fig. 4-2). Experiments have been repeated at least three times for each growth condition and for each protein.

Measurement of the total cellular protein

At OD_{450} of 0.16 (for M9 glucose) and at OD_{450} of 0.275 (for M9complete), 0.9 ml of the wt cell culture was added to 0.1 ml ice-cold 50% TCA, incubated on ice for 15 min, centrifuged to pellet precipitated proteins and resuspended in 0.1 ml of 5% SDS, 0.1 M TrisBase by vortexing and boiling for 5 min. These samples were used to measure total cellular protein. To obtain a calibration curve for total cellular protein quantification, 0.9 ml samples containing different concentrations of BSA suspended either in M9 glucose or in M9 complete medium were TCA precipitated and resuspended in the same way as described above for cellular proteins. 0.1 ml of the resuspended cellular protein samples and the BSA standards were mixed with 2 ml of BCA working reagent (from BCA protein kit) and incubated for 30 min at 37°C. The signal was measured at OD_{590} versus water. The signals of the BSA standards were fitted by a straight line (in the linear range), which was used to calculate total cellular protein concentration. Experiments were repeated 2 times.

Measurement of the number of cells

Aliquots of wt cell cultures in M9 minimal or in M9 complete medium at OD_{450} of 0.16 and OD_{450} of 0.275 respectively were taken and 0.1 ml of consecutive dilutions plated on Luria broth (LB) plates. The plates were incubated at 37°C overnight. The numbers of cells in the medium were calculated from the numbers of colonies on the plates. Experiments were repeated 3 times.

Development of equilibrium model

A mathematical model was developed to study partitioning of RNAP between specific (promoters) and nonspecific sites on DNA, and a pool of free RNAP in the cytoplasm. The model considers one major σ factor, labeled as σ^{70}, and one alternative σ factor, labeled as σ^{A}. It describes equilibrium binding between (i) free E and the σs, (ii) Eσs and promoters, and (iii) E and Eσs binding to nonspecific DNA sites (Fig. 4-3). The equilibrium model is based on the following assumptions: (i) binding of E and Eσs to DNA is reversible; (ii) σ^{70} promoters can be occupied only by $E\sigma^{70}$ (and σ^{A} promoters only by $E\sigma^{A}$); (iii) σ^{70} and σ^{A} have the same binding affinity for free E; (iv) all σ^{70} promoters have the same binding affinity for $E\sigma^{70}$ (and all σ^{A} promoters have the same affinity for $E\sigma^{A}$); (v) E, $E\sigma^{70}$ and $E\sigma^{A}$ bind to nonspecific DNA sites with the same affinity. For simulation of RNA polymerase partitioning between various pools, we set $\sigma^{A} = 0$, since under "normal" growth conditions the alternative sigma factors available for binding to E comprise a small fraction of total σs. For simulation of σ competition, we set σ^{A} promoters = 0, because there are many, many more promoter sites for σ^{70} than for alternative σ's [201, 202]. Parameters used in calculations are summarized in Table 4-5, row 3. The equation system was solved in Mathematica software using the function Nsolve.

Equilibrium model equations:

In the equations below, p = σ^{70} promoters; d = nonspecific RNAP binding sites on DNA. For subscripts, t = total, f = free, NS = nonspecific DNA binding and S =

specific DNA binding (to promoters). The equation system is solved using the function Nsolve in Mathematica software. The Nsolve function computes a numerical Gröbner basis followed by extraction of numerical roots using an eigensystem method.

Conservation equations:

$$E_t = E_f + E_{NS} + E\sigma_f + E\sigma^A{}_f + E\sigma_{NS} + E\sigma^A{}_{NS} + E\sigma_S + E\sigma^A{}_S$$
$$\sigma_t = \sigma_f + E\sigma_f + E\sigma_{NS} + E\sigma_S$$
$$\sigma^A{}_t = \sigma^A{}_f + E\sigma^A{}_f + E\sigma^A{}_{NS} + E\sigma^A{}_S$$
$$d = d_f + E_{NS} + E\sigma_{NS} + E\sigma^A{}_{NS}$$
$$p = p_f + E\sigma_S$$
$$p^A = p^A{}_f + E\sigma_S$$

Mass-action equations:

$$K_\sigma = \frac{\sigma_f \cdot E_f}{E\sigma_f}; \quad K_\sigma = \frac{\sigma^A{}_f \cdot E_f}{E\sigma^A{}_f};$$
$$K_{NS} = \frac{E_f \cdot d_f}{E_{NS}}; \quad K_{NS} = \frac{E\sigma_f \cdot d_f}{E\sigma_{NS}}; \quad K_{NS} = \frac{E\sigma^A{}_f \cdot d_f}{E\sigma^A{}_{NS}}$$
$$K_S = \frac{E\sigma_f \cdot p_f}{E\sigma_S}; \quad K_S = \frac{E\sigma^A{}_f \cdot p_f}{E\sigma^A{}_S}$$

Discussion of some assumptions used in the model:

The assumption that E and Ęσs bind to nonspecific DNA sites with the same affinity was based on *in vitro* data, indicating that K_{NS} of E and K_{NS} of $E\sigma^{70}$ differ by less than one order of magnitude [175]. When modeling sigma competition we

assumed equal binding affinity of σ^A and σ for E (dissociation constant K_σ), since *in vitro* data indicates that binding of various σs to E differs less than one order of magnitude [203]. .

In vivo values utilized in the model

Values for parameters that we used in the model and their derivation are reported in Table 4-5. The derivation of critical parameters is described in detail below.

(1) To estimate how much E is not involved in elongation, we calculate the number of E expected to be involved in elongation and subtract that number from the total number of E that we measured. The elongation rate of stable RNA is almost twice that of mRNA [204], therefore, to estimate the pool of elongating E, the fraction of RNA synthesis devoted to mRNA and stable RNA must be determined. We determined this fraction by interpolating our growth rate into compendia of data reporting the fraction of m- and rRNA synthesis at many different growth rates [160, 205]. We then calculated the number of E necessary to achieve the observed rate of synthesis for each RNA class. These calculations revealed that at each growth rate, < 20% of the E is in the elongation phase. This estimate of elongating E is smaller than commonly quoted values, primarily because the total number of E/cell is larger than the generally quoted value [159, 160].

(2) We take the number of σ^{70} promoters/cell growing in M9 complete as the number of predicted σ^{70} promoters/genome (obtained from Regulon DB [201, 202]) multiplied by the number of genome equivalents per cell obtained by interpolation (Table 4-5). These values may be significantly higher than the actual number of $E\sigma^{70}$

promoters/cell as only ~20% of these predicted promoters have been validated experimentally.

(3) The number of nonspecific binding sites is calculated as the # bp/genome multiplied by # genome equivalents/cell.

(4) Cell volume values are for cells growing at 1.3 doubling per hour, reported from measurements determined either by electron microscopy [206] or by particle size analyzer [207]. The contribution of the periplasmic space is ignored. This value is the same (within error) as the volume of cytoplasmic water per cell, calculated from the amount of cytoplasmic water per mg of dry weight in osmotically stressed E. coli (measured by Cayley et. al. [208]) and the total protein per cell (measured in this work).

Parameters used in simulations

Initial simulation studies showed that RNAP partitioning is qualitatively similar whether we used parameters obtained for cells growing in M9 minimal or for cells growing in M9 complete. We have chosen to demonstrate simulations made with parameters obtained for cells growing fast (in M9 complete), because the extent of possible promoter saturation with these parameters is higher and is therefore a better illustration for the predictions of the model. The simulations were carried out with the following parameters of the model (E_T that is nonelongating E, σ_T that is σ^{70}, number of promoters and nonspecific binding sites, and cell volume) set to in vivo values derived for cells growing in M9 complete (see Table 4-5; column 3), and K_σ (dissociation constant for E to σ) taken to be 1 nM [203, 209]. When calculating

Table 4-1. *Quantification of the concentrations of purified his_6 - σ^{70} and E used to generate the standard curves*

Protein quantification	his_6 - σ^{70} mg/mL	E	
		mg/mL	μM
Coomassie staining	2.8 ± 0.4	(β-subunit) 5.85	39
UV A_{280} absorbance	4.1 ± 0.7	($\beta\beta'\alpha_2\omega$) 6.9	18

Table 4-2. *The numbers of cells and the total protein mass per cell in MG1655 wt cells, growing in M9 glucose media at 30° C*

M9 glucose Media	OD_{450nm}	# of cells / mL culture x 10^7	Total protein / mL culture [b] μg	Total protein /cell μg/10^9 cells
Complete	0.275	7.5 ± 1	34 ± 5	450 ± 70
Minimal	0.16	8.9 ± 0.5	27 ± 3	300 ± 35

[a] - Measured by the plating assay, described in Materials and Methods
[b] - Measured in TCA-precipitated cells using the BCA protein kit, as described in Materials and Methods

Table 4-3. *E, σ^{70}, σ^E, and σ^{32} intracellular levels during log phase in MG1655 wt cells, grown in M9 glucose media at 30°C*

M9 glucose Media	Complete		Minimal	
	fmoles / μg of total protein	# of molec / cell 10^3	fmoles / μg of total protein	# of mole / cell 10^3
E [c]	46 ± 15	13 ± 4	14 ± 7	2.6 ± 1.3
σ^{70}	62 ± 17	17 ± 4	26 ± 13	4.7 ± 2.4
σ^E	20 ± 5	5.5 ± 1.2	17 ± 4	3.2 ± 0.6
σ^{32}	0.44 ± 0.14	0.120 ± 0.034	0.1 ± 0.03	0.020 ± 0.005

These values are based on measurements from 3 independent cultures.
[a] – Calculated by dividing moles of the protein inl mL of culture by the total protein / mL culture (Table 4-2)
[b] – Converted into # of molecules / cell by multiplying moles of protein inl mL of culture by Avogadro's number and dividing that value by the # of cells /1 mL culture (Table 4-2)
[c] – Concentration of purified E, used for quantification, was measured by UV A_{280} absorbance;
while concentration of the three purified sigma factors, used for quantification, was measured by Coomassie staining, as described in Materials and Methods

Table 4-4. *α_p, % of RNA Polymerase of total cellular protein, in the literature*

#	Method	Quantitatio	Strain	Medium	DT,	α_p, %	Reference
1	WC	D	B/r	Glucose +	25	1.29	[210]
2	WC	R	B	Glucose +	28	1.62 [a]	[187]
3	WC	R	B /r	Glucose +	29	1.5	[181]

				Glucose	44	1.05	
				Succinate	90	0.82	
4	WC	R	B/r	Glucose + a/a	26	1.6	[184]
				Glucose	40	1.4	
				Acetate	136	1.05	
			K12	Glucose + a/a	40	1.53	
				Glucose	60	1.16	
				Acetate	136	0.85	
5	WC	D	K12	Glucose + a/a	45	$(1.8 \pm 0.6)^{b}$	This work
				Glucose	133	$(0.53 \pm 0.27)^{c}$	
6	L	R	K12	Glucose + a/a		1.08^{d}	[188]
7	L	R	K12	Glucose + a/a	39	1.7^{e}	[183]
				Glucose	79	1.2^{f}	
				Succinate	133	0.98^{g}	
8	L	R	K12	Glucose + leu		1.08^{h}	[211]

DT – doubling time; **WC** – solubilized whole cell extracts applied to SDS gel; **L** - RNAP immunnoprecipitated from treated and fractionated cell lysate and applied to SDS gel; **R** – radioactivity; **D** – densitometry.

[a] The original work quoted α_p = 0.9% based on quantifying the β' subunit; however β was 1.8 fold more abundant than β'. As we know now that β'and β are produced in stoichiometric amounts, we used the β value to calculate α_p.

[b], [c] – converted into α_p from fmoles of RNAP / μg of total protein (Table 4-3) by multiplying by RNAP MW (380 kD)

[d], [e], [f], [g], [h] - α_p (RNAP) was calculated from α_p(β') by multiplying by 2.5, which is the ratio of the MW of RNAP to that of β'-subunit MW; [d] $\alpha_p(\beta') = 0.43\%$; [e] $\alpha_p(\beta') = 0.68\%$; [f] $\alpha_p(\beta') = 0.48\%$; [g] $\alpha_p(\beta') = 0.39\%$; [h] $\alpha_p(\beta') \sim 0.43\%$;

Table 4-5. *Parameters measured and calculated for cells growing in M9 complete and minimal*

Parameter	*Symbol, unit*	*M9 complete*	*M9 minimal*	*Calculations /References*
Doubling time	τ, min	45	133	Measured at 30°C (this work)
Doubling per hour	ν	1.33	0.45	60 min / τ
Average cell volume	V, 10^{-15} L	0.8^{a}	0.39^{b}	V^{a} [206, 207] $V^{b} = N^{a} \cdot V^{a} / N^{b}$
Number of cells (exp. grow OD_{450} = 1 mL	N, 10^{8}	2.7^{a}	5.6^{b}	Measured (this work) extrapolated from Table 2
Genome equivalents per OD_{46}	G, 10^{8}	6.5^{a}	7.8^{b}	G^{a} [205], Table 4-1 G^{b} interpolation of [205]
Number of genome equivalent per cell	g	2.4	1.4	g = G / N
RNA per OD_{460} = 1	RNA, 10^{16} ntps	4.6^{a}	3.3^{b}	RNA^{a} [205], Table 4-1 RNA^{b} interpolation of [205] Table 4-1
RNA per cell	rna, 10^{7} ntps	17	6	rna = RNA / N
Rate of stable RNA synthesis	ν_s, 10^{5} ntps/min/cell	31.3	3.7	$\nu_s = rna \cdot f_s \cdot \ln 2 / \tau$ $f_s = 1.2$ [c]
Stable RNA synthesized per total RNA synthesis	r_s/r_t, %	62	37	r_s/r_t interpolation of [212], Table 4-3 [d]
Rate of mRNA synthesis	ν_m, 10^{5}	19	6.3	$\nu_m = \nu_s \cdot (100 - r_s/r_t) / (r_s/r_t)$ [e]

	ntps/min/cell			
mRNA elongation rate	c_m, ntps/ sec	49	37	c_m averaged interpolation of [204], Table 4-2
rRNA elongation rate	c_s, ntps / sec	86	70	c_s interpolation of [204], Table 4-2
Number of RNAP, elongating mRNA	$RNAP_m$, molec / cell	646	284	$RNAP_m = \nu_m / (c_m \cdot 60$ sec)
Number of RNAP, elongating rRNA	$RNAP_r$, molec / cell	607	88	$RNAP_r = \nu_s / (c_s \cdot 60$ sec)
Total RNAP, involved into elongation	$RNAP_E$, molec / cell	1250	370	$RNAP_T = RNAP_m + RNAP_r$
Total number of core RNAP	$RNAP_T$, molec / cell	13,000	2,600	Measured experimentally, this work, Table 4-3
Number of RNAP, not involved into elongation	RNAP, molec / cell	11,750	2,230	$RNAP = RNAP_T - RNAP_E$
Total number of σ^{70}	σ^{70}, molec / cell	17,000	4,700	Measured experimentally, this work, Table 4-3
Number of σ^{70} per non-elongating RNAP	σ^{70} / RNAP	~ 1.5	~ 2.1	
Total number of σ^{70} promoter	p, per cell, 10	10.5	6.1	$p = pr \cdot g$ $pr = 4{,}379$ [f]
Number of nonspecific bindin locations	d, per cell, 10	11.04	6.44	$d = g \cdot bp$; $bp = 4.6 \cdot 10^6$ [g]
Number of non-elongating RNAP per σ^{70} promoter	RNAP / p	~ 1.1	~ 0.37	

The number of molecules per cell were converted into concentrations by dividing them by $V \cdot N_A$, where V is the cell volume in M9 complete media ($0.8 \cdot 10^{-15}$L), and N_A is the Avogadro's number ($6.01 \cdot 10^{23}$ molecules/mole).

[a] – stands for values calculated for cells, growing exponentially with doubling time 45'. That corresponds to the upper line of the *Calculations/Refences* pannel

[b] – stands for values calculated for cells , growing exponentially with doubling time 133'. That corresponds to the lower line of the *Calculations/Refences* pannel

[c] - f_s corrects for the 20% of the rRNA and tRNA primary transcripts that are unstable spacer or flanking sequences, [212] Table 4-3

[d] - measured in B/r cells

[e] - underestimated due to decay of labeled mRNA during the pulse-labeling period, [212] Table 4-3

[f] – the number of predicted Sigma70 promoters (among them 974 promoters confirmed), [201]

[g] –bp is the number of DNA base pairs per genome

Figure legends:

Figure 4-1. The efficiency of staining with antibodies of the purified proteins and these same proteins mixed with cell extracts after their transfer to the PVDV membranes.

The same amounts of the purified GST – σ^E on its own or mixed with the wt MG1655 cell extracts were loaded onto the same Tris-glycine SDS gel (left panel), separated and electroblotted onto PVDV membrane. The same procedure was done for the purified periplasmic domain of RseA (peri) (right panel). The blots were developed and visualized as described in Materials and Methods. Three separate experiments are shown.

Figure 4-2. Quantification of the intracellular protein concentrations by quantitative westerns with the calibration curves from purified proteins mixed with cell extracts, prepared as described in Materials and Methods.

(A) The calibration curve for σ^{70} built from the purified his_6-σ^{70} mixed with a wt MG1655 cell extract as described in Materials and Methods

(B) The calibration curve for σ^E was built from the purified his_6-σ^E mixed with Δ*rpoE* (CAG22216) cell extract as described in Materials and Methods.

(C) The calibration curve for the β-subunit of E, built from the purified E mixed with RL1120 cell extract as described in Materials and Methods.

β* - endogenous β subunit of E mixed of RL1120 cells, that runs at a position distinct from that of wt β

Figure 4-3. Equilibrium model reaction channels:

E can bind to either of the two sigma factors: σ^{70} and σ^{A} to form $E\sigma^{70}$ or $E\sigma^{A}$ with the same disassociation constant K_σ. $E\sigma^{70}$ can specifically bind to σ^{70} promoters (and $E\sigma^{A}$ can specifically bind to σ^{A} promoters) with a disassociation constant K_S. E, $E\sigma^{70}$ and $E\sigma^{A}$ can also bind to DNA non-specifically with a disassociation constant K_{NS}.

Figure 4-4. Free RNAP and promoter saturation vs K_S and K_{NS}.

Calculated according to the Equilibrium model. See Materials and Methods for a complete discussion of the binding constants and approximations used in the models. The number of $\sigma^{A} = 0$; The numbers of total σ^{70}, σ^{70} promoters (p) and DNA binding sites (d) are indicated in Table 4-5, column 3. E_T =12,000 molec/cell.

(A) Solid lines represent sets of K_S (the dissociation constant for $E\sigma^{70}$ binding to promoters) and K_{NS} (the dissociation constant of non-specific binding between E or $E\sigma^{70}$ and the random DNA) for which the number of free RNAP (free E + free $E\sigma^{70}$) is equal to 5%, 1% or 0.1% of total nonelongating RNAP. Everything on the right of the line, where $K_S > K_{NS}$, is considered nonphysiological. Dashed area is the space of K_S and K_{NS} where $RNAP_{free} < 1\%$.

(B) Fraction of σ^{70} promoters occupied by $E\sigma^{70}$ plotted vs K_S as a function of K_{NS}.

Figure 4-5. Decrease in σ^{70} promoters' occupancy by $E\sigma^{70}$, induced by sigma competition.

Calculated according to the Equilibrium model. See Materials and Methods for a complete discussion of the binding constants and approximations used in the model. The number of σ^{A} promoters = 0. The numbers of σ^{70} promoters (p) and DNA binding sites (d) are indicated in Table 4-5, row 3. E_T =12,000 molec/cell.

(A) Decrease in σ^{70} promoters' occupancy by $E\sigma^{70}$ for various numbers of σ^{70} molecules per cell.

Concentration of free RNAP = free E + free $E\sigma^{70}$ is 1%. $E\sigma^{70}{}_S$ – the occupancy of σ^{70} promoters with $E\sigma^{70}$ (at σ^A =0) is 48%.

Dotted line: σ^{70} =8,000 molec/cell ($K_S = 1.19 \cdot 10^{-7}$, $K_{NS} = 4.01 \cdot 10^{-4}$)

Solid line: σ^{70} =17,000 molec/cell ($K_S = 2.76 \cdot 10^{-7}$, $K_{NS} = 4.01 \cdot 10^{-4}$)

Competition starts when $\sigma_T = \sigma^{70} + \sigma^A > E_T$ = 12,000 molec/cell

An arbitrary line of "perfect competition" is calculated for a "symmetrical" case, when $E\sigma^A$ has the same number of specific binding sites as σ^{70} and the same K_S.

(B) Decrease in σ^{70} promoters' occupancy by $E\sigma^{70}$ for various occupancies of σ^{70} promoters with $E\sigma^{70}$. Concentration of free RNAP is 1%. σ^{70} =17,000 molec/cell.

$E\sigma^{70}{}_S$ – the occupancy of σ^{70} promoters with $E\sigma^{70}$ (at σ^A =0) is 99% ($K_S = 2.07 \cdot 10^{-9}$, $K_{NS} = 1.88 \cdot 10^{-3}$); 48% ($K_S = 2.76 \cdot 10^{-7}$, $K_{NS} = 4.01 \cdot 10^{-4}$); and 5% ($K_S = 5.01 \cdot 10^{-6}$, $K_{NS} = 2.42 \cdot 10^{-4}$).

Figure 4-1

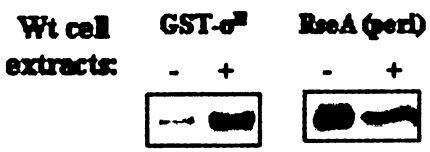

Figure 4-2

A

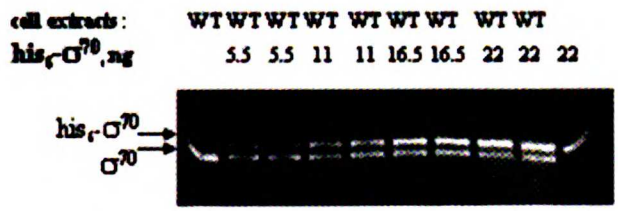
cell extracts :
WT WT WT WT WT WT WT WT WT
his$_6$-σ^{70}, ng
5.5 5.5 11 11 16.5 16.5 22 22 22
his$_6$-σ^{70}
σ^{70}

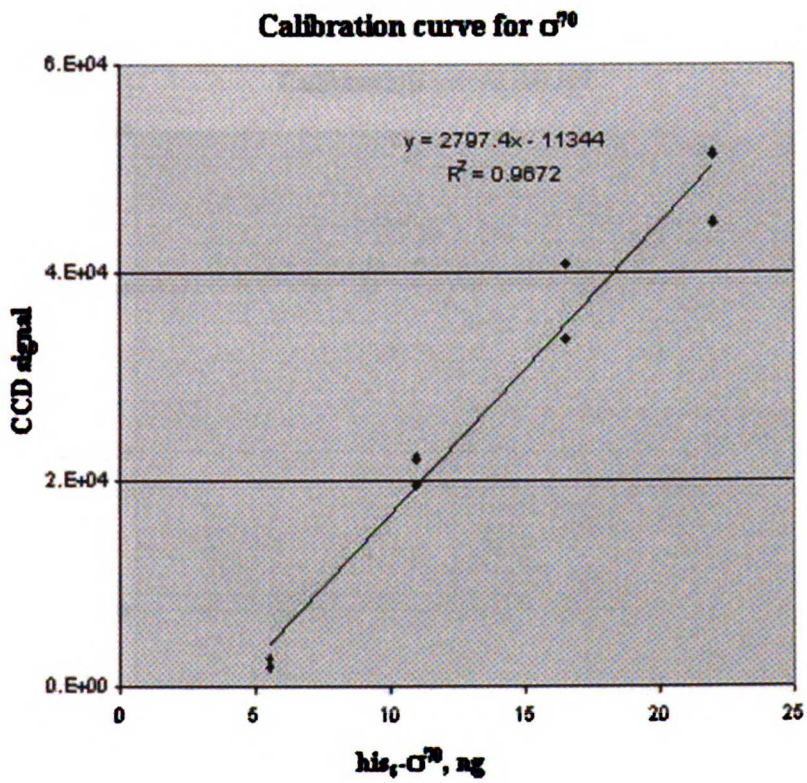
Calibration curve for σ^{70}
y = 2797.4x - 11344
R^2 = 0.9672
CCD signal
6.E+04
4.E+04
2.E+04
0.E+00
0
5
10
15
20
25
his$_6$-σ^{70}, ng

Figure 4-2

B

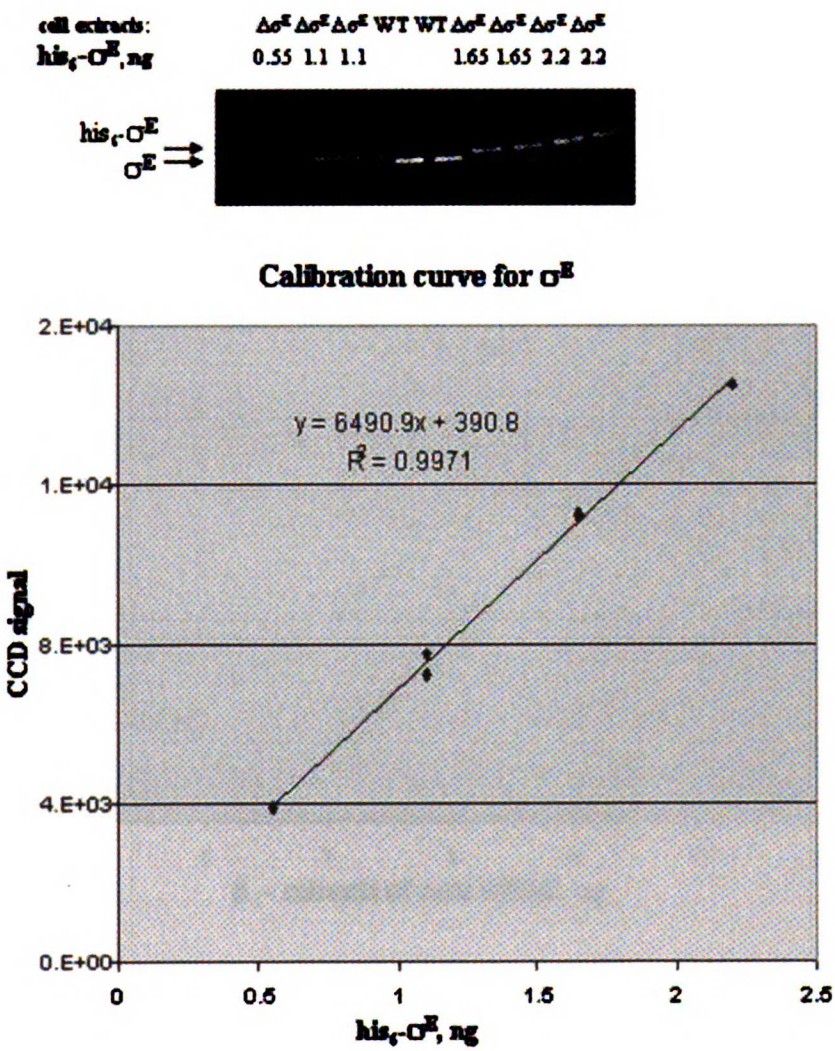
cell extracts:
Δσ^E Δσ^E Δσ^E WT WT Δσ^E Δσ^E Δσ^E Δσ^E
his_6-σ^E, ng
0.55 1.1 1.1 1.65 1.65 2.2 2.2
his_6-σ^E
σ^E
Calibration curve for σ^E
y = 6490.9x + 390.8
R^2 = 0.9971
CCD signal
2.E+04
1.E+04
8.E+03
4.E+03
0.E+00
0
0.5
1
1.5
2
2.5
his_6-σ^E, ng

Figure 4-2

C

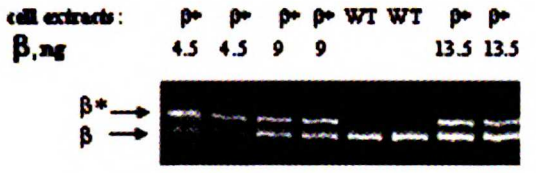
cell extracts :
β*
β
β, ng
4.5
4.5
9
9
13.5
13.5

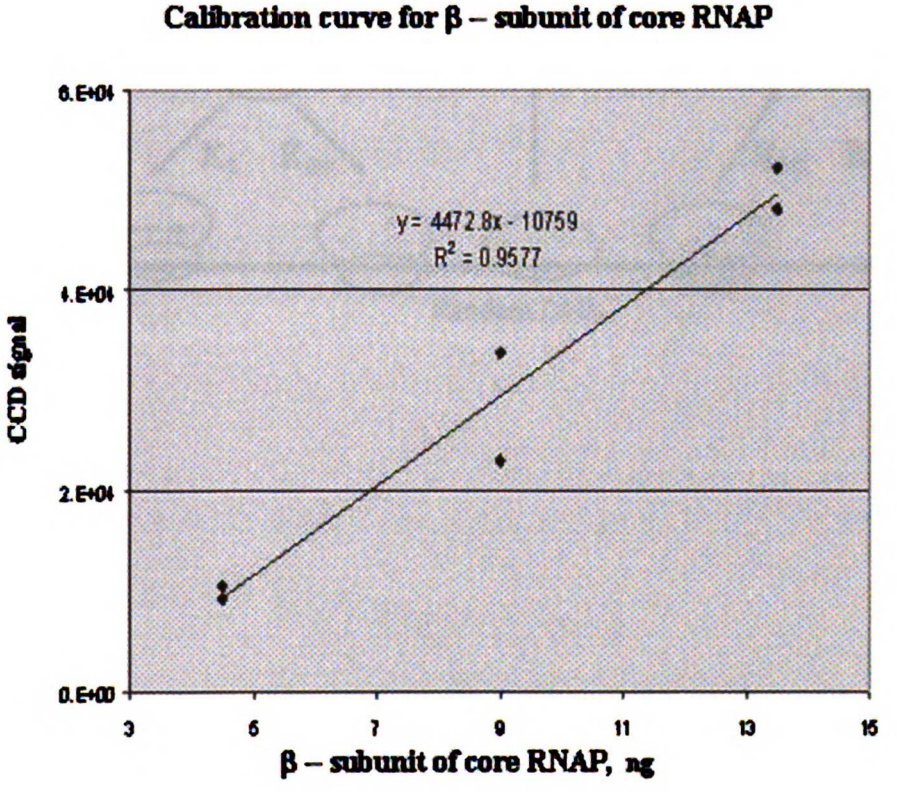
Calibration curve for β – subunit of core RNAP
y = 4472.8x - 10759
R² = 0.9577
CCD signal
β – subunit of core RNAP, ng

Figure 4-3

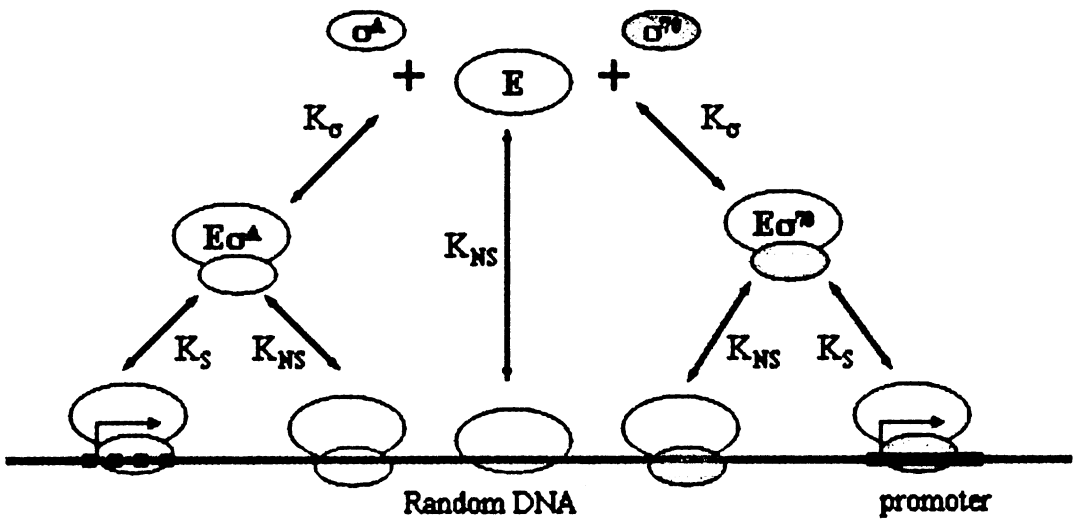

Figure 4-4

A

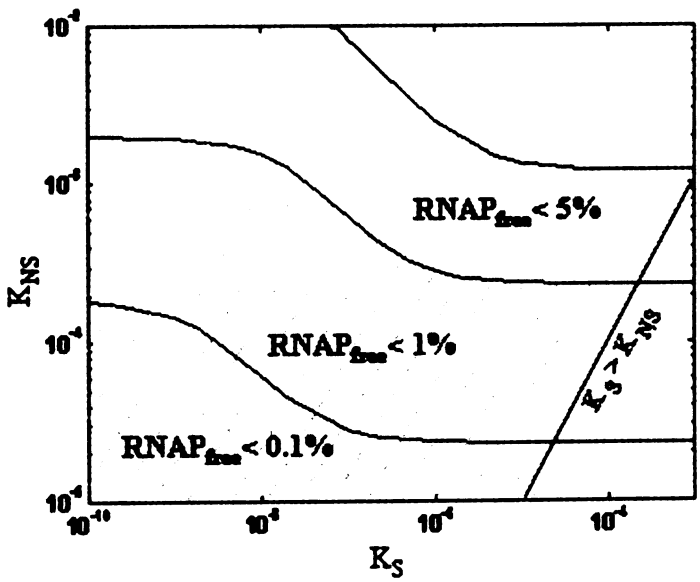
RNAP$_{free}$< 5%
RNAP$_{free}$< 1%
RNAP$_{free}$< 0.1%
$K_S > K_{NS}$
K_{NS}
K_S

B

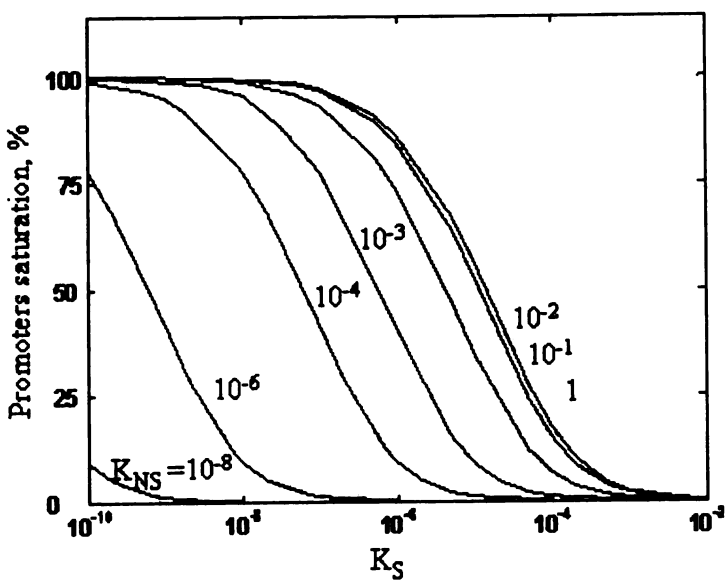
Promoters saturation, %
100
75
50
25
0
10^{-2}
10^{-1}
1
10^{-3}
10^{-4}
10^{-6}
$K_{NS}=10^{-8}$
K_S

Figure 4-5

A

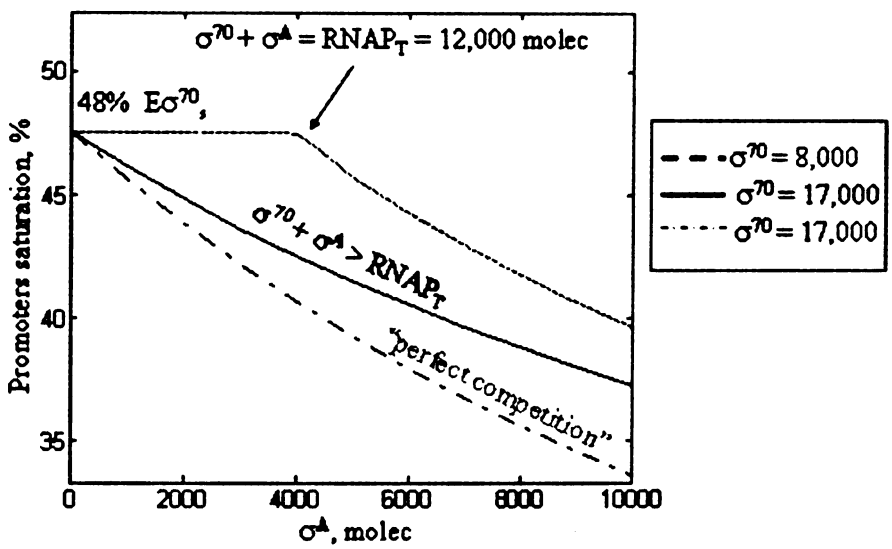
σ70+ σA = RNAPT = 12,000 molec
48% Eσ70s
σ70+ σA > RNAPT
"perfect competition"
σ70 = 8,000
σ70 = 17,000
σ70 = 17,000
Promoters saturation, %
σA, molec

B

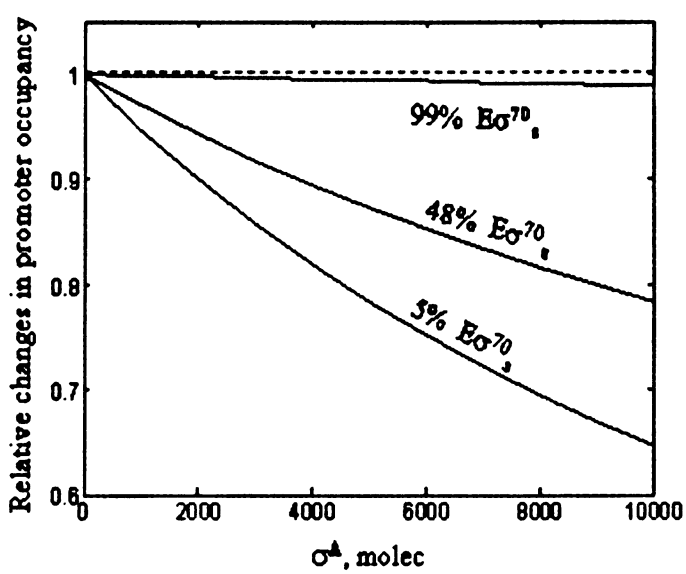
99% Eσ70s
48% Eσ70s
5% Eσ70s
Relative changes in promoter occupancy
σA, molec

Chapter Five

Conclusions and future directions

Conclusions

Extracytoplasmic stress, induced by heat, induces σ^E activity. In Chapter 2 of this Thesis we have shown that changes in σ^E activity, induced by temperature upshift or downshift (from 30° C to 43 ° C, and *vice versa*), correlate with an increase (decrease) in the rate of RseA degradation. This work suggests that the temperature-induced extracytoplasmic signal is transduced to σ^E by the regulated degradation of RseA.

In addition, *in vitro* experiments demonstrated that σ^E dissociates from the cytoplasmic domain of RseA extremely slowly. Therefore *in vivo*, σ^E is likely to be only released from the inhibitory interaction with RseA predominantly upon RseA degradation. This mechanism enables cells to respond to the changes in RseA degradation rate rapidly and explains the fast shut off in σ^E activity (that is not due to the changes in the relative levels of RseA and σ^E) caused by RseA stabilization.

This thesis also presented evidence that RseB and DegS function to make the system sensitive to a wide range of OMP concentrations and unresponsive to variations in the levels of DegS and RseP proteases. These features rely on the inability of RseP to cleave intact RseA. In the present report, we demonstrate that RseB, which binds to the periplasmic face of RseA, and DegS each independently inhibit RseP cleavage of intact RseA.

Finally, this work describes estimation of the levels of E, σ^{70}, σ^E and σ^{32} in *E. coli*. These values were then used in an equilibrium model to calculate the partitioning of RNAP between σs, promoters, nonspecific DNA binding sites, and the cytoplasm. The model suggests that the nonspecific binding of holoenzyme to DNA plays a

critical role in the extent of promoter saturation. Consequently, in order for activators to function by recruiting RNAP to promoters, nonspecific binding needs to be relatively strong. In addition, the new estimates indicate that the numbers of σ^{70} molecules/cell and thus total σs exceeds the number of non-elongating E molecules/cell: a condition that is necessary for σ competition. Moreover, the model predicts that σ competition preferentially affects promoters that are far from saturation.

Future directions:

Other inducers of the σ^E pathway

The transmembrane pathway that regulates σ^Eaccording to the folded state of OMPs is well characterized; however, little is known about other extracytoplasmic signals that may induce σ^E. The present work shows that similar to the OMP signal, heat induced extracytoplasmic signal is transduced via a regulated degradation of RseA. However, the nature of inducing signals and the proteases that induce temperature-dependent proteolysis of RseA are yet to be determined. One possible mechanism is that stresses in the envelope either directly perturb OMP maturation (e.g. by decreasing OMP stability) or titrate away OMP folding catalysts (due to accumulation of other unfolded proteins), thus increasing the flux of unassembled OMPs in the envelope. This scenario can be tested *in vivo* by measuring heat induced changes in σ^E activity and the rate of RseA degradation in strains that have reduced OMP synthesis. If the timing and the magnitude of the σ^E response does not change,

compared to the wild type cells – this would imply that heat-induced activation of the pathway is independent of the OMP pathway. Another possibility is that unfolded proteins activate the pathway via an OMP–independent way that does not require activation of DegS. For example, the ability of RseP to cleave full-length RseA without preliminary cleavage by DegS is inhibited by RseB. This activity of RseP could be increased by titrating away RseB in response to periplasmic signals such as unfolded proteins [25]. In the wild type cells this possibility would be partially masked by the proteolytic activity of DegS. Therefore, titration away of RseB away by unfolded proteins should be tested in a DegSΔPDZ (possibly a catalytic site mutant) strain, since under those conditions removal of RseB results into a strong induction of σ^E activity.

Structural mechanisms of RseP inhibition by RseB and DegS

Based on the present in the Thesis data it can be suggested that RseB and DegS each independently inhibit RseP cleavage of intact RseA. However, the molecular mechanisms of this inhibition are unknown. Since RseP inhibition requires periplasmic domain of RseA (specifically, its Gln-rich region) [38], RseB, and the PDZ domain of RseP, we suggest that these components participate in the same inhibitory reaction. For example, RseB binding to RseA might facilitate a conformational change in RseA that makes its Gln-rich regions more accessible to binding by the PDZ domain of RseP, thereby facilitating the inhibitory reaction. Alternatively RseB could independently bind to the RseP PDZ domain. The second mechanism for inhibiting RseP cleavage of intact RseA involves DegS and is

independent of the PDZ domain of RseP. DegS could negatively regulate RseP by forming a complex with RseA, thereby either blocking or altering the RseA recognition sites for RseP. Alternatively, DegS could form a complex with RseP thereby reducing its ability to cleave intact RseA. Although current experimental evidence is more consistent with a second scenario, both of these hypotheses should be tested. Interactions between DegS, RseP, RseA and RseB can be probed by a combination of *in vitro* binding assays, crosslinking and mutational analysis. In addition, determining the structures of these proteins or modeling them based on protein homology, might suggest potential interaction sites that can be later tested experimentally.

Testing predictions of the equilibrium model of RNA polymerase binding to DNA.

The four major predictions of the equilibrium model of RNA polymerase partitioning between promoters, nonspecific sites on DNA and the cytoplasm are: (i) significant amounts of RNA polymerase are bound to DNA nonspecifically *in vivo*; (ii) competition between the sigma factors is possible only when total amount of σs exceed that of the non-elongating core RNA polymerase; (iii) promoters that bind holoenzyme weakly are more sensitive to regulation by competition than the strong promoters; (iv) specific binding of the holoenzyme with alternative σs to their promoters should be stronger (or their nonspecific binding to DNA – weaker) compared to σ^{70} holoenzyme. Testing competition between the sigma factors for core RNA polymerase can shad light on (i), (ii) and (iii) predictions of the model. GFP expression system under control of σ^{32} or σ^{E} promoters of various strengths can be

used to asses the extent of competition between the sigma factors. To measure the competition differential plots of GFP accumulation with cell growth should be measured both at wild type levels of σ^{70} and when σ^{70} is overexpressed. Simultaneous overexpression of core RNA polymerase might be useful to asses conditions when sigma competition does not exist (number of core RNAP molecules/cell, not involved into elongation is higher than the number of total σs). Abolishment of competition between σs would also indirectly support conclusion that a large fraction of RNA polymerase is nonspecifically bound to DNA. Indeed, if the amount of RNA polymerase involved in elongation is much higher than that estimated from the literature, then the σs must be competing for a limiting amount of free core. In that case 2, 3-fold overproduction of core should not eliminate sigma competition. Specific and nonspecific binding of holoenzymes with alternative σs to DNA can be tested by *in vitro* binding assays.

Finally, to address the timing of transcriptional responses upon changes in the levels of σs, one would need to develop a dynamical model that would take into account the synthesis of new core and σs, as well as the release of core upon mRNA synthesis.

Appendix

Measurements of the association and dissociation rate constants of σ^E binding to the cytoplasmic domain of RseA.

Summary:

In these experiments we show that σ^E / RseA binding is extremely tight, suggesting that σ^E could be released from the complex only upon RseA degradation. In this case by changing the rate of RseA degradation cells can directly regulate σ^E release rate (and therefore its activity). This finding explains the observed correlation between σ^E activity and the rate of RseA proteolysis, that could not be explained by changes in the levels of RseA and σ^E per se [34].

Introduction:

The experiments described earlier [34] demonstrated that in cells that are shifted from 43° C to 30° C RseA is rapidly (within 3 min) stabilized. In parallel, within 10 min after the temperature downshift σ^E activity decreases more than 10-fold. The observed decrease can not be explained by changes in the relative levels of RseA and σ^E, since within that time RseA levels do not change. To explain this result it was suggested that in addition to being regulated by the relative levels of RseA and σ^E, σ^E activity is also regulated directly by the rate of σ^E release from RseA upon degradation. That scenario would apply if σ^E dissociates from RseA with a rate constant slower that of RseA degradation.

To test this suggestion we have undertaken to measure the rate constant of σ^E dissociation from RseA *in vitro* by monitoring fluorescent anisotropy of the cytoplasmic domain of RseA, (RseA1-100) labeled with rhodamine.

Results:

Based on the crystal structure of σ^E / RseA1-90 complex, only [1-66] region of cyto-RseA is involved into σ^E binding, while the residues 67-90 are disordered and do not appear to play a role in the binding [28]. In accord with that RseA1-100 is sufficient for anti-σ activity *in vivo* [26, 27]. Thus, to measure the dissociation rate of σ^E from RseA *in vitro* we have used a 1-100 fragment of RseA C-terminally coupled to a hexahistidine tag. To label his_6-RseA1-100 with rhodamine, glutamic acid at position 28 was mutated into cystein. In accord with prediction of the structural data [28], E28C mutation and rhodamine labeling did not affect σ^E binding, since premixed labeled his_6-RseA1-100(E23C) and unlabeled his_6-RseA1-100 bound his_6-σ^E equally well. The dissociation rate of his_6-σ^E from RseA was measured by competing off bound labeled his_6-RseA1-100(E23C) by 10 fold excess of his_6-RseA1-100. Within 2 hours there was no decrease in fluorescent anisotropy, indicating that the dissociation rate constant of his_6-σ^E from his_6-RseA1-100(E23C) is much less than 10^{-4} s^{-1} (Fig. A-1). This very slow dissociation rate is not an artifact of E23C mutation and/or rhodamine labeling of his_6-RseA1-100, since 100 nM labeled his_6-RseA1-100(E23C) could not compete off 100 nM of unlabeled his_6-RseA1-100 prebound to his_6-σ^E within 2 hours.

The association rate of the labeled his_6-RseA1-100(E23C) and his_6-σ^E, measured by changes in rhodamine fluorescence upon the binding, is $(1.5 \pm 0.2)10^7$ $M^{-1}s^{-1}$ (Fig. A-2). Thus the binding constant of his_6-σ^E and his_6-RseA1-100 is tighter than 10 pM.

Materials and Methods:

Plasmids:

pJT6 plasmid utilizes the Novagen T7 expression vector pET28b. It expresses the cytoplasmic domain of RseA (the N-terminal 100 amino acids), C-terminally coupled to a hexahistidine tag by a linker containing a thrombin cleavage site. This plasmid was constructed using primers that add a 5' NcoI site (RSEA/LC-15, 5'-GGGTATTAGCCATGGAGAAAGAAC-3') and a 3'HindIII site plus thrombin-cleavable linker (JTO-16, 5'-TACGCAAAGCTTGCTGCCGCGCGGCACCAGCTGTGCCGCCCACGGACG-3') The 5' NcoI site changes the second amino acid from Q to E.

pRseA1-100(E28C) (glutamic acid changed to cystein) was constructed by quick-change mutagenesis with primers rseAE28C28-1 5'-CTGGCTCATAACCCATGTATGCAGAAAACCTGG-3' and rseAE28C28-1r 5'-CCAGGTTTTCTGCATACATGGGTTATGAGCCAG-3' using pJT6 as a template.

σ^E with N-terminal His6-tag was expressed from pPER76 [42]. Overproduced from CAG36039 (BL21, pLysS)

Protein expression and purification:

The plasmids carrying his_6-σ^E, his_6-RseA1-100 and his_6-RseA1-100(E28C) were individually transformed into *E. coli* BL21 cells. Transformants were grown with aeration at 37°C in LB medium with ampicillin, 100 μg/mL (pPER76) or with 30 mg/ml kanamycin (pJT6, px) to 0.5 OD600 and induced with 1 mM IPTG for 1-2

hours. Cultures were then pelleted, flash-frozen in liquid nitrogen, pellets were thawed in ice water and refrozen in liquid nitrogen two more times to weaken cell walls, and resuspended in $1/50^{th}$ volume of initial induction culture in BufferI (10 mM Tris-HCl pH 9.0, 5% glycerol, 0.1 mM aminoethylbenzenesulfonic acid [AEBSF], 0.5mM β-mercaptoethanol [BME]) plus 500 mM NaCl, 10 mM imidazole (pH 7.9). 200 μg/ml lysozyme was added and the suspension was incubated on ice for 15 minutes, then tip-sonicated with a Branson micro-tip at setting #6, 100%, with 2 second pulses until the solution was thin and homogenous. Cellular debris was pelleted at 25,000 g for 30 min at 4°C, and the supernatant containing the overexpressed protein was applied to a 5-mL Co^{2+} metal ion affinity column (Talon resin, Clontech) equilibrated in Buffer I/500 mM NaCl/10 mM imidazole at 4oC. The column was washed with 50 ml of Buffer I/500 mM NaCl/20 mM imidazole, then step eluted with 15 ml each of Buffer I/150 NaCl/40,60,100,200 mM imidazole. 1 ml fractions were analyzed by SDS-PAGE followed by Coomassie blue staining, and those containing protein were pooled and incubated overnight at 4°C against the dialysis buffer (Buffer I/50 mM NaCl plus 25% glycerol (30% total), 0.1% Tween20). The Co^{2+} elution pool was then loaded onto 1 ml HiTrap Q (Pharmacia) anion exchange column equilibrated in Buffer I/50 mM NaCl at 4°C. The Q column was washed with 5 ml of the equilibrating buffer, then step-eluted with 5 ml each of Buffer I/100, 250 mM NaCl. 1 ml fractions were analyzed by SDS-PAGE followed by Coomassie blue staining and those containing protein were pooled and dialyzed at 4°C overnight against the dialysis buffer. Dialyzed pools were flash-frozen in liquid nitrogen and stored at –80°C.

Fluorescent Labeling:

Prior to fluorescent labeling of his_6-RseA1-100(E28C) - with rhodamine on cystein 28, it was loaded on a PD10 desalting column, and then washed and eluted with dialysis buffer, that did not contain β-mercaptoethanol [BME]). 250 µl fractions were collected, analyzed by UV absorbance at A_{280} and A_{290} and the fractions with protein were pooled together. Pooled his_6-RseA1-100(E28C) was incubated with 10 fold molar excess of rhodamine maleimide (Molecular Probes, Eugene, OR) at 4°C for 2 hours, the reaction was quenched with 1000 fold excess of DTT, and the sample was spun at 80,000 rpm for 20 min at 4°C to remove precipitated dye. To remove unreacted dye the supernatant was chromatographed on a PD10 desalting column prewashed with 25mL of the dialysis buffer with 2 mM DTT. 0.5mL fractions were analyzed by SDS-PAGE followed by Coomassi staining and by Fluorescent imaging with Alpha Imager 2000.

Polarization Anisotropy:

Prior to each experiment fresh probes of rhodamine-labeled his_6-RseA1-100(E28C) and unlabeled his_6-σ^E, his_6-RseA1-100 were taken from –80°C freezer, defrozen on ice, and centrifuged at 80,000 rpm for 20 min to remove aggregated proteins. Concentrations of the purified proteins were then measured by UV A_{280} absorbance. Proteins were diluted (over 10 fold) to the appropriate concentrations by dialysis buffer without added glycerol (5% remaining) and mixed together. The samples were degassed under vacuum at room temperature before data collection.

Data were collected with a K2 Multifrequency Fluorometer (ISS, Champagne, IL) set to λ_{ex} = 543 nm and λ_{em} = 575 nm.

Binding curve of his_6-RseA1-100(E28C) and his_6-σ^E was obtained by measuring polarization anisotropy for 100 nM of labeled his_6-RseA1-100(E28C) in the presence of various concentrations of his_6-σ^E. Relative affinities of labeled his_6-RseA1-100(E28C) and unlabeled his_6-RseA1-100 were measured by adding various concentrations of his_6-σ^E to the mix of the two proteins (100 nM each). Labeled his_6-RseA1-100(E28C) and unlabeled his_6-RseA1-100 bound his_6-σ^E equally tight. The dissociation rate of his_6-RseA1-100(E28C) / his_6-σ^E complex (100 nM) was measured by monitoring anisotropy of the complex upon addition of excess of his_6-RseA1-100 (1.5 μM). In the same way it was measured for his_6-RseA1-100/ his_6-σ^E complex.

Kinetic assay:

We measured the time course of his_6-σ^E binding to his_6-RseA1-100(E28C) by the increase in intensity of rhodamine fluorescence (λ_{ex} = 543 nm, λ_{em} = 575 nm) upon formation of the complex, using a stopped flow hand-operated mixing system (SFA-20; HiTech Scientific, Salisbury, U.K.) and fluorimeter (K2; ISS, Champagne, IL). To calculate the association rate constant of his_6-σ^E and labeled his_6-RseA1-100(E28C), we measured the time course of their binding for various concentrations of his_6-σ^E and labeled his_6-RseA1-100(E28C) (125nM and 128 nM; 247 nM and 128 nM; 250 nM and 100 nM; 370 nM and 128 nM). The data obtained were analyzed using KaleidaGraph (Synergy Software, Reading, PA) by fitting to the function shown in Equation 1.

$$I = I_0 + \Delta I \cdot C, \quad where \qquad \text{(Eq. 1)}$$

$$C = \frac{\sigma^E \cdot \exp\{-k \cdot |(\sigma^E - RseA_{cyto})| \cdot t\} - 1}{RseA_{cyto} \cdot \exp\{-k \cdot |(\sigma^E - RseA_{cyto})| \cdot t\} - \sigma^E}$$

where I_0 - is the fluorescence intensity of the labeled his_6-RseA1-100(E28C) when it is not in complex with his_6-σ^E, ΔI - is the increase in the fluorescence intensity upon his_6-σ^E binding, C- fraction of his_6-RseA1-100(E28C) that is in complex with his_6-σ^E, σ^E and $RseA_{cyto}$ - concentrations of his_6-σ^E and his_6-RseA1-100(E28C) mixed together; k - the association rate constant.

Figure A. Kinetic measurements of the dissociation and association rate constants of σ^E binding to RseA cyto.

(A-1) Changes in fluorescent anisotropy of the complex between his_6-RseA1-100(E28C), labeled with rhodamine, and his_6-σ^E (100 nM) after addition of the excess of unlabled his_6-RseA1-100 (1.5 μM).

(A-2) Changes in fluorescent intensity of his_6-RseA1-100(E28C), labeled with rhodamine, induced by binding of his_6-σ^E. 128 nM of his_6-RseA1-100(E28C) were rapidly mixed with various concentrations of his_6-σ^E: 125 nM, 240 nM, 370 nM using a stopped flow technique.

Figure A

A-1

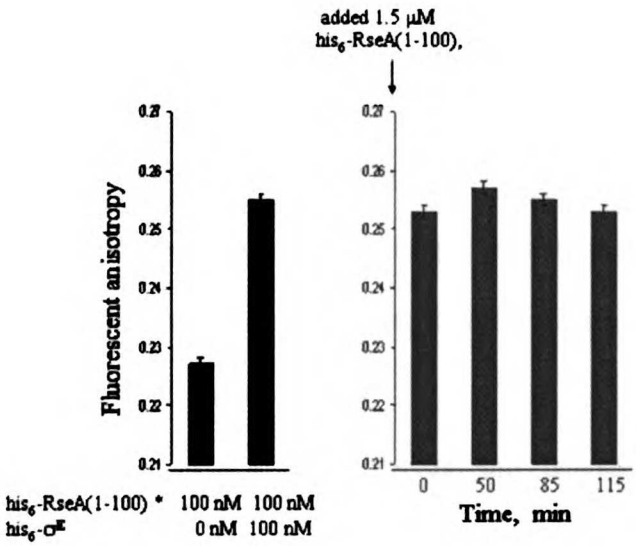

A-2

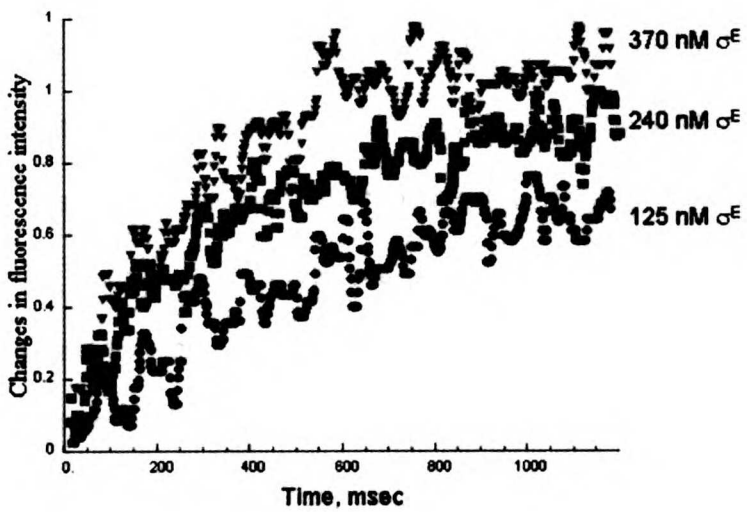

Bibliography

1. Cell Communication, in Molecular biology of the cell, A.J. Bruce Alberts, Julian Lewis, Martin Raff, Keith Roberts, Peter Walter, Editor. 2002, Garland Science: New York. p. 831-907.

2. Brown, M.S., et al., Regulated intramembrane proteolysis: a control mechanism conserved from bacteria to humans. Cell, 2000. **100**(4): p. 391-8.

3. Rawson, R.B., et al., Complementation cloning of S2P, a gene encoding a putative metalloprotease required for intramembrane cleavage of SREBPs. Mol Cell, 1997. **1**(1): p. 47-57.

4. Duncan, E.A., et al., Second-site cleavage in sterol regulatory element-binding protein occurs at transmembrane junction as determined by cysteine panning. J Biol Chem, 1998. **273**(28): p. 17801-9.

5. Weihofen, A. and B. Martoglio, Intramembrane-cleaving proteases: controlled liberation of proteins and bioactive peptides. Trends Cell Biol, 2003. **13**(2): p. 71-8.

6. Rudner, D.Z., P. Fawcett, and R. Losick, A family of membrane-embedded metalloproteases involved in regulated proteolysis of membrane-associated transcription factors. Proc Natl Acad Sci U S A, 1999. **96**(26): p. 14765-70.

7. Cutting, S., S. Roels, and R. Losick, Sporulation operon spoIVF and the characterization of mutations that uncouple mother-cell from forespore gene expression in Bacillus subtilis. J Mol Biol, 1991. **221**(4): p. 1237-56.

8. Sakai, J., et al., Sterol-regulated release of SREBP-2 from cell membranes requires two sequential cleavages, one within a transmembrane segment. Cell, 1996. **85**(7): p. 1037-46.

9. Haze, K., et al., Mammalian transcription factor ATF6 is synthesized as a transmembrane protein and activated by proteolysis in response to endoplasmic reticulum stress. Mol Biol Cell, 1999. **10**(11): p. 3787-99.

10. Ye, J., et al., ER stress induces cleavage of membrane-bound ATF6 by the same proteases that process SREBPs. Mol Cell, 2000. **6**(6): p. 1355-64.

11. Wang, X., et al., SREBP-1, a membrane-bound transcription factor released by sterol-regulated proteolysis. Cell, 1994. **77**(1): p. 53-62.

12. Selkoe, D. and R. Kopan, Notch and Presenilin: regulated intramembrane proteolysis links development and degeneration. Annu Rev Neurosci, 2003. **26**: p. 565-97.

13. Becker-Herman, S., et al., CD74 Is a Member of the Regulated Intramembrane Proteolysis-processed Protein Family. Mol Biol Cell, 2005. **16**(11): p. 5061-9.

14. Nikaido, H., Outer membrane, in Escherichia coli and Salmonella: Cellular and Molecular Biology, C.R.I. Neidhardt FC, Ingraham JL, Lin ECC, Low KB, Magasanik B, Reznikoff WS, Riley M, Schaechter M, Umbarger HE, Editor. 1996, ASM Press: Washington DC. p. 29-47.

15. Oliver, D.B., Periplasm, in Escherichia coli and Salmonella: Cellular and Molecular Biology, C.R.I. Neidhardt FC, Ingraham JL, Lin ECC, Low KB, Magasanik B, Reznikoff WS, Riley M, Schaechter M, Umbarger HE, Editor. 1996, ASM Press: Washington DC. p. 88-103.

16. Park, J.T., The murein sacculus, in Escherichia coli and Salmonella: Cellular and Molecular Biology, C.R.I. Neidhardt FC, Ingraham JL, Lin ECC, Low KB,

Magasanik B, Reznikoff WS, Riley M, Schaechter M, Umbarger HE, Editor. 1996, ASM Press: Washington DC. p. 48-57.

17. Kadner, R.J., Cytoplasmic membrane, in Escherichia coli and Salmonella: Cellular and Molecular Biology, C.R.I. Neidhardt FC, Ingraham JL, Lin ECC, Low KB, Magasanik B, Reznikoff WS, Riley M, Schaechter M, Umbarger HE, Editor. 1996, ASM Press: Washington DC. p. 58-87.

18. Nikaido, H., Molecular basis of bacterial outer membrane permeability revisited. Microbiol Mol Biol Rev, 2003. **67**(4): p. 593-656.

19. Onufryk, C., et al., Characterization of six lipoproteins in the sigmaE regulon. J Bacteriol, 2005. **187**(13): p. 4552-61.

20. Wu, T., et al., Identification of a multicomponent complex required for outer membrane biogenesis in Escherichia coli. Cell, 2005. **121**(2): p. 235-45.

21. Rizzitello, A.E., J.R. Harper, and T.J. Silhavy, Genetic evidence for parallel pathways of chaperone activity in the periplasm of Escherichia coli. J Bacteriol, 2001. **183**(23): p. 6794-800.

22. Mecsas, J., et al., The activity of sigma E, an Escherichia coli heat-inducible sigma-factor, is modulated by expression of outer membrane proteins. Genes Dev. Vol. 7. 1993. 2618-28.

23. Walsh, N.P., et al., OMP peptide signals initiate the envelope-stress response by activating DegS protease via relief of inhibition mediated by its PDZ domain. Cell, 2003. **113**(1): p. 61-71.

24. Rhodius, V.A., Conserved and variable functions of the sigmaE stress response in related genomes. PLos Biol, 2006. **in press**.

25. Grigorova, I.L., et al., Fine-tuning of the Escherichia coli sigmaE envelope stress response relies on multiple mechanisms to inhibit signal-independent proteolysis of the transmembrane anti-sigma factor, RseA. Genes Dev, 2004. **18**(21): p. 2686-97.

26. De Las Penas, A., L. Connolly, and C.A. Gross, The sigmaE-mediated response to extracytoplasmic stress in Escherichia coli is transduced by RseA and RseB, two negative regulators of sigmaE. Mol Microbiol, 1997. **24**(2): p. 373-85.

27. Missiakas, D., et al., Modulation of the Escherichia coli sigmaE (RpoE) heat-shock transcription-factor activity by the RseA, RseB and RseC proteins. Mol Microbiol, 1997. **24**(2): p. 355-71.

28. Campbell, E.A., et al., Crystal structure of Escherichia coli sigmaE with the cytoplasmic domain of its anti-sigma RseA. Mol Cell, 2003. **11**(4): p. 1067-78.

29. Ades, S.E., et al., The Escherichia coli sigma(E)-dependent extracytoplasmic stress response is controlled by the regulated proteolysis of an anti-sigma factor. Genes Dev, 1999. **13**(18): p. 2449-61.

30. Wilken, C., et al., Crystal structure of the DegS stress sensor: How a PDZ domain recognizes misfolded protein and activates a protease. Cell, 2004. **117**(4): p. 483-94.

31. Karshikoff, A., et al., Electrostatic properties of two porin channels from Escherichia coli. J Mol Biol, 1994. **240**(4): p. 372-84.

32. Cowan, S.W., et al., The structure of OmpF porin in a tetragonal crystal form. Structure, 1995. **3**(10): p. 1041-50.

33. Flynn, J.M., et al., Modulating substrate choice: the SspB adaptor delivers a regulator of the extracytoplasmic-stress response to the AAA+ protease ClpXP for degradation. Genes Dev, 2004. **18**(18): p. 2292-301.

34. Ades, S.E., I.L. Grigorova, and C.A. Gross, Regulation of the alternative sigma factor sigma(E) during initiation, adaptation, and shutoff of the extracytoplasmic heat shock response in Escherichia coli. J Bacteriol, 2003. **185**(8): p. 2512-9.

35. Ades, S.E., Control of the alternative sigma factor sigmaE in Escherichia coli. Curr Opin Microbiol, 2004. **7**(2): p. 157-62.

36. Alba, B.M., et al., DegS and YaeL participate sequentially in the cleavage of RseA to activate the sigma(E)-dependent extracytoplasmic stress response. Genes Dev, 2002. **16**(16): p. 2156-68.

37. Kanehara, K., K. Ito, and Y. Akiyama, YaeL (EcfE) activates the sigma(E) pathway of stress response through a site-2 cleavage of anti-sigma(E), RseA, in Genes Dev. 2002. p. 2147-55.

38. Kanehara, K., K. Ito, and Y. Akiyama, YaeL proteolysis of RseA is controlled by the PDZ domain of YaeL and a Gln-rich region of RseA. Embo J, 2003. **22**(23): p. 6389-98.

39. Bohn, C., J. Collier, and P. Bouloc, Dispensable PDZ domain of Escherichia coli YaeL essential protease. Mol Microbiol, 2004. **52**(2): p. 427-35.

40. Akiyama, Y., K. Kanehara, and K. Ito, RseP (YaeL), an Escherichia coli RIP protease, cleaves transmembrane sequences. Embo J, 2004. **23**(22): p. 4434-42.

41. Hengge-Aronis, R., Interplay of global regulators and cell physiology in the general stress response of Escherichia coli. Curr Opin Microbiol, 1999. **2**(2): p. 148-52.

42. Rouviere, P.E., et al., rpoE, the gene encoding the second heat-shock sigma factor, sigma E, in Escherichia coli. Embo J, 1995. **14**(5): p. 1032-42.

43. Raina, S., D. Missiakas, and C. Georgopoulos, The rpoE gene encoding the sigma E (sigma 24) heat shock sigma factor of Escherichia coli. Embo J, 1995. **14**(5): p. 1043-55.

44. Missiakas, D., J.M. Betton, and S. Raina, New components of protein folding in extracytoplasmic compartments of Escherichia coli SurA, FkpA and Skp/OmpH. Mol Microbiol, 1996. **21**(4): p. 871-84.

45. Wang, Q.P. and J.M. Kaguni, A novel sigma factor is involved in expression of the rpoH gene of Escherichia coli. J Bacteriol, 1989. **171**(8): p. 4248-53.

46. Erickson, J.W. and C.A. Gross, Identification of the sigma E subunit of Escherichia coli RNA polymerase: a second alternate sigma factor involved in high-temperature gene expression. Genes Dev, 1989. **3**(9): p. 1462-71.

47. Alba, B.M. and C.A. Gross, Regulation of the Escherichia colisigma-dependent envelope stress response. Mol Microbiol, 2004. **52**(3): p. 613-9.

48. Gilligan, P.H., Microbiology of airway disease in patients with cystic fibrosis. Clin Microbiol Rev, 1991. **4**(1): p. 35-51.

49. Govan, J.R.W., Bacterial infections of respiratory and gastrointestinal mucosae., S.J. Donachie W, Editor. 1988: IRL, Oxford. p. 67-96.

50. Penketh, A., et al., The relationship of phenotype changes in Pseudomonas aeruginosa to the clinical condition of patients with cystic fibrosis. Am Rev Respir Dis, 1983. **127**(5): p. 605-8.

51. Govan, J.R. and J.W. Nelson, Microbiology of lung infection in cystic fibrosis. Br Med Bull, 1992. **48**(4): p. 912-30.

52. Lam, J., et al., Production of mucoid microcolonies by Pseudomonas aeruginosa within infected lungs in cystic fibrosis. Infect Immun, 1980. **28**(2): p. 546-56.

53. Martin, D.W., et al., Mechanism of conversion to mucoidy in Pseudomonas aeruginosa infecting cystic fibrosis patients. Proc Natl Acad Sci U S A, 1993. **90**(18): p. 8377-81.

54. Martin, D.W., et al., Differentiation of Pseudomonas aeruginosa into the alginate-producing form: inactivation of mucB causes conversion to mucoidy. Mol Microbiol, 1993. **9**(3): p. 497-506.

55. Martin, D.W., B.W. Holloway, and V. Deretic, Characterization of a locus determining the mucoid status of Pseudomonas aeruginosa: AlgU shows sequence similarities with a Bacillus sigma factor. J Bacteriol, 1993. **175**(4): p. 1153-64.

56. Martin, D.W., et al., Analysis of promoters controlled by the putative sigma factor AlgU regulating conversion to mucoidy in Pseudomonas aeruginosa: relationship to sigma E and stress response. J Bacteriol, 1994. **176**(21): p. 6688-96.

57. DeVries, C.A. and D.E. Ohman, Mucoid-to-nonmucoid conversion in alginate-producing Pseudomonas aeruginosa often results from spontaneous mutations in algT, encoding a putative alternate sigma factor, and shows evidence for autoregulation. J Bacteriol, 1994. **176**(21): p. 6677-87.

58. Dartigalongue, C., D. Missiakas, and S. Raina, Characterization of the Escherichia coli sigma E regulon. J Biol Chem, 2001. **276**(24): p. 20866-75.

59. Firoved, A.M. and V. Deretic, Microarray analysis of global gene expression in mucoid Pseudomonas aeruginosa. J Bacteriol, 2003. **185**(3): p. 1071-81.

60. Firoved, A.M., J.C. Boucher, and V. Deretic, Global genomic analysis of AlgU (sigma(E))-dependent promoters (sigmulon) in Pseudomonas aeruginosa and implications for inflammatory processes in cystic fibrosis. J Bacteriol, 2002. **184**(4): p. 1057-64.

61. Malhotra, S., et al., Proteome analysis of the effect of mucoid conversion on global protein expression in Pseudomonas aeruginosa strain PAO1 shows induction of the disulfide bond isomerase, dsbA. J Bacteriol, 2000. **182**(24): p. 6999-7006.

62. Chitnis, C.E. and D.E. Ohman, Genetic analysis of the alginate biosynthetic gene cluster of Pseudomonas aeruginosa shows evidence of an operonic structure. Mol Microbiol, 1993. **8**(3): p. 583-93.

63. Boucher, J.C., et al., Two distinct loci affecting conversion to mucoidy in Pseudomonas aeruginosa in cystic fibrosis encode homologs of the serine protease HtrA. J Bacteriol, 1996. **178**(2): p. 511-23.

64. Missiakas, D. and S. Raina, The extracytoplasmic function sigma factors: role and regulation. Mol Microbiol, 1998. **28**(6): p. 1059-66.

65. Schurr, M.J. and V. Deretic, Microbial pathogenesis in cystic fibrosis: co-ordinate regulation of heat-shock response and conversion to mucoidy in Pseudomonas aeruginosa. Mol Microbiol, 1997. **24**(2): p. 411-20.

66. Schurr, M.J., et al., Multiple promoters and induction by heat shock of the gene encoding the alternative sigma factor AlgU (sigma E) which controls mucoidy in cystic fibrosis isolates of Pseudomonas aeruginosa. J Bacteriol, 1995. **177**(19): p. 5670-9.

67. Learn, D.B., E.P. Brestel, and S. Seetharama, Hypochlorite scavenging by Pseudomonas aeruginosa alginate. Infect Immun, 1987. **55**(8): p. 1813-8.

68. Simpson, J.A., S.E. Smith, and R.T. Dean, Scavenging by alginate of free radicals released by macrophages. Free Radic Biol Med, 1989. **6**(4): p. 347-53.

69. Yu, H., M.J. Schurr, and V. Deretic, Functional equivalence of Escherichia coli sigma E and Pseudomonas aeruginosa AlgU: E. coli rpoE restores mucoidy and reduces sensitivity to reactive oxygen intermediates in algU mutants of P. aeruginosa. J Bacteriol, 1995. **177**(11): p. 3259-68.

70. Mathee, K., C.J. McPherson, and D.E. Ohman, Posttranslational control of the algT (algU)-encoded sigma22 for expression of the alginate regulon in Pseudomonas aeruginosa and localization of its antagonist proteins MucA and MucB (AlgN). J Bacteriol, 1997. **179**(11): p. 3711-20.

71. Boucher, J.C., et al., Mucoid Pseudomonas aeruginosa in cystic fibrosis: characterization of muc mutations in clinical isolates and analysis of clearance in a mouse model of respiratory infection. Infect Immun, 1997. **65**(9): p. 3838-46.

72. Fyfe, J.A. and J.R. Govan, Alginate synthesis in mucoid Pseudomonas aeruginosa: a chromosomal locus involved in control. J Gen Microbiol, 1980. **119**(2): p. 443-50.

73. Rowen, D.W. and V. Deretic, Membrane-to-cytosol redistribution of ECF sigma factor AlgU and conversion to mucoidy in Pseudomonas aeruginosa isolates from cystic fibrosis patients. Mol Microbiol, 2000. **36**(2): p. 314-27.

74. Jonsson, A.B., G. Nyberg, and S. Normark, Phase variation of gonococcal pili by frameshift mutation in pilC, a novel gene for pilus assembly. Embo J, 1991. **10**(2): p. 477-88.

75. Broschard, T.H., N. Koffel-Schwartz, and R.P. Fuchs, Sequence-dependent modulation of frameshift mutagenesis at NarI-derived mutation hot spots. J Mol Biol, 1999. **288**(1): p. 191-9.

76. Reiling, S.A., et al., Prc protease promotes mucoidy in mucA mutants of Pseudomonas aeruginosa. Microbiology, 2005. **151**(Pt 7): p. 2251-61.

77. Schurr, M.J., et al., Gene cluster controlling conversion to alginate-overproducing phenotype in Pseudomonas aeruginosa: functional analysis in a heterologous host and role in the instability of mucoidy. J Bacteriol, 1994. **176**(11): p. 3375-82.

78. Raivio, T.L., Envelope stress responses and Gram-negative bacterial pathogenesis. Mol Microbiol, 2005. **56**(5): p. 1119-28.

79. Korbsrisate, S., et al., The Burkholderia pseudomallei RpoE (AlgU) operon is involved in environmental stress tolerance and biofilm formation. FEMS Microbiol Lett, 2005. **252**(2): p. 243-9.

80. Matson, J.S. and V.J. DiRita, Degradation of the membrane-localized virulence activator TcpP by the YaeL protease in Vibrio cholerae. Proc Natl Acad Sci U S A, 2005. **102**(45): p. 16403-8.

81. Hase, C.C. and J.J. Mekalanos, TcpP protein is a positive regulator of virulence gene expression in Vibrio cholerae. Proc Natl Acad Sci U S A, 1998. **95**(2): p. 730-4.

82. Carroll, P.A., et al., Phase variation in tcpH modulates expression of the ToxR regulon in Vibrio cholerae. Mol Microbiol, 1997. **25**(6): p. 1099-111.

83. Krukonis, E.S., R.R. Yu, and V.J. Dirita, The Vibrio cholerae ToxR/TcpP/ToxT virulence cascade: distinct roles for two membrane-localized transcriptional activators on a single promoter. Mol Microbiol, 2000. **38**(1): p. 67-84.

84. Krukonis, E.S. and V.J. DiRita, DNA binding and ToxR responsiveness by the wing domain of TcpP, an activator of virulence gene expression in Vibrio cholerae. Mol Cell, 2003. **12**(1): p. 157-65.

85. Beck, N.A., E.S. Krukonis, and V.J. DiRita, TcpH influences virulence gene expression in Vibrio cholerae by inhibiting degradation of the transcription activator TcpP. J Bacteriol, 2004. **186**(24): p. 8309-16.

86. DiRita, V.J. and J.J. Mekalanos, Periplasmic interaction between two membrane regulatory proteins, ToxR and ToxS, results in signal transduction and transcriptional activation. Cell, 1991. **64**(1): p. 29-37.

87. Yu, R.R. and V.J. DiRita, Analysis of an autoregulatory loop controlling ToxT, cholera toxin, and toxin-coregulated pilus production in Vibrio cholerae. J Bacteriol, 1999. **181**(8): p. 2584-92.

88. Dziejman, M. and J.J. Mekalanos, Analysis of membrane protein interaction: ToxR can dimerize the amino terminus of phage lambda repressor. Mol Microbiol, 1994. **13**(3): p. 485-94.

89. Makinoshima, H. and M.S. Glickman, Regulation of Mycobacterium tuberculosis cell envelope composition and virulence by intramembrane proteolysis. Nature, 2005. **436**(7049): p. 406-9.

90. Glickman, M.S., J.S. Cox, and W.R. Jacobs, Jr., A novel mycolic acid cyclopropane synthetase is required for cording, persistence, and virulence of Mycobacterium tuberculosis. Mol Cell, 2000. **5**(4): p. 717-27.

91. Reed, M.B., et al., A glycolipid of hypervirulent tuberculosis strains that inhibits the innate immune response. Nature, 2004. **431**(7004): p. 84-7.

92. Rao, V., et al., Mycobacterium tuberculosis controls host innate immune activation through cyclopropane modification of a glycolipid effector molecule. J Exp Med, 2005. **201**(4): p. 535-43.

93. Glickman, M.S. and W.R. Jacobs, Jr., Microbial pathogenesis of Mycobacterium tuberculosis: dawn of a discipline. Cell, 2001. **104**(4): p. 477-85.

94. Schaible, U.E., et al., Apoptosis facilitates antigen presentation to T lymphocytes through MHC-I and CD1 in tuberculosis. Nat Med, 2003. **9**(8): p. 1039-46.

95. Rhoades, E., et al., Identification and macrophage-activating activity of glycolipids released from intracellular Mycobacterium bovis BCG. Mol Microbiol, 2003. **48**(4): p. 875-88.

96. Schobel, S., et al., The Bacillus subtilis sigmaW anti-sigma factor RsiW is degraded by intramembrane proteolysis through YluC. Mol Microbiol, 2004. **52**(4): p. 1091-105.

97. Helmann, J.D., The extracytoplasmic function (ECF) sigma factors. Adv Microb Physiol, 2002. **46**: p. 47-110.

98. Helmann, J.D., Moran, C.P., RNA polymerase and sigma factors., in Bacillus subtilis and its closest relatives. From genes to cells., H.J. Sonenshein AL, and

Lousick R., Editor. 2002, American Society for Microbiology Press: Washington, DC. p. 289-312.

99. Cao, M., et al., Antibiotics that inhibit cell wall biosynthesis induce expression of the Bacillus subtilis sigma(W) and sigma(M) regulons. Mol Microbiol, 2002. **45**(5): p. 1267-76.

100. Petersohn, A., et al., Global analysis of the general stress response of Bacillus subtilis. J Bacteriol, 2001. **183**(19): p. 5617-31.

101. Wiegert, T., et al., Alkaline shock induces the Bacillus subtilis sigma(W) regulon. Mol Microbiol, 2001. **41**(1): p. 59-71.

102. Errington, J., Regulation of endospore formation in Bacillus subtilis. Nat Rev Microbiol, 2003. **1**(2): p. 117-26.

103. Kroos, L. and Y.T. Yu, Regulation of sigma factor activity during Bacillus subtilis development. Curr Opin Microbiol, 2000. **3**(6): p. 553-60.

104. Cutting, S., et al., A forespore checkpoint for mother cell gene expression during development in B. subtilis. Cell, 1990. **62**(2): p. 239-50.

105. Lu, S., R. Halberg, and L. Kroos, Processing of the mother-cell sigma factor, sigma K, may depend on events occurring in the forespore during Bacillus subtilis development. Proc Natl Acad Sci U S A, 1990. **87**(24): p. 9722-6.

106. Zhang, B., A. Hofmeister, and L. Kroos, The prosequence of pro-sigmaK promotes membrane association and inhibits RNA polymerase core binding. J Bacteriol, 1998. **180**(9): p. 2434-41.

107. Yu, Y.T. and L. Kroos, Evidence that SpoIVFB is a novel type of membrane metalloprotease governing intercompartmental communication during Bacillus subtilis sporulation. J Bacteriol, 2000. **182**(11): p. 3305-9.

108. Lu, S., S. Cutting, and L. Kroos, Sporulation protein SpoIVFB from Bacillus subtilis enhances processing of the sigma factor precursor Pro-sigma K in the absence of other sporulation gene products. J Bacteriol, 1995. **177**(4): p. 1082-5.

109. Resnekov, O. and R. Losick, Negative regulation of the proteolytic activation of a developmental transcription factor in Bacillus subtilis. Proc Natl Acad Sci U S A, 1998. **95**(6): p. 3162-7.

110. Kroos, L., et al., Forespore signaling is necessary for pro-sigmaK processing during Bacillus subtilis sporulation despite the loss of SpoIVFA upon translational arrest. J Bacteriol, 2002. **184**(19): p. 5393-401.

111. Resnekov, O., S. Alper, and R. Losick, Subcellular localization of proteins governing the proteolytic activation of a developmental transcription factor in Bacillus subtilis. Genes Cells, 1996. **1**(6): p. 529-42.

112. Ricca, E., S. Cutting, and R. Losick, Characterization of bofA, a gene involved in intercompartmental regulation of pro-sigma K processing during sporulation in Bacillus subtilis. J Bacteriol, 1992. **174**(10): p. 3177-84.

113. Rudner, D.Z., Q. Pan, and R.M. Losick, Evidence that subcellular localization of a bacterial membrane protein is achieved by diffusion and capture. Proc Natl Acad Sci U S A, 2002. **99**(13): p. 8701-6.

114. Rudner, D.Z. and R. Losick, A sporulation membrane protein tethers the pro-sigmaK processing enzyme to its inhibitor and dictates its subcellular localization. Genes Dev, 2002. **16**(8): p. 1007-18.

115. Zhou, R. and L. Kroos, BofA protein inhibits intramembrane proteolysis of pro-sigmaK in an intercompartmental signaling pathway during Bacillus subtilis sporulation. Proc Natl Acad Sci U S A, 2004. **101**(17): p. 6385-90.

116. Gomez, M., S. Cutting, and P. Stragier, Transcription of spoIVB is the only role of sigma G that is essential for pro-sigma K processing during spore formation in Bacillus subtilis. J Bacteriol, 1995. **177**(16): p. 4825-7.

117. Wakeley, P.R., et al., Proteolysis of SpoIVB is a critical determinant in signalling of Pro-sigmaK processing in Bacillus subtilis. Mol Microbiol, 2000. **36**(6): p. 1336-48.

118. Dong, T.C. and S.M. Cutting, SpoIVB-mediated cleavage of SpoIVFA could provide the intercellular signal to activate processing of Pro-sigmaK in Bacillus subtilis. Mol Microbiol, 2003. **49**(5): p. 1425-34.

119. Pan, Q., R. Losick, and D.Z. Rudner, A second PDZ-containing serine protease contributes to activation of the sporulation transcription factor sigmaK in Bacillus subtilis. J Bacteriol, 2003. **185**(20): p. 6051-6.

120. Zhou, R. and L. Kroos, Serine proteases from two cell types target different components of a complex that governs regulated intramembrane proteolysis of pro-sigmaK during Bacillus subtilis development. Mol Microbiol, 2005. **58**(3): p. 835-46.

121. Cutting, S., et al., Forespore-specific transcription of a gene in the signal transduction pathway that governs Pro-sigma K processing in Bacillus subtilis. Genes Dev, 1991. **5**(3): p. 456-66.

122. Jiang, X., et al., Engulfment-regulated proteolysis of SpoIIQ: evidence that dual checkpoints control sigma activity. Mol Microbiol, 2005. **58**(1): p. 102-15.

123. Chen, J.C., P.H. Viollier, and L. Shapiro, A membrane metalloprotease participates in the sequential degradation of a Caulobacter polarity determinant. Mol Microbiol, 2005. **55**(4): p. 1085-103.

124. Viollier, P.H., N. Sternheim, and L. Shapiro, Identification of a localization factor for the polar positioning of bacterial structural and regulatory proteins. Proc Natl Acad Sci U S A, 2002. **99**(21): p. 13831-6.

125. Hinz, A.J., et al., The Caulobacter crescentus polar organelle development protein PodJ is differentially localized and is required for polar targeting of the PleC development regulator. Mol Microbiol, 2003. **47**(4): p. 929-41.

126. Becker, J. and E.A. Craig, Heat-shock proteins as molecular chaperones. Eur J Biochem, 1994. **219**(1-2): p. 11-23.

127. Gross, C.A., Function and Regulation of the Heat Shock Proteins, in Escherichia coli and Salmonella: Cellular and Molecular Biology, e.a. F. C. Neidhardt, Editor. 1996, ASM Press: Washington, D.C. p. 1382-1399.

128. Bukau, B., Regulation of the Escherichia coli heat-shock response. Mol Microbiol, 1993. **9**(4): p. 671-80.

129. Morimoto, R.I., Regulation of the heat shock transcriptional response: cross talk between a family of heat shock factors, molecular chaperones, and negative regulators. Genes Dev, 1998. **12**(24): p. 3788-96.

130. Yura, T. and K. Nakahigashi, Regulation of the heat-shock response. Curr Opin Microbiol, 1999. **2**(2): p. 153-8.

131. Yura, T., H. Nagai, and H. Mori, Regulation of the heat-shock response in bacteria. Annu Rev Microbiol, 1993. **47**: p. 321-50.

132. Grossman, A.D., J.W. Erickson, and C.A. Gross, The htpR gene product of E. coli is a sigma factor for heat-shock promoters. Cell, 1984. **38**(2): p. 383-90.

133. Hiratsu, K., et al., The rpoE gene of Escherichia coli, which encodes sigma E, is essential for bacterial growth at high temperature. J Bacteriol, 1995. **177**(10): p. 2918-22.

134. Landick, R., et al., Nucleotide sequence of the heat shock regulatory gene of E. coli suggests its protein product may be a transcription factor. Cell, 1984. **38**(1): p. 175-82.

135. Yura, T., et al., Heat shock regulatory gene (htpR) of Escherichia coli is required for growth at high temperature but is dispensable at low temperature. Proc Natl Acad Sci U S A, 1984. **81**(21): p. 6803-7.

136. Gamer, J., et al., A cycle of binding and release of the DnaK, DnaJ and GrpE chaperones regulates activity of the Escherichia coli heat shock transcription factor sigma32. Embo J, 1996. **15**(3): p. 607-17.

137. Grossman, A.D., et al., Sigma 32 synthesis can regulate the synthesis of heat shock proteins in Escherichia coli. Genes Dev, 1987. **1**(2): p. 179-84.

138. Morita, M.T., et al., Dynamic interplay between antagonistic pathways controlling the sigma 32 level in Escherichia coli. Proc Natl Acad Sci U S A, 2000. **97**(11): p. 5860-5.

139. Morita, M.T., et al., Translational induction of heat shock transcription factor sigma32: evidence for a built-in RNA thermosensor. Genes Dev, 1999. **13**(6): p. 655-65.

140. Straus, D., W. Walter, and C.A. Gross, DnaK, DnaJ, and GrpE heat shock proteins negatively regulate heat shock gene expression by controlling the synthesis and stability of sigma 32. Genes Dev, 1990. **4**(12A): p. 2202-9.

141. Straus, D.B., W.A. Walter, and C.A. Gross, The activity of sigma 32 is reduced under conditions of excess heat shock protein production in Escherichia coli. Genes Dev, 1989. **3**(12A): p. 2003-10.

142. Straus, D.B., W.A. Walter, and C.A. Gross, The heat shock response of E. coli is regulated by changes in the concentration of sigma 32. Nature, 1987. **329**(6137): p. 348-51.

143. Rouviere, P.E. and C.A. Gross, SurA, a periplasmic protein with peptidyl-prolyl isomerase activity, participates in the assembly of outer membrane porins. Genes Dev, 1996. **10**(24): p. 3170-82.

144. Connolly, L., et al., The response to extracytoplasmic stress in Escherichia coli is controlled by partially overlapping pathways. Genes Dev, 1997. **11**(15): p. 2012-21.

145. Danese, P.N., et al., The Cpx two-component signal transduction pathway of Escherichia coli regulates transcription of the gene specifying the stress-inducible periplasmic protease, DegP. Genes Dev, 1995. **9**(4): p. 387-98.

146. Alba, B.M., et al., degS (hhoB) is an essential Escherichia coli gene whose indispensable function is to provide sigma (E) activity. Mol Microbiol, 2001. **40**(6): p. 1323-33.

147. Baker, T.A., A.D. Grossman, and C.A. Gross, A gene regulating the heat shock response in Escherichia coli also affects proteolysis. Proc Natl Acad Sci U S A, 1984. **81**(21): p. 6779-83.

148. Collinet, B., et al., RseB binding to the periplasmic domain of RseA modulates the RseA:sigmaE interaction in the cytoplasm and the availability of sigmaE.RNA polymerase. J Biol Chem, 2000. **275**(43): p. 33898-904.

149. Sambrook, J., Fritsch, E., and T. Maniatis, Molecular cloning: A laboratory manual. 1989, Cold Spring Harbor, NY: Cold Spring Harbor Laboratory Press.

150. De Las Penas, A., L. Connolly, and C.A. Gross, SigmaE is an essential sigma factor in Escherichia coli. J Bacteriol, 1997. **179**(21): p. 6862-4.

151. Forst, S., et al., Regulation of ompC and ompF expression in Escherichia coli in the absence of envZ. J Bacteriol, 1988. **170**(11): p. 5080-5.

152. Mizuno, T. and S. Mizushima, Signal transduction and gene regulation through the phosphorylation of two regulatory components: the molecular basis for the osmotic regulation of the porin genes. Mol Microbiol, 1990. **4**(7): p. 1077-82.

153. Betton, J. and M. Hofnung, Folding of a mutant maltose-binding protein of Escherichia coli which forms inclusion bodies. J Biol Chem, 1996. **271**(14): p. 8046-52.

154. Hunke, S. and J.M. Betton, Temperature effect on inclusion body formation and stress response in the periplasm of Escherichia coli. Mol Microbiol, 2003. **50**(5): p. 1579-89.

155. Raivio, T.L. and T.J. Silhavy, Periplasmic stress and ECF sigma factors. Annu Rev Microbiol, 2001. **55**: p. 591-624.

156. Clausen, T., C. Southan, and M. Ehrmann, The HtrA family of proteases: implications for protein composition and cell fate. Mol Cell, 2002. **10**(3): p. 443-55.

157. Li, W., et al., Structural insights into the pro-apoptotic function of mitochondrial serine protease HtrA2/Omi. Nat Struct Biol, 2002. **9**(6): p. 436-41.

158. Miller, J.H., Experiments in molecular genetics. 1972, Cold Spring Harbor Laboratory Press: Cold Spring Harbor, NY. p. 274-281.

159. Ishihama, A., Functional modulation of Escherichia coli RNA polymerase. Annu Rev Microbiol, 2000. **54**: p. 499-518.

160. Hans Bremer, P.P.D., Modulation of Chemical Composition and Other Parameters of the Cell by Growth Rate, in Escherichia coli and Salmonella cellular and molecular biology, F.C. Neidhardt, Editor. 1996, ASM Press: Washington, D. C. p. 1553-1569.

161. Hicks, K.A. and A.D. Grossman, Altering the level and regulation of the major sigma subunit of RNA polymerase affects gene expression and development in Bacillus subtilis. Mol Microbiol, 1996. **20**(1): p. 201-12.

162. Zhou, Y.N., W.A. Walter, and C.A. Gross, A mutant sigma 32 with a small deletion in conserved region 3 of sigma has reduced affinity for core RNA polymerase. J Bacteriol, 1992. **174**(15): p. 5005-12.

163. Jishage, M., et al., Regulation of sigma factor competition by the alarmone ppGpp. Genes Dev, 2002. **16**(10): p. 1260-70.

164. Nystrom, T., Growth versus maintenance: a trade-off dictated by RNA polymerase availability and sigma factor competition? Mol Microbiol, 2004. **54**(4): p. 855-62.

165. Laurie, A.D., et al., The role of the alarmone (p)ppGpp in sigma N competition for core RNA polymerase. J Biol Chem, 2003. **278**(3): p. 1494-503.

166. Gross, C.A., et al., The functional and regulatory roles of sigma factors in transcription. Cold Spring Harb Symp Quant Biol, 1998. **63**: p. 141-55.

167. deHaseth, P.L., M.L. Zupancic, and M.T. Record, Jr., RNA polymerase-promoter interactions: the comings and goings of RNA polymerase. J Bacteriol, 1998. **180**(12): p. 3019-25.

168. McClure, W.R., Mechanism and control of transcription initiation in prokaryotes. Annu Rev Biochem, 1985. **54**: p. 171-204.

169. Buc, H. and W.R. McClure, Kinetics of open complex formation between Escherichia coli RNA polymerase and the lac UV5 promoter. Evidence for a sequential mechanism involving three steps. Biochemistry, 1985. **24**(11): p. 2712-23.

170. Saecker, R.M., et al., Kinetic studies and structural models of the association of E. coli sigma(70) RNA polymerase with the lambdaP(R) promoter:

large scale conformational changes in forming the kinetically significant intermediates. J Mol Biol, 2002. **319**(3): p. 649-71.

171. Schlax, P.J., M.W. Capp, and M.T. Record, Jr., Inhibition of transcription initiation by lac repressor. J Mol Biol, 1995. **245**(4): p. 331-50.

172. Zhou, Y.N. and C.A. Gross, How a mutation in the gene encoding sigma 70 suppresses the defective heat shock response caused by a mutation in the gene encoding sigma 32. J Bacteriol, 1992. **174**(22): p. 7128-37.

173. Farewell, A., K. Kvint, and T. Nystrom, Negative regulation by RpoS: a case of sigma factor competition. Mol Microbiol, 1998. **29**(4): p. 1039-51.

174. Jishage, M. and A. Ishihama, Transcriptional organization and in vivo role of the Escherichia coli rsd gene, encoding the regulator of RNA polymerase sigma D. J Bacteriol, 1999. **181**(12): p. 3768-76.

175. deHaseth, P.L., et al., Nonspecific interactions of Escherichia coli RNA polymerase with native and denatured DNA: differences in the binding behavior of core and holoenzyme. Biochemistry, 1978. **17**(9): p. 1612-22.

176. von Hippel, P.H., et al., Non-specific DNA binding of genome regulating proteins as a biological control mechanism: I. The lac operon: equilibrium aspects. Proc Natl Acad Sci U S A, 1974. **71**(12): p. 4808-12.

177. Kao-Huang, Y., et al., Nonspecific DNA binding of genome-regulating proteins as a biological control mechanism: measurement of DNA-bound Escherichia coli lac repressor in vivo. Proc Natl Acad Sci U S A, 1977. **74**(10): p. 4228-32.

178. Jishage, M., et al., Regulation of RNA polymerase sigma subunit synthesis in Escherichia coli: intracellular levels of four species of sigma subunit under various growth conditions. J Bacteriol, 1996. **178**(18): p. 5447-51.

179. Maeda, H., et al., Two extracytoplasmic function sigma subunits, sigma(E) and sigma(FecI), of Escherichia coli: promoter selectivity and intracellular levels. J Bacteriol, 2000. **182**(4): p. 1181-4.

180. Jishage, M. and A. Ishihama, Regulation of RNA polymerase sigma subunit synthesis in Escherichia coli: intracellular levels of sigma 70 and sigma 38. J Bacteriol, 1995. **177**(23): p. 6832-5.

181. Dalbow, D.G., Synthesis of RNA polymerase in Escherichia coli B-r growing at different rates. J Mol Biol, 1973. **75**(1): p. 181-4.

182. Iwakura, Y. and A. Ishihama, Biosynthesis of RNA polymerase in Escherichia coli. II. control of RNA polymerase synthesis during nutritional shift up and down. Mol Gen Genet, 1975. **142**(1): p. 67-84.

183. Iwakura, Y., K. Ito, and A. Ishihama, Biosynthesis of RNA polymerase in Escherichia coli. I. Control of RNA polymerase content at various growth rates. Mol Gen Genet, 1974. **133**(1): p. 1-23.

184. Matzura, H., B.S. Hansen, and J. Zeuthen, Biosynthesis of the beta and beta' subunits of RNA polymerase in Escherichia coli. J Mol Biol, 1973. **74**(1): p. 9-20.

185. Matzura, H., S. Molin, and O. Maaloe, Sequential biosynthesis of the and ' subunits of the DNA-dependent RNA polymerase from Escherichia coli. J Mol Biol, 1971. **59**(1): p. 17-25.

186. Pedersen, S., et al., Patterns of protein synthesis in E. coli: a catalog of the amount of 140 individual proteins at different growth rates. Cell, 1978. **14**(1): p. 179-90.

187. Engbaek, F., C. Gross, and R.R. Burgess, Quantitation of RNA polymerase subunits in Escherichia coli during exponential growth and after Bacteriophage T4 infection. Mol Gen Genet, 1976. **143**(3): p. 291-5.

188. Nakamura, Y. and T. Yura, Evidence for a positive regulation of RNA polymerase synthesis in Escherichia coli. J Mol Biol, 1975. **97**(4): p. 621-42.

189. Soupene, E., et al., Physiological studies of Escherichia coli strain MG1655: growth defects and apparent cross-regulation of gene expression. J Bacteriol, 2003. **185**(18): p. 5611-26.

190. Shepherd, N., P. Dennis, and H. Bremer, Cytoplasmic RNA Polymerase in Escherichia coli. J Bacteriol, 2001. **183**(8): p. 2527-34.

191. Singer, P.T. and C.W. Wu, Kinetics of promoter search by Escherichia coli RNA polymerase. Effects of monovalent and divalent cations and temperature. J Biol Chem, 1988. **263**(9): p. 4208-14.

192. Ricchetti, M., W. Metzger, and H. Heumann, One-dimensional diffusion of Escherichia coli DNA-dependent RNA polymerase: a mechanism to facilitate promoter location. Proc Natl Acad Sci U S A, 1988. **85**(13): p. 4610-4.

193. Ricchetti, M., W. Metzger, and H. Heumann, Directed one-dimensional diffusion of Escherichia coli RNA-polymerase, a mechanism to facilitate promoter location. Biochem Pharmacol, 1988. **37**(9): p. 1805-6.

194. Guthold, M., et al., Direct observation of one-dimensional diffusion and transcription by Escherichia coli RNA polymerase. Biophys J, 1999. **77**(4): p. 2284-94.

195. Sharp, M.M., et al., The interface of sigma with core RNA polymerase is extensive, conserved, and functionally specialized. Genes Dev, 1999. **13**(22): p. 3015-26.

196. Young, B.A., et al., A coiled-coil from the RNA polymerase beta' subunit allosterically induces selective nontemplate strand binding by sigma(70). Cell, 2001. **105**(7): p. 935-44.

197. Gross, T.M.G.a.C.A., Assay of Escherichia coli RNA polymerase: sigma-core interactions, in Methods Enzymol. 2003. p. 206-212.

198. Burgess, R.R., in RNA Polymerase, R. Losick, Chamberlin, M. J., Editor. 1976, Cold Spring Harbor Press: Cold Spring Harbor, NY. p. 69-100.

199. Kusukawa, N. and T. Yura, Heat shock protein GroE of Escherichia coli: key protective roles against thermal stress. Genes Dev, 1988. **2**(7): p. 874-82.

200. Opalka, N., et al., Direct localization of a beta-subunit domain on the three-dimensional structure of Escherichia coli RNA polymerase. Proc Natl Acad Sci U S A, 2000. **97**(2): p. 617-22.

201. RegulonDB (version 4.0): Transcriptional Regulation, Operon Organization and Growth Conditions in Escherichia coli K-12. 2004: Nucleic Acids Research 32. p. 303-306.

202. Salgado, H., et al., RegulonDB (version 4.0): transcriptional regulation, operon organization and growth conditions in Escherichia coli K-12. Nucleic Acids Res, 2004. **32**(Database issue): p. D303-6.

203. Maeda, H., N. Fujita, and A. Ishihama, Competition among seven Escherichia coli sigma subunits: relative binding affinities to the core RNA polymerase. Nucleic Acids Res, 2000. **28**(18): p. 3497-503.

204. Vogel, U. and K.F. Jensen, The RNA chain elongation rate in Escherichia coli depends on the growth rate. J Bacteriol, 1994. **176**(10): p. 2807-13.

205. Liang, S., et al., Activities of constitutive promoters in Escherichia coli. J Mol Biol, 1999. **292**(1): p. 19-37.

206. Bremer, H. and S. Lin-Chao, Analysis of the physiological control of replication of ColE1-type plasmids. J Theor Biol, 1986. **123**(4): p. 453-70.

207. Churchward, G., E. Estiva, and H. Bremer, Growth rate-dependent control of chromosome replication initiation in Escherichia coli. J Bacteriol, 1981. **145**(3): p. 1232-8.

208. Cayley, S. and M.T. Record, Jr., Roles of cytoplasmic osmolytes, water, and crowding in the response of Escherichia coli to osmotic stress: biophysical basis of osmoprotection by glycine betaine. Biochemistry, 2003. **42**(43): p. 12596-609.

209. Gill, S.C., S.E. Weitzel, and P.H. von Hippel, Escherichia coli sigma 70 and NusA proteins. I. Binding interactions with core RNA polymerase in solution and within the transcription complex. J Mol Biol, 1991. **220**(2): p. 307-24.

210. Churchward, G., H. Bremer, and R. Young, Transcription in bacteria at different DNA concentrations. J Bacteriol, 1982. **150**(2): p. 572-81.

211. Kawakami, K., T. Saitoh, and A. Ishihama, Biosynthesis of RNA polymerase in Escherichia coli. IX. Growth-dependent variations in the synthesis rate, content and distribution of RNA polymerase. Mol Gen Genet, 1979. **174**(2): p. 107-16.

212. Dennis, H.B.a.P.P., Modulation of Chemical Composition and Other Parameters of the Cell by Growth Rate, in Escherichia coli and Salmonella cellular and molecular biology, F.C. Neidhardt, Editor. 1996, ASM Press: Washington, D. C. p. 1553-1569.